SUMMARY OF DIPLOMA SHEET

AUTHOR	**Surname** Marchevka	**Name** Petr
FIELD OF STUDY	2301T001 “Transport and handling machinery“	
SUPERVISOR	**Surname (Inclusive of Degrees)** Doc. Ing. Němec,CSc.	**Name** Ladislav
INSTITUTION	ZČU - FST - KKS	

TYPE OF WORK	**DIPLOMA**	~~**BACHELOR**~~	**Delete when not applicable**
TITLE OF THE WORK	4-Stroke engine for hybrid vehicle		

FACULTY	Mechanical Engineering		**DEPARTMENT**	Machine Design		**SUBMITTED IN**	2016

NUMBER OF PAGES (A4 and eq. A4)

TOTALLY	95		**TEXT PART**	92		**GRAPHICAL PART**	3

BRIEF DESCRIPTION **TOPIC, GOAL, RESULTS AND CONTRIBUTIONS**	The diploma thesis deals with a conceptual design of a 4-stroke, 2 cylinder in-line turbocharged engine for an hybrid electric vehicle. The main purpose of this work is the design of a crankshaft assembly, a cylinder head and an engine block. Thesis includes a background research of the various HEV powertrain configuration. Calculation analysis is mainly focused on the connection-rod stress analysis. The numerical analysis, modeling and drawing were performed in SIEMENS NX 10 software environment.
KEY WORDS	Combustion engine, construction, stress analysis, Hybrid electric vehicle (HEV), FEM

ANOTAČNÍ LIST DIPLOMOVÉ PRÁCE

AUTOR	**Přijmení** Marchevka		**Jméno** Petr
STUDIJNÍ OBOR	2301T001 „Dopravní a manipulační technika“		
VEDOUCÍ PRÁCE	**Příjmení (včetně titulů)** Doc. Ing. Němec,CSc.		**Jméno** Ladislav
PRACOVIŠTĚ	ZČU - FST - KKS		
DRUH PRÁCE	DIPLOMOVÁ	~~BAKALÁŘSKÁ~~	Nehodící se škrtněte
NÁZEV PRÁCE	Návrh 4-dobého spalovacího motoru pro hybridní vozidlo		

FAKULTA	strojní		KATEDRA	KKS		ROK ODEVZD.	2016

POČET STRAN (A4 a ekvivalentů A4)

CELKEM	95		TEXTOVÁ ČÁST	92		GRAFICKÁ ČÁST	3

STRUČNÝ POPIS (MAX 10 ŘÁDEK) ZAMĚŘENÍ, TÉMA, CÍL POZNATKY A PŘÍNOSY	Diplomová práce se zabývá koncepčním návrhem čtyřtaktního, 2 válcového přeplňovaného motoru. Navrhovaný motor je konstruován jako součást pohonné jednotky pro hybridní vozidlo. Hlavním cíle práce byl návrh klikové soustavy, hlavy motoru a bloku motoru. Práce také obsahuje rešeršní část zabývající se popisem konfigurace hnacího ústrojí hybridních vozidel. Výpočtová analýza je primárně zaměřena na pevnostní kontrolu ojnice. Výpočtová analýza, modelování a výkresy byly provedené v prostřední programu SIEMENS NX 10.
KLÍČOVÁ SLOVA	Spalovací motor, konstrukce, pevnostní výpočet, hybridní vozidlo

Declaration of Own Work

I hereby declare that this master thesis is completely my own work and that I used only the cited sources.

Pilsen: …………………….   . . . .

Signature

Acknowledgement

I would like to thank to my thesis supervisor doc. Ing. Ladislav Němec, CSc. and my consultant Ing. Miroslav Kalčík for assistance, time and valuable remarks.

Contents

List of symbols and abbreviations

Symbol	Name	Unit
a_K	Piston acceleration	mms^{-2}
a_{Kx}	Piston acceleration direction -X	mms^{-2}
a_{Ky}	Piston acceleration direction -Y	mms^{-2}
A_{piston}	Piston area	mm^2
AA	Distance between bosses -piston	mm
C_f	Surface finish Factor	-
C_p	Stress concentrator factor	-
C_S	Size factor	-
CT	Crown thickness - piston	mm
D	Diameter of bore	mm
d_0	Nominal thread diameter	mm
d_c	Crankpin diameter	mm
D_d	Big-end diameter	mm
D_h	Small-end diameter	mm
d_j	Main journal diameter	mm
D_0	Hole diameter	mm
D_1	Head diameter - bolt	mm
d_2	Shank diameter	mm
d_3	Thread root diameter	mm
DL	Crown under side to pin hole - piston	mm
E	Young's modulus	MPa
F	Top land width -piston	mm
F_A	Internal axis force of a bolt connection	N
F_g	Gas pressure force	N
f_H	Under-head friction	-
F_i	Preload force of a bolt connection	N
F_{IS}	Inertial force of the moving parts of the crank mechanism	N
F_N	Piston normal force	N
F_{PP}	Overall piston pin force	N
F_R	Radial force at the crankshaft	N
F_S	Connection – rod force	N
f_s	Safety factor	-
$F_{Scylinder}$	Inertia force of the reciprocating mass of the crankshaft assembly for one cylinder	N
F_T	Tangential force at the crankshaft	N
f_T	Thread friction	-

Symbol	Name	Unit
F_{Tmax}	Maximal tensile force acting on the bolt	N
H_h	Small-end width	mm
CH	Compression height -piston	mm
i	Number of bolts of connection rod	-
L_0	Hole length	mm
L_1	Threated length	mm
L_2	Shank length	mm
L_{bal}	Length of the counterbalance	mm
l_c	Crankpin width	mm
l_{cs}	Big-end bearing	mm
l_j	Main journal width	mm
l_{js}	Main bearing width	mm
l_{mj}	Main journal distance	mm
L_{oj}	Connection rod length	mm
L_R	Distance between center of gravity and center of big end	mm
L_S	Distance between center of gravity and center of small end	mm
$m_{counterbal}$	Counterbalance mass	kg
$m_{counterweight}$	Crankshaft counterweight mass	kg
m_{CW}	Counterweight mass	kg
m_{Ezal}	Equivalent Mass of the crank arm	kg
m_{oj}	Connection rod weight	kg
m_p	Piston assembly weight	kg
m_R	Rotation mass of the connection rod	kg
$m_{Rcylinder}$	Rotating mass of the crankshaft assembly for one cylinder	kg
m_S	Reciprocation mass of the connection rod	kg
$m_{Scylinder}$	Reciprocating mass of the crankshaft assembly for one cylinder	kg
m_{zal}	Mass of the crank arm	kg
n	Engine speed	rpm
OL	Overall length -piston	mm
p	Pressure	MPa
P	Thread pitch	mm
PB	Pin hole diameters -piston	mm
r_{T_bal}	Distance between balance shaft axis and center of mass of the counterbalance	mm
$r_{T\_counterweight}$	Distance between crankshaft axis and center of mass of counterweight	mm
r_{bal}	Radius of the counterbalance	mm
R_{CW}	Effective counterweight radius	mm

Symbol	Name	Unit
R_e	Yield strength	MPa
r_K	Crank radius	mm
r_{Tzal}	Distance between crankshaft axis and center of mass of the crank arm	mm
s	Piston stroke	mm
S_0	Contact surface (one bolt)	mm^2
SL	Skirt length -piston	mm
St	Ring land width	mm
T_T	Tightening torque	Nm
v	Piston velocity	mm/s
α	Crank angle	degree
β	Pivoting angle of connection rod	degree
γ	Connection rod ratio	-
ε_{CR}	Connection rod - angular acceleration	rad*s-2
κ	Overall flexibility coefficient of the connection	-
κ_B	Coefficient of flexibility of the connecting rod bolt	Nm^(-1)
κ_S	Flexibility coefficient of the connection rod:	Nm-1
ν	Poisson ratio	-
ρ	Density	kg/m3
σ_A	Stress amplitude	MPa
σ_m	Mean stress in the cycle	MPa
σ_{MAX}	Maximum stress in the cycle	MPa
σ_{max}	Maximum stress	MPa
σ_{MIN}	Minimum stress in the cycle	MPa
σ_T	Tensile stress	MPA
ϕ_z	Thread angle	degree
ω	Crankshaft angular velocity	rad*s-1
ω_{CR}	Connection rod - angular velocity	rad*s-1

Abbreviation	Name
BDC	Botton Dead Center
CAD	Computer Aided Design
DOHC	Double Over Head Camshaft
FEM	Finite Elements Method
HEV	Hybrid Electriv Vehicle
hp	Horse Power
ICE	Internal Combustio Engine
PHEV	Plug- In Hybrid Vehicle
PSA	French multinational manufacturer of automobiles and motorcycles sold under the Peugeot, Citroën and DS Automobiles[6] brands
TDC	Top Dead Center

1 Introduction

The environmental pollution problem concerning a limited storage of an oil and a limited range capability of today's purely electric vehicles led to increasing interest in the concept of hybrid vehicles. Moreover, hybrid vehicles could be a compromise or a solution to problems of today. It seems that especially hybrid electric vehicles can provide a short-term solution until limitation and infra-structure problems of pure electric vehicles will be solved.

The first part of the thesis is focused on a theoretical description of hybrid vehicles. This part also describes a different hybrid vehicle powertrain configuration. The thesis includes a background research of important design features and engineering principles of combustion engine as well.

The main part of the thesis deals with conceptual design of 4-stroke,2 cylinder in-line engine. This part is composed of a few subsections which provide a brief overview about a process modeling. The description of the process modeling is not exhaustive due to lack of given time. This is the reason that some parts are simplified just to show the geometry. The purpose is to show basic steps in modeling of the main parts of ICE.

The calculation analysis is mainly focused on the connection-rod stress analysis. It was necessary to performed many calculations to obtain input data for stress analysis. That includes calculation of the basic crank mechanism quantities (crank radius, angular velocity, connection rod ratio), calculation of crankshaft drive kinematics (piston acceleration, angular velocity and angular acceleration of connection rod etc.) In the last step, the calculation of a crankshaft was provided – assembly kinetics.

During developing the thesis many abbreviation were used. In order to avoid any confusion using the same abbreviation for different things, thesis does not always follow commonly used symbols and abbreviation. The list of symbols and abbreviation is attached.

The numerical analysis, modeling and drawing were performed in SIEMENS NX 10 software environment. Microsoft Excel 356 was used to provide all analytic calculations and graphs.

2 Hybrid vehicle

2.1 Introduction

A hybrid vehicle use two or more different sources of energy. We can also find one of the official definitions proposed by Technical Committee 69 of Electric Road Vehicles of the International Electrotechnical Commission.

Definition: *„ A hybrid road vehicle is one in which the propulsion energy during specified operational missions is available from two or more kinds or types of energy stores, sources, or converters, of which at least one store or converter must be on board.“* [1]

Different combinations of energy sources exist, for example, electric and mechanical energy sources or electric and chemical energy sources. However, the combination of fuel energy and electric energy sources has been found as the most acceptable, due to the combined usage of mature ICE techniques and well-established modern power electronics. The most widely used hybrid combination is a combustion engine and an electric motor in a different powertrain configuration.

The main reasons for development of hybrid vehicles are environmental pollution problem, a limited storage of oil and limited range capability of today's purely electric vehicle. The hybrid vehicle serves as a compromise or a solution of these issue. Especially as a short- term solution until the limitation and infra-structure problems of purely electric vehicles are solved.

The different types of sources of energy, energy carries and vehicles is shown on Figure 1. For conventinal vehicles (gasoline/diesel – powered) are typically rely on liquid fuel which is derived only from fossil fuel. Event thought that hybrid vehicles are considering as a short term solution, could play a vital role in a transisson from conventional vehicles to future vehicles which will use variety sources of energy based on renewable source of energy. [1]

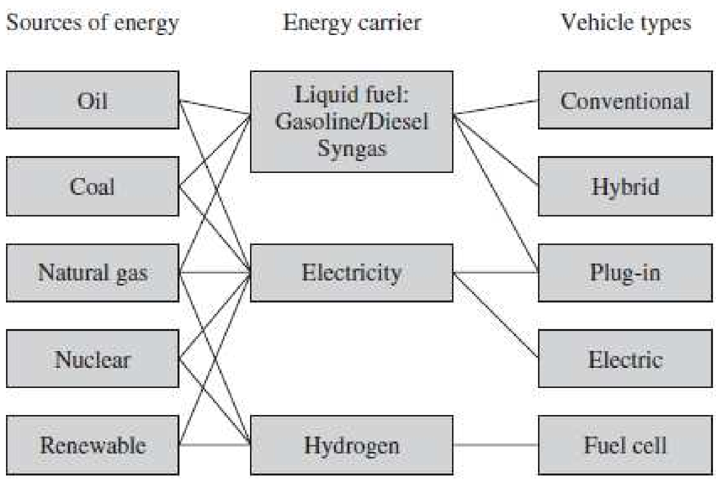

Figure 1 Different sources of energy, carriers and types of vehicle [1]

2.2 Engine type

In these days, many different engine types could be found. The main attention will be focused focus on a description of the most important of them.

2.2.1 Continuously outboard recharged electric vehicle

For this type of engine are necessary suitable infrastructure, permission and vehicles. Hybrid vehicle can be recharged while the user drives. For the vehicle is crucial to established the contact with an electrified rail, plate or overhead wire. The contact is established via an attached conduction wheel or similar mechanism. The vehicle is recharged on the highway using an attached mechanism and can be normally used on other roads without electrified rail, plate, wire using internal battery.

The main advantages are theoretical unrestricted highway range as long as you stay on electric infrastructure access, this mean reduction of the need of expensive battery system.

However, the problem is that such electrical infrastructure is old, is not widely distributed outside of cities and a private use of the existing electrical system is prohibited.[1,5]

2.2.2 Fluid power hybrid vehicle

Another subtype is thefluid power hybrid including Petro-air hybrid (hydraulic hybrid) and the Petro-hydraulic hybrid (pneumatic hybrid). These types of hybrid use an engine to charge a pressure accumulator to drive wheel through hydraulic or pneumatic drive units. Mostly the engine is detached from the final drive, similarly as a series HEV, serving just to charge the energy accumulator. The transmission is eliminated as well as the final drive. This concept allows regenerative braking to recover some of the supplied drive energy back

In recent years, there have been only a few car producers introducing the fluid power hybrid vehicle, but the concept from PSA Peugeot Citroen is a promising exception. This concept uses an 82-hp 1.2-liter gasoline engine which, provides most of the power driven via an epicyclic automatic transmission. While during deceleration, the energy of the wheel drives hydraulic pump that pushed hydraulic fluid into an accumulator and compresses the nitrogen gas within. The system works in the opposite way during the acceleration. The hydraulic motor connected to the transmission is driven by the hydraulic fluid. [8]

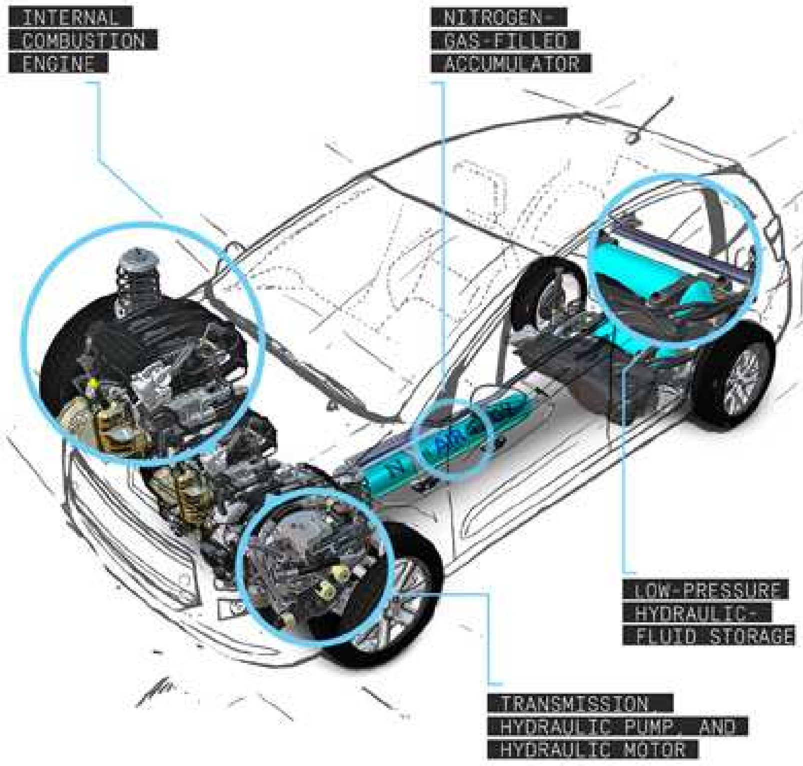

Figure 2. Hybrid Air car by PSA Peugoet Citroen [8]

2.2.3 Electric – human power hybrid vehicle

The special form of hybrid vehicle is electric- human power vehicles, including electric bicycles, scooters, and electric skateboards and so on.

2.2.4 Hybrid electric- petroleum vehicles

This is the most known hybrid type, usually called Hybrid Electric Vehicle (HEV). In most cases a petroleum –electric hybrid uses Internal Combustion Engine (ICE) and an electric motor as source of drive energy. The ICE can use a variety of fuel as natural gas, gasoline or diesel. The energy is stored in an electric battery set and in the fuel of the internal combustion engine. There are many types of petroleum – electric hybrid drivetrains from the Full-hybrid to the Micro hybrid, offering different advantages and disadvantages.

This thesis will be mainly focus on hybrid electric vehicles, because HEV is seen as one of the most promising means to improve the near-term sustainability.

2.3 Hybrid vehicle powertrain configuration

2.3.1 Series hybrid electric vehicle

The configuration of series HEV is shown on Figure 3. The main energy source is ICE, which converts the original energy in gasoline in to the mechanical power. Later, the mechanical output is converted to electricity using a generator. The final drive is provided by the electric motor using electricity generated by the generator or by a battery. The engine speed can be controlled independently of vehicle speed, because the engine is decoupled from the wheels. This provides operation of the engine at its optimum speed to achieve the best fuel economy. Besides, fuel economy it allows simplification of the control of the engine. Another big advantage is no need of a traditional mechanical transmission. Due to elimination of the transmission and the final drive, the efficiency of the vehicle can be increased. This configuration also provides capability of all-wheel drive. [1,5]

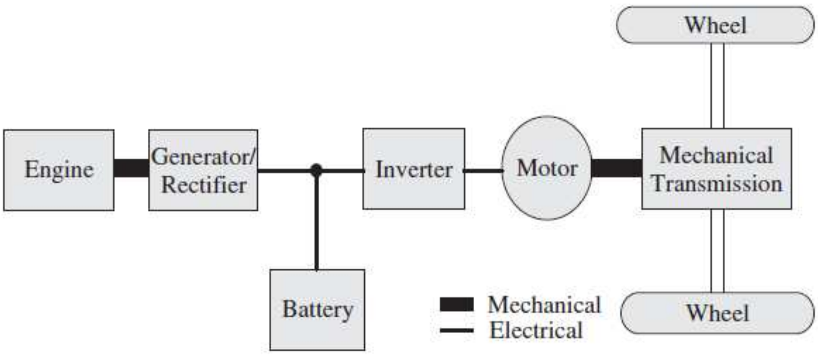

Figure 3 Series hybrid vehicle – configuration [5]

2.3.2 Parallel hybrid electric vehicle

The configuration of series HEV is shown on Figure 4. The electric motor and the ICE can both deliver power in parallel to the wheels, either in combined form or separately. The electric motor and the ICE are coupled to the final drive via a mechanisms such as clutch, belts, pulley and gears. The electric motor could be used in different modes for example as a generator to recover the kinetic energy during braking or absorbing a portion of power from the ICE or as a propulsion devices.

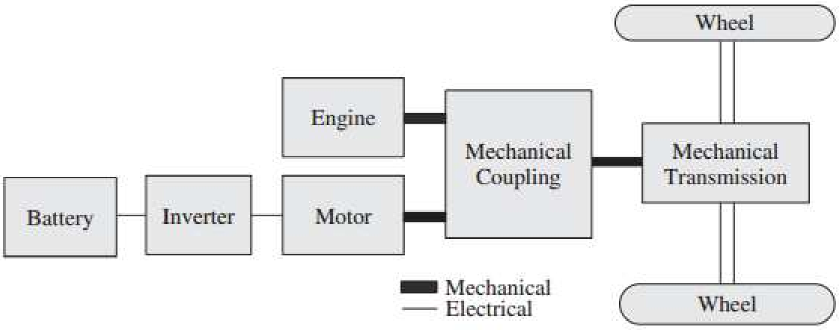

Figure 4. Parallel hybrid vehicle – configuration [5]

2.3.3 Series – Parallel hybrid electric vehicle

The configuration of series – Parallel HEV is shown on Figure 5. This configuration involves the features of both series and parallel hybrid electric vehicles. For that reason, it can be operated as a series or parallel. The main difference between a series HEV and the series – parallel HEV is a mechanical link between engine and the final drive. Therefore, the engine can drive the wheels directly. In comparison to a parallel HEV, the series- parallel HEV adds a second electric motor, which serves primary as a generator.

These features of series- parallel HEV increase efficiency and drivability, but due to increased components and complexity is more expensive than series or parallel HEV.

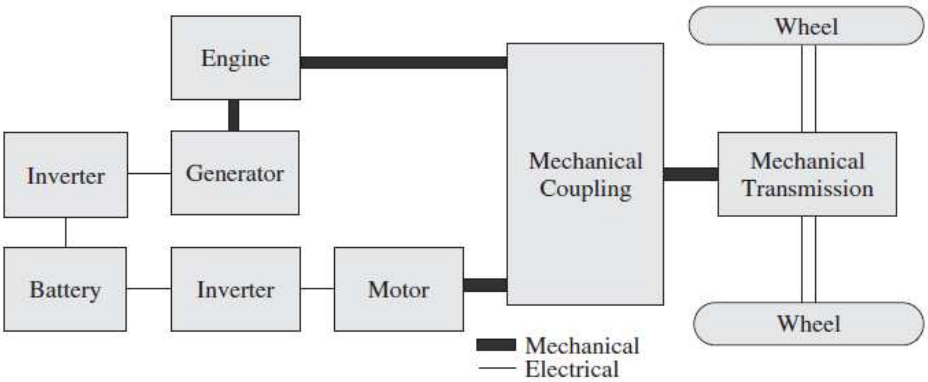

Figure 5. Series - Parallel hybrid electric vehicle – configuration [5]

2.3.4 Complex hybrid electric vehicle

The configuration of Complex HEV is shown on Figure 6. This configuration usually involves the use of a multiple electric motor and planetary gear systems. A typical example is a four-wheel drive system which is realized using separate drive axles. This system uses the generator to realize series operation such as control the engine operating condition in order to achieve maximum efficiency. Using of two electric motors increase performance in regenerating braking, vehicle stability control and antilock braking control. [1,5]

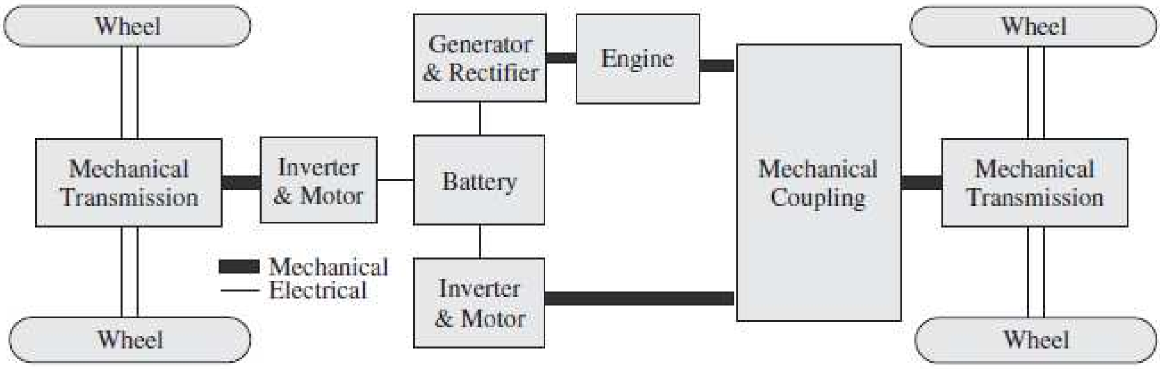

Figure 6 Complex hybrid electric vehicle – configuration [5]

2.3.5 Plug-in hybrid electric vehicle

The configuration of Plug-in hybrid vehicle is shown on Figure 7. In recent time, automotive industry has been focused on another subtype of HEV Plug- in hybrid vehicle. PHEVs are usually a general serial or parallel hybrid with increased energy storage capacity, mostly through a lithium- ion battery. The battery allows the hybrid vehicle to drive on electric mode distance that depends on the battery. PHEVs has been identified as one of the most promising means to improve the near-term sustainability of the transportation as well as stationary energy sectors. [6]

Generally, the only difference between the HEV and PHEV is related to the size of the battery and the charging process

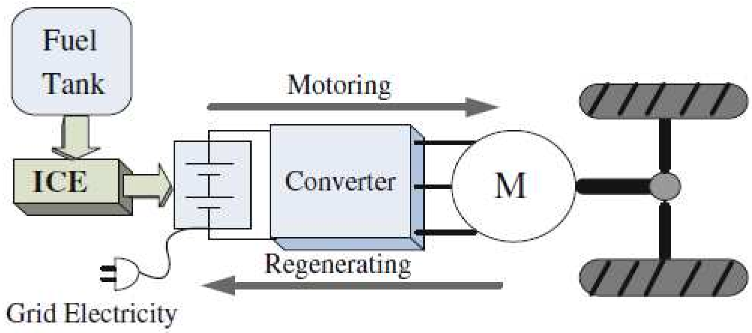

Figure 7 Plug - in hybrid vehicle – configuration [6]

3 Four – Stroke Combustion engine

3.1 Design and engineering principles

A four – stroke engine is an internal combustion engine in which the piston completed four separate strokes while turning a crankshaft. Typical four-stroke combustion engine is consist of four main design parts and accessories: [2]

- Engine housing - head , cylinder, crankshaft case, engine block, oil pan
- Crankshaft mechanism - piston, connection rod, crankshaft
- Valve train valves, valves springs, camshaft, rocker arm, rocker arm shaft, gears, timing belt
- Fuel system -carburetor, fuel injection, fuel pump
- Accessories -starter system, lubrication system, cooling system, exhaust system

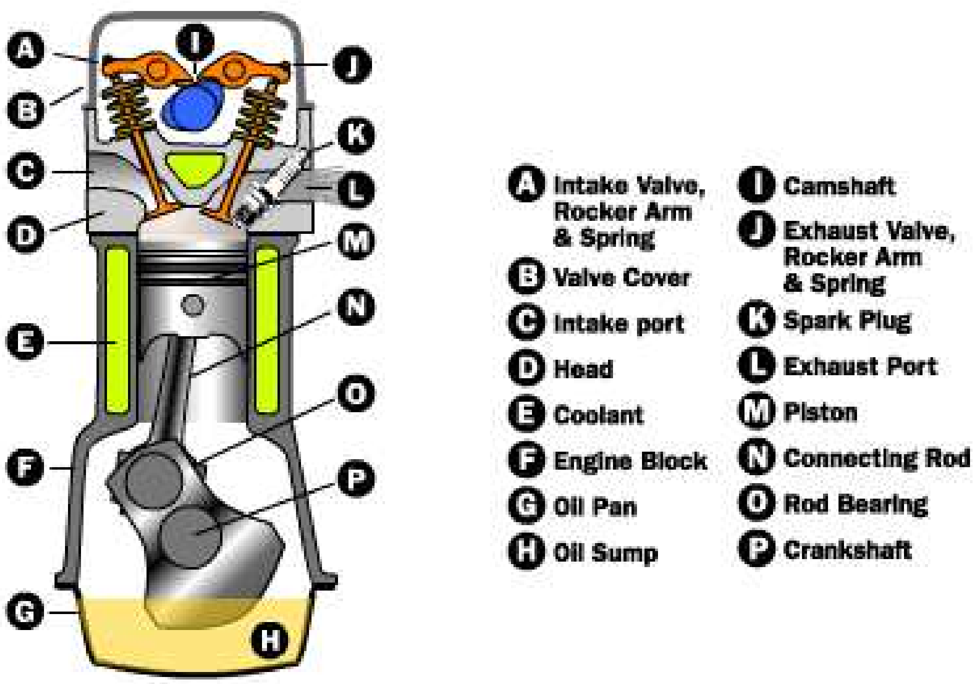

Figure 8. Four - stroke combustion engine – scheme [3]

A stroke refers to the full travel of the piston in the cylinder, in both direction. A whole cycle lasts two rotations of the crankshaft (720 degrees). The four separates strokes are termed [2]:

I. Intake

- The piston starts at Top Dead Center (T.D.C.) and ends at Bottom Dead Center (BDC). Due to the downward motion of the piston and open intake valve the piston pulls the air –fuel mixture into the cylinder by producing a negative pressure (-0,01 ÷-0,03 MPa). In order to the best filling process intake valve is opened at 45 degrees before T.D.C. and it is closed 35÷90 degrees after T.D.C. The exhaust valve is closed a whole stroke.

II. **Compression**

- The piston starts few degrees after B.D.C goes upward and compresses air-fuel mixture to 1/7÷1/20 of a normal volume. Piston ends at T.D.C Due to the compression, the temperature of the mixture is rising to 500 Celsius degree, and the final pressure is around 1,8MPa. After that, the mixture is prepared for the ignition. Both the intake and exhaust valves are closed during this stroke.

III. Power

- This is the start of the second revolution, while the piston is at T.D.C spark plug is activated and ignites the air – fuel mixture. However, due to time delay spark plug is activated 0-40 degrees before T.D.C The piston is forcefully returned to B.D.C. This stroke produces mechanical work.

IV. Exhaust

- The exhaust valve opens 40÷90 degree before B.D.C. The point at which the exhaust valve opens must be carefully chosen to ensure that as much gas as possible will escape. Due to a combination of pressure (0.5MPa) and piston’s upward movement exhaust gas is pushed from the cylinder.

A whole 4-stroke cycle is shown on Figure 9 with an explanation.

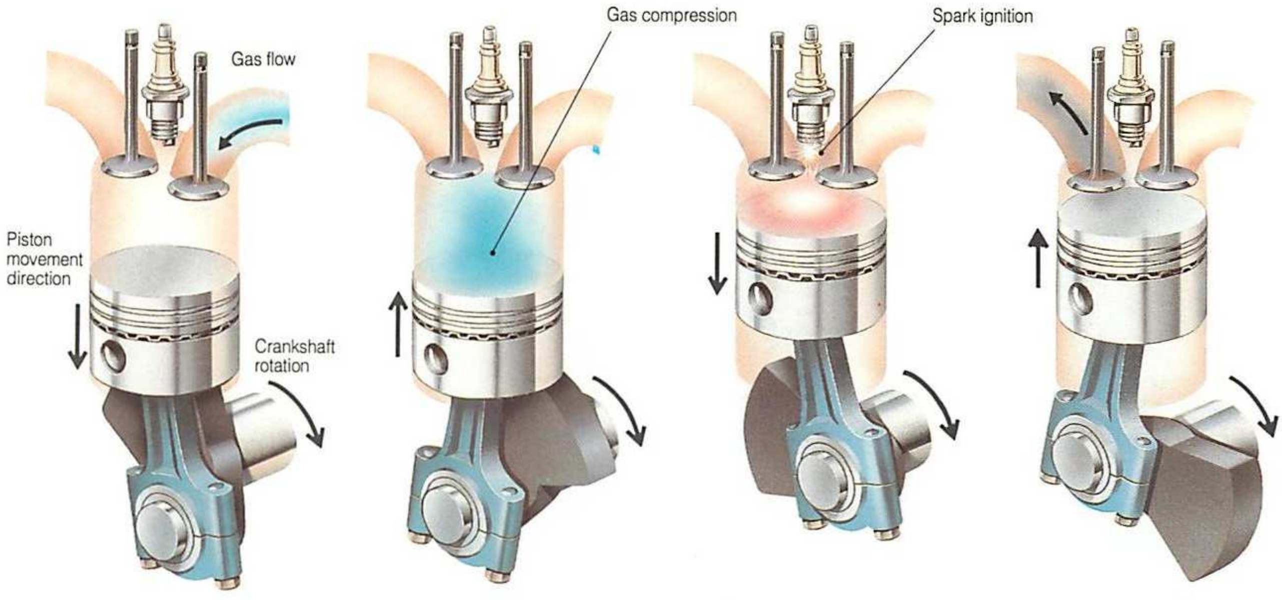

Figure 9. Four- stroke engine - a whole cycle [4]

3.2 Main parts of IC engine

3.2.1 Crankshaft

Figure 10 shows a crankshaft formed of a number of parts (section). The crankshaft is compound from main journals rotate in main bearings, and the crank pins (crank journals) that are fitted to the connection rod. Main journals are connected to the crank pin by the webs. Crankshafts are subjected to particularly heavy loads, so it is very important to focus on avoiding a sharp corner. It is necessary to formed fillets or radius between the journals and the webs. There are one-piece crankshaft of a buildup construction (the shaft is made in sections and assembled.)

Since the connection rod and piston are moving in a reciprocating way, the crankshaft is subjected to momentum forces, centrifugal forces which leads to torsion tension, bending tension and torsional vibration. This is the reason crankshaft's design play the vital role in the ICE construction.

When the engine is running the rotating parts must be balanced as effectively as possible to ensure that the parts will cause no vibration, or as little as possible. Mostly, webs are extended to improve balancing in order to form balance masses. It is impossible to balance completely the rotating parts of all types of engine. Balancing of the crankshaft will be more discuss in later chapter Engine balancing.

The rear end of the crankshaft is usually attached to the flywheel. It is necessary to provide perfectly secure attachment to avoid any vibration and other reasons for stress accumulation in the crankshaft. Thy flywheel should be assembly in one position only, partly because the flywheels is mostly marked on to indicate the position of the first crank pin. Another reason is that some imperfections of balance may arise which may cause vibration. This is the reason that the flywheel and the crankshaft must be balanced as an assembly. [2,10]

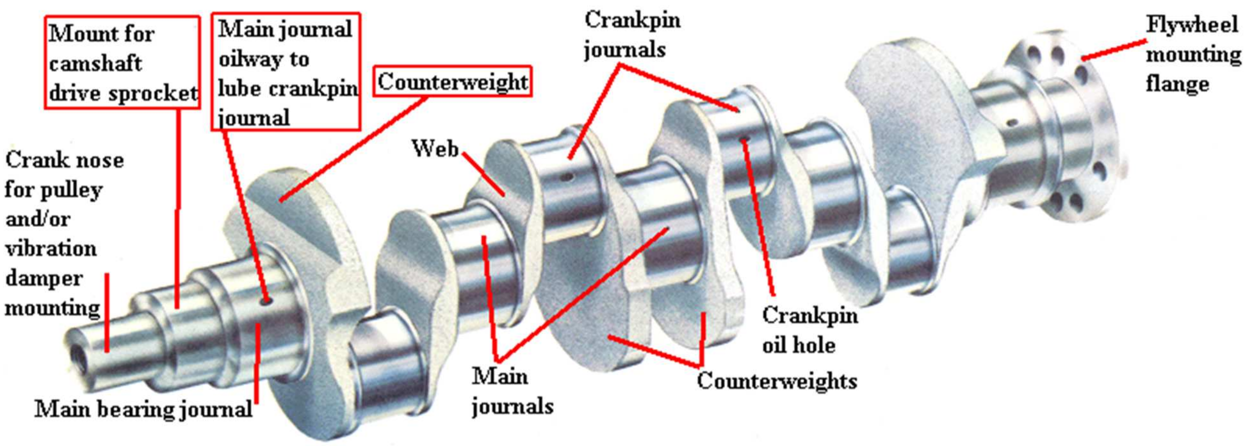

Figure 10 The terminology of a crankshaft [9]

The engine lubrication system delivers oil under pressure to the main bearings, where it is fed into the groove running around the bearing at about middle of its length. Mostly through the crankshaft is drilled set of holes running from the main journals, through the webs to the surface of the crank pins seen on Figure 11.

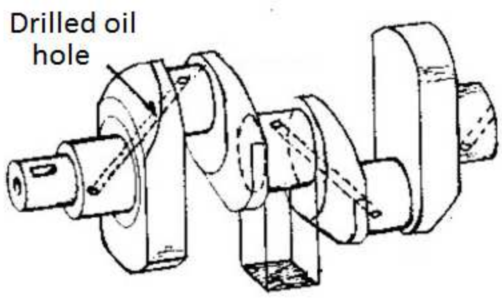

Figure 11. Oilways drilled through the crankshaft [11]

3.2.2 Connection rod

Figure 12 shows the terminology of a typical connection rod. Due to limitation of space inside the piston, the end which connects to the gudgeon pin is smaller than that which connects to the crankshaft. These ends are called the small end and the big end, as it shown on Figure 12. The load caused by gas pressure on the piston has buckling effect on the middle part of the rod. The middle part, which connects the small end and the big end, is generally made of H or I section, which gives better possible resistance to sideway buckling.

Usually the big end is split in two pieces, because usually the crankshaft is not in sections assembled and suitably fixed together, but it is made by one piece. This is the reason that the big-end is split across the center of the crank pin. Two halves are bolted by high- tensile steel bolts. The inside surface of the big-end is lined with a thin coating of a special bearing metal, which helps to provide suitable surface resistance for running on the steel crank pin.

Connection rods are usually made from steel forgings and it is accurately machined. In some cases, an aluminum alloys could be used. The connection rod is machined to reduce weight and polished to remove surface scratches that may lead to fatigue failure. [2]

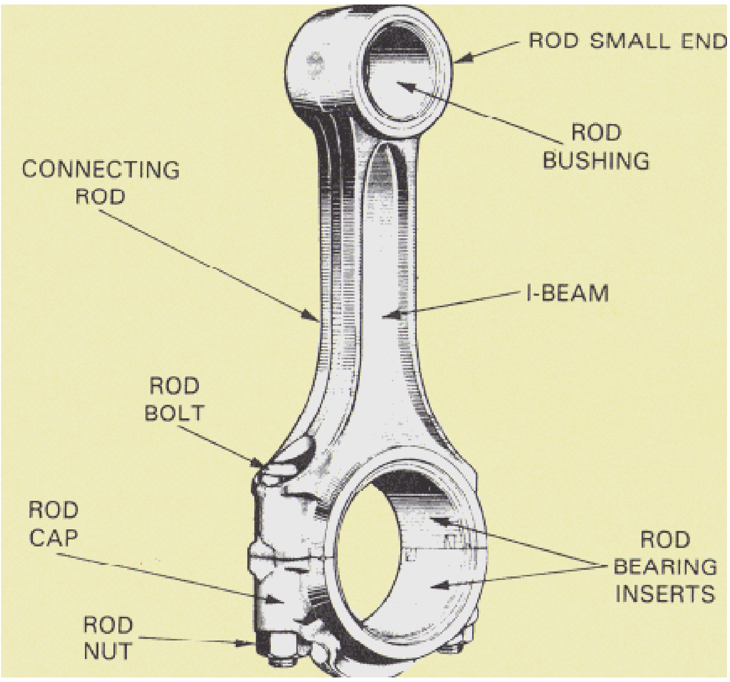

Figure 12 The terminology of a connection rod [12]

3.2.3 Piston, rings and piston pins

Figure 13 shows the main parts of the pistons assembly and the terminology. The piston head forms the upper surface on which the gas pressure acts. The pressure force is equal to the cross-sectional area of the cylinder head multiplied by the gas pressure. This force, acting along the center-line of the cylinder, is transmitted through the piston to the piston pin bosses and then trough the piston pin to the connection rod. The connecting operates at an angle to the center-line of the piston during the greater part of the strokes which causes side force of the piston applied on the cylinder wall. The skirt is bearing surface formed to provide contact surface on the piston to carry this side force. In order to move piston in the cylinder freely there must be some clearance. However, the clearance allows gas leak from the combustion chamber past the piston. To reduce leakage as much as possible the ring grooves are formed on the piston just below the piston head. These ring grooves divide the ring belt into three parts; the top land, second, land and third land. The top ring, the second ring and the oil ring are fitted into particular grooves. The pistons are made of cast iron, especially early engine, or aluminum. Both materials have advantages and disadvantages relate to the mechanical and physical properties. Generally aluminum alloys are mostly used because they combine a low coefficient of thermal expansion and a high yield strength.[2, 10]

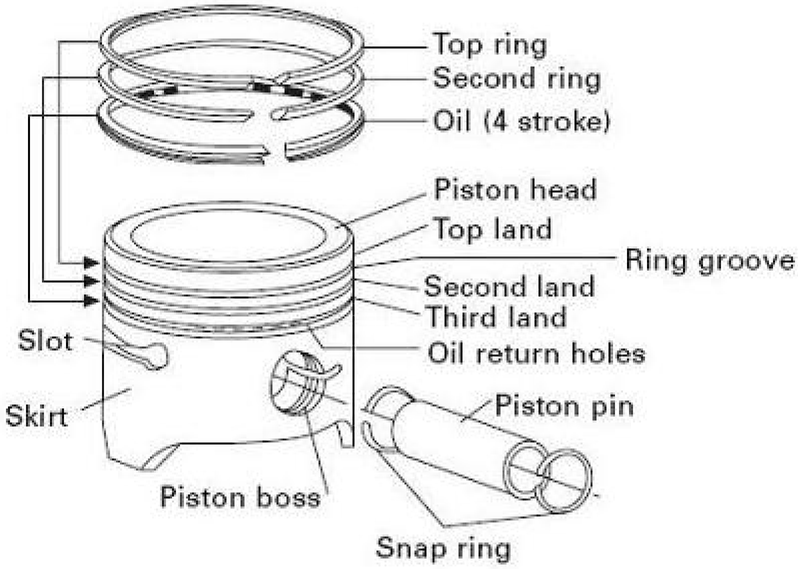

Figure 13 The terminology of a piston assembly [13]

The purpose of the piston rings , as it was mentioned earlier, is to prevent gas leakage througout the clearance that must be between the piston and the cylinder. However, the piston rings also control the oil film on the cylinder wall. This provides adequate lubrication without excessive quatnitites of oil getting along the pisotn and into the combustion chamber. This piston ring is called an oil-control or a scraper ring.

Piston pin carries the high loads imposed upon them by gas pressure through the piston thererore they are made of steel aloys. To provide a wear-resistance of the surface and case – hardened steel alloys with 3-4 per cent of nickel are used. It is necessary to avoid any contact between the ends of the piston pin and the cylinder wall that could lead to deep grooves in the cylinde surface. There are two types of piston pin; Semi-floating (securely fixed int either the piston or the connection rod) and Fully floating (free to turn in both the piston and the connection rod).

3.2.4 Engine block and crankcase

Figure 14 shows a four cylinder engine assembly including engine block, crankcase and other parts. Nowadays almost universal structure is a monoblock construction. This arrangement has all the cylinders of an engine in one casting. Main advantages of this construction are providing the great rigidity, reducing machining and assembly operations to the minimum. The main disadvantage is that the construction is heavy and large structure that could lead to handle problems. Older constructions of an engine had usually cylinders made with integral cylinder head, later when the monoblock construction was developed there were advantages in making all the cylinder heads in a single separate casting. This cylinder head is attached to the cylinder block by screws or studs and nuts. However, it is difficult to obtain a gas- and water tight joint between the head and the block. Nevertheless the adoption of the monoblock construction makes the detachable the cylinder head a necessity, and this is now the common practice. [2,10]

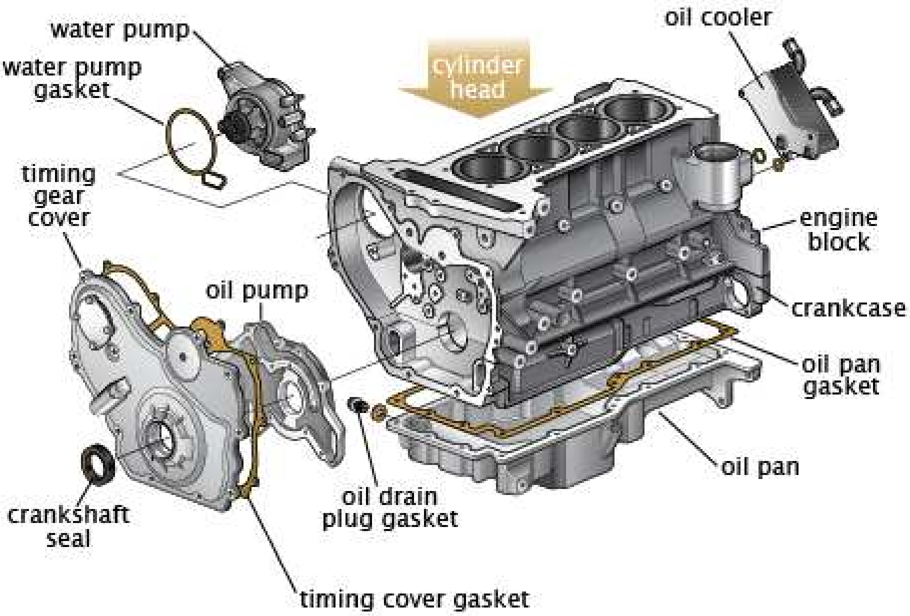

Figure 14 Engine assembly [12]

The crankcase carries the crankshaft main bearings in webs, which lie transversely across the crankcase. These webs form the front wall, rear wall and stiffen the structure besides acting as supports for the main bearings. These main bearing are typically split across their diameters to allow assembly of the crankshaft. If lower faces of the block is level with the center of the main bearings then is easier the machining operation of the block.

The oil pan, which typically collects the supply of oil used of lubrication the engine, is attached to lower part of the crankcase by screws or bolts and nuts. A cork gasket is commonly install between oil pan and the crankcase to help to make the joint oil-tight.

The cylinder block and the cylinder head are usually made of cast iron. However, in some cases aluminum alloys are preferred, giving lots of advantages. Aluminum alloys reduce weight, improve heat conductivity, which later results in lower and more uniform temperatures of combustion chamber walls. This also allows higher compression ration compare with a cast iron head. [2,10]

4 Turbochargers

4.1 Introduction

Turbosupercharger also known as a turbocharger or only turbo. The turbo is an exhaust gas turbine driven by centrifugal supercharger. In a piston engine, approximately 2/3rds of the heat generated in combustion is normally wasted. The advantage of turbocharging is obvious - instead of wasting thermal energy through exhaust, we can make use of such energy to increase engine power. A turbocharger places a small radial inflow turbine in the exhaust gas stream to recapture a portion of that energy, and use it to supercharge the engine. The turbine is driven at extremely high speeds (300 000 rpm) by the exhaust energy, and a shaft transmits this rotation to a centrifugal compressor, which is used to boost the engine. The centrifugal compressor pump fresh air into the combustion chambers at a pressure higher than normal atmosphere, a small capacity engine can deliver power comparable with much bigger opponents. [14,16,17,18]

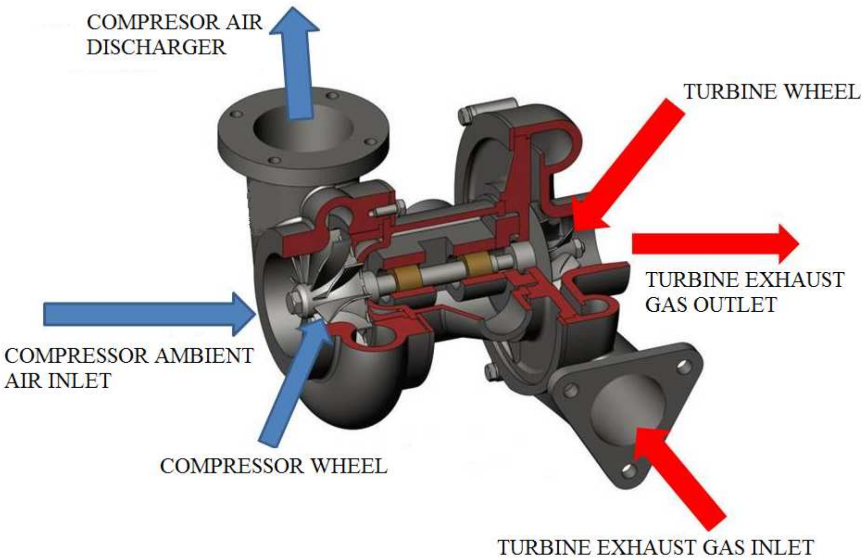

Figure 15 Scheme of a turbocharger

As turbochargers are able to increase the volumetric efficiency make turbochargers a key enabler of phenomena called downsizing, perhaps the most important automotive trend of the modern era. [19]

Downsizing is the reduction the volume of the engine chambers. For example we could substitute large V8 naturally aspirated engine with turbocharged V6 or we could replace non-turbo V6 with boosted 4 cylinders, whilst maintain a similar levers of torque and engine power as we can see on Figure 16.

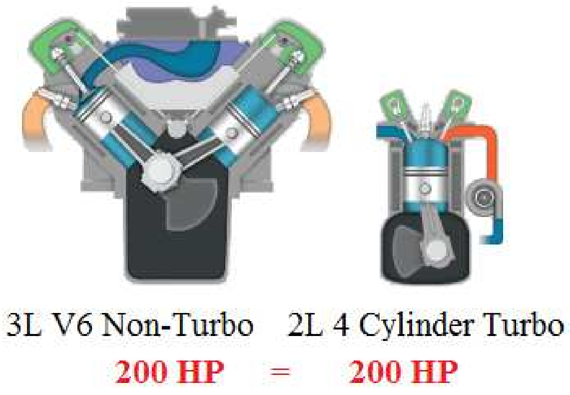

Figure 16 Turbocharger helps a smaller engine to perform like a bigger engine [15]

There are more additional advantages beside better efficiency such as quicker engine warm-up, reducing cold-start emissions, lower weight, better acceleration, handling and braking although fuel consumption is not necessarily better.

We can expect big impact of turbo over the next 10 years. That will include a reduction of average engine displacement in the US from 3.6L to 3.0L. In Europe, 4 cylinders will remain the architecture of choice, but reducing from an average 1.7L to 1.5L or smaller. China – where the turbo experience is more recent will see a downsizing of a similar magnitude. Figure 17 shows most probably development in a future. [15]

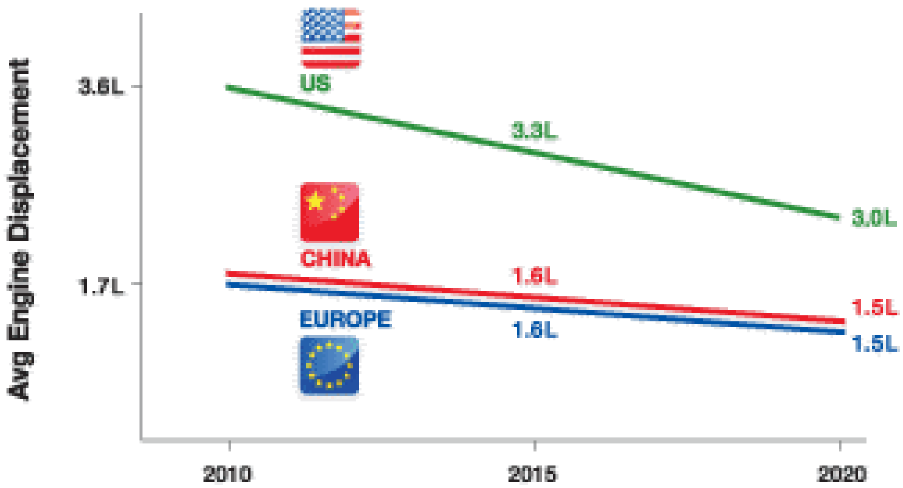

Figure 17 Turbo characteristics will increasingly support an automotive industry downsizing focused on meeting fuel efficiency targets whilst maintaining impressive drive ability [15]

5 Engine passive resistance

5.1 General overview

Several kinds of mechanical losses are present in every engine. The friction or mechanical losses of an engine include bearing friction, piston and piston ring friction, pumping losses caused by water pumps, lubrication pumps, and scavenging air blowers, power required to propel valves. Friction losses can be kept to a minimum by maintain the engine in its best mechanical conditions, but they cannot be eliminated. Lubrication and cooling systems must be at highest operating efficiency to minimize friction of bearings, pistons and piston rings etc. [20] Table 1 shows engine losses.

Losses	Gasoline engine [%]	Diesel engine [%]
Piston and piston ring friction	45	50
Bearing friction	23	24
Cylinder charge replacement	20	14
Power required auxiliary componetns	6	6
Power required to propel valves	6	6

Table 1 Engine losses (Gasoline, Diesel) [20]

In ICE engine piston ring friction losses account for approximately 45 % of total losses as shows Table 1. A reduction in piston ring friction can be obtained by improving friction surfaces and improving lubrication system.

The piston with the piston rings and bearing surface is highly complex tribological systems. To be able to provide wear resistance, it is necessary to build up a hydrodynamics lubrication film. It is vital that the oil film must be higher than the surface roughness of two contact surfaces. For piston rings, the oil film must be built up dynamically as an oil wedge. However, when the relative speed of contact surfaces is zero, the oil wedge always collapses. This occurs for piston rings at top and bottom dead centers. Therefore, it is important to ensure that sufficient oil-retaining volume can be maintained in the contact surfaces. [1,20,21]

Modern engine ring surface can be modified using variation coatings. Special coatings of metallic or ceramic material can be applied to the ring faces of piston rings to increase durability and to minimize friction. The most common for this purpose is chromium coatings. Few experiments study used laser modification of the piston rings. [22]

6 Concept of engine

6.1 General design strategy

The designed engine is developed as a part of a propulsion unit for series Hybrid Electric vehicle. Figure 18 shows scheme of the vehicle configuration. More precisely, it will be a part of Plug-in hybrid electric vehicle with increased energy storage capacity. Using the advantages of both series and plug-in HEV. The engine speed will be controlled independently of vehicle speed. This provides operation of the engine at its optimum speed to achieve the best fuel economy. Thanks to this configuration, it also provides capability of all wheel-drive of a vehicle.

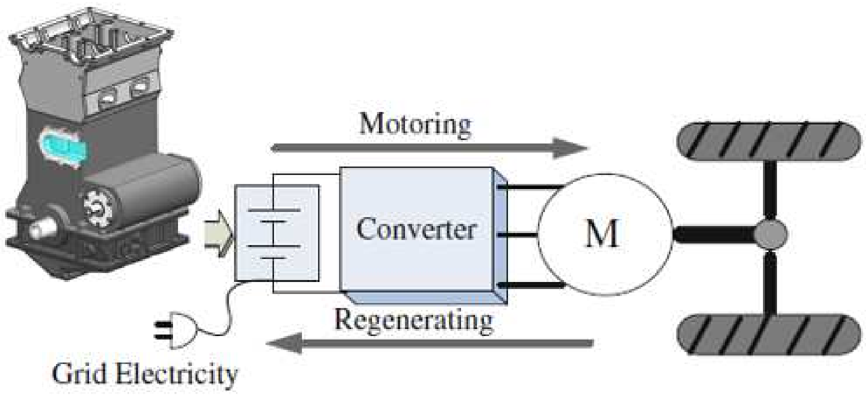

Figure 18 Scheme of the designed configuration of the hybrid vehicle

The conceptual design of the engine did not consider surrounding of the engine, because the conceptual design would be too complex for the thesis.

The conceptual design engine is designed with several pre-defined attributes:

- Cylinder arrangement In – line two cylinder engine
- Crankshaft configuration 360 (Figure 19)
- Cooling Air/ water-cooled system
- Lubrication Forced – feed lubrication system (wet – sump system)
- Valve- timing design Double overhead camshaft
- Valves per cylinder 4

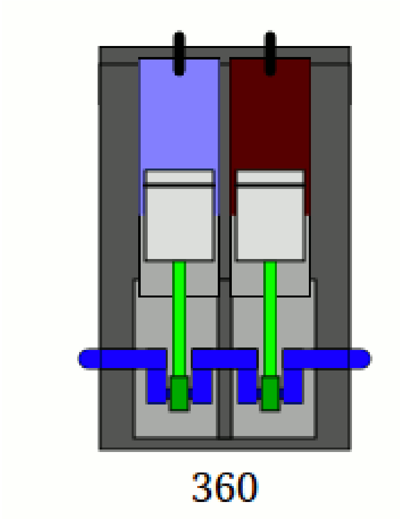

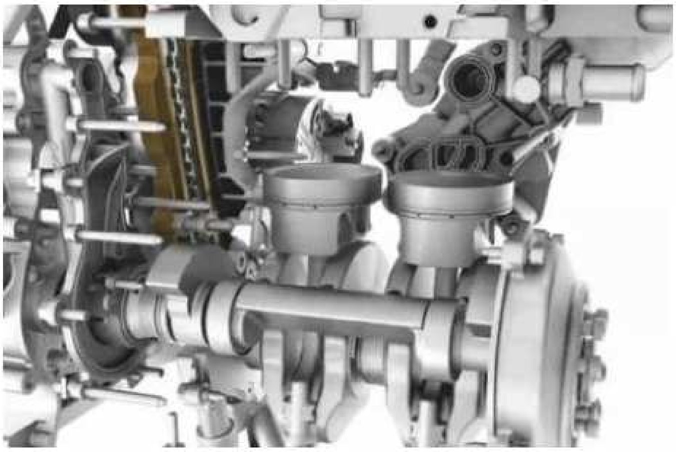

Figure 19 Crankshaft configurations of the engine [23,24]

The scheme of conceptual engine is in Figure 20. This schematic figure show all parts of the engine and connection between them. Not all of them will be designed and modeled in following chapters.

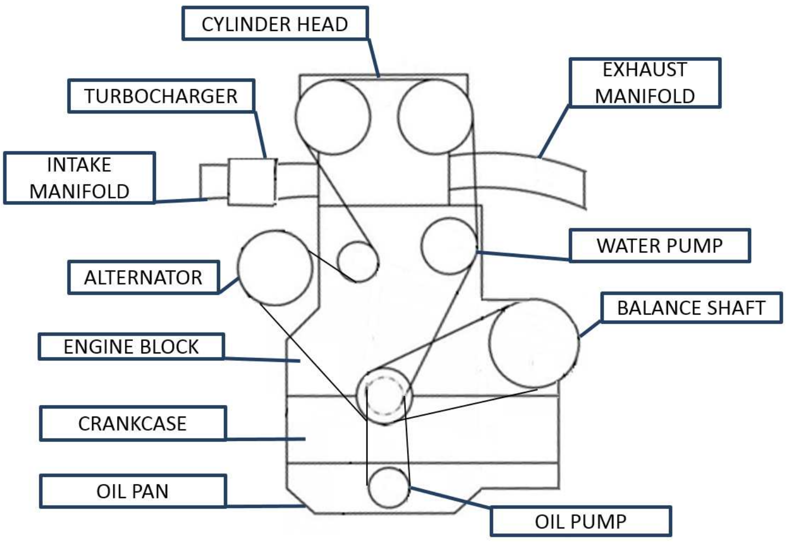

Figure 20 Scheme of conceptual engine

6.2 Strategy and scheme of lubrication system

The main function of the lubrication system is to lubricate the tribologically critical pairings of the crankshaft drive, the cylinder head and other components. The oil supply serves other functions as removing local contaminants, combustion residues and wear particle, which are filtered out in the oil-filter unit. Further functions include the dissipation of heat in areas subjected the thermal load, such as the friction bearing in the crankshaft drive and damping of vibration in bearings.[21]

The system of forced-feed lubrication with wet sump was chosen as the most suitable for designed concept of the engine. Figure 21 shows typical force-feed lubrication system. Oil pump delivers a defined volumetric flow from the oil sump through an oil-filter unit to all bearing surfaces in the engine while sliding parts are lubricated by splash lubrication systems and oil mist. After flowing through the bearing surfaces and sliding parts the engine oil is forced by the gravity back into the oil sump and into the oil pan located underneath the crankcase. The direct supply of oil by the oil pump and the rotational motion of the crankshaft effect a fine condition of the required oil mist.[1,21]

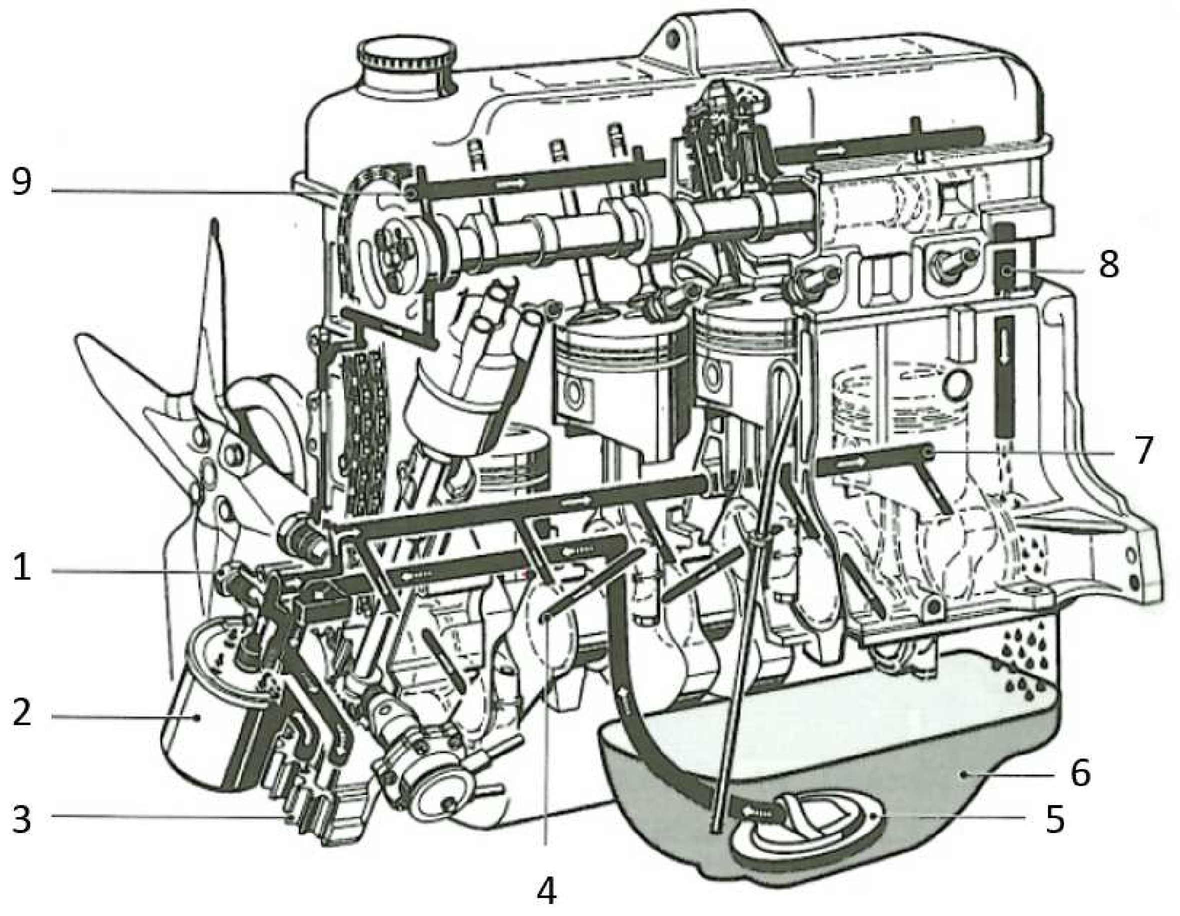

Figure 21 Force-feed lubrication system (1 Pressure – relief valve, 2 Oil filter, 3 Gear pump, 4 From main bearing to connection- rod bearing, 5 intake bell housing with strainer, 6 oil pan, 7 main oil feed line to crankshaft bearings, 8 return flow from timing case to crankcase, 9 To camshaft bearings [21]

Since a trochoid oil pump is the most common used in this application, this type of oil pump was also chosen as the most appropriate in the designed concept.

Figure 22 to Figure 24 show part of the lubrication system of the designed engine (orange part of the figure). It consists of sets of the drilled feedholes in the engine block, cylinder head and in the crankshaft. The sets are also called an oil gallery. The figures also show the sliding bearings which are supplied with the oil.

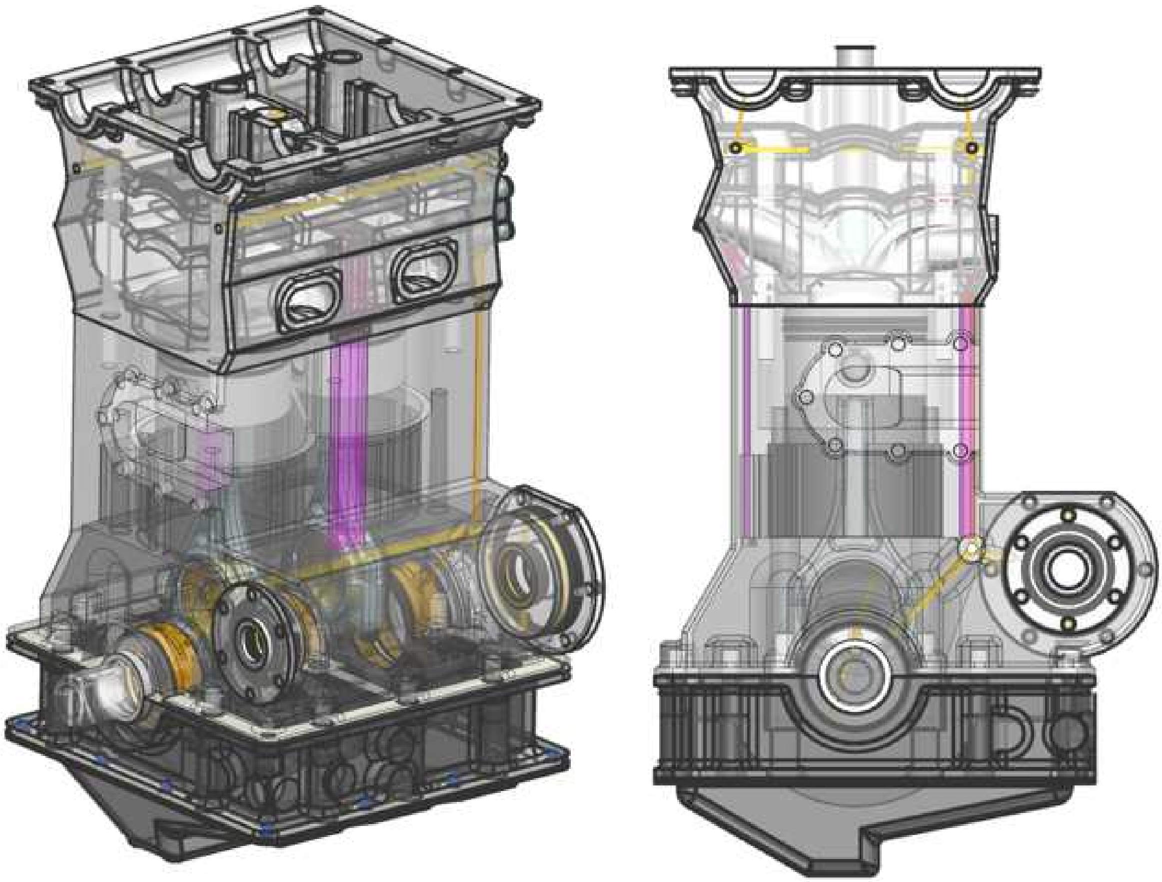

Figure 22 Designed lubrication system - (orange - feedholes, purple- return lines)

The purple channels in the cylinder head and the engine block are the return lines for used oil. (Figure 22 to Figure 24)

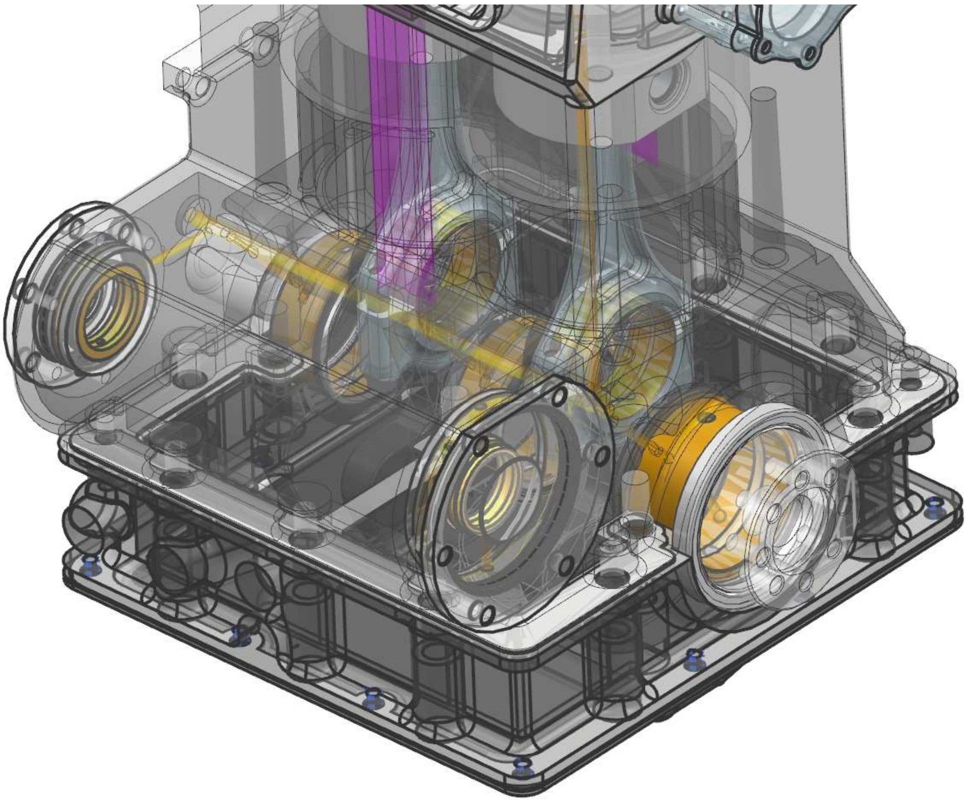

Figure 23 Detail of designed lubrication system - (orange - feedholes, purple- return lines)

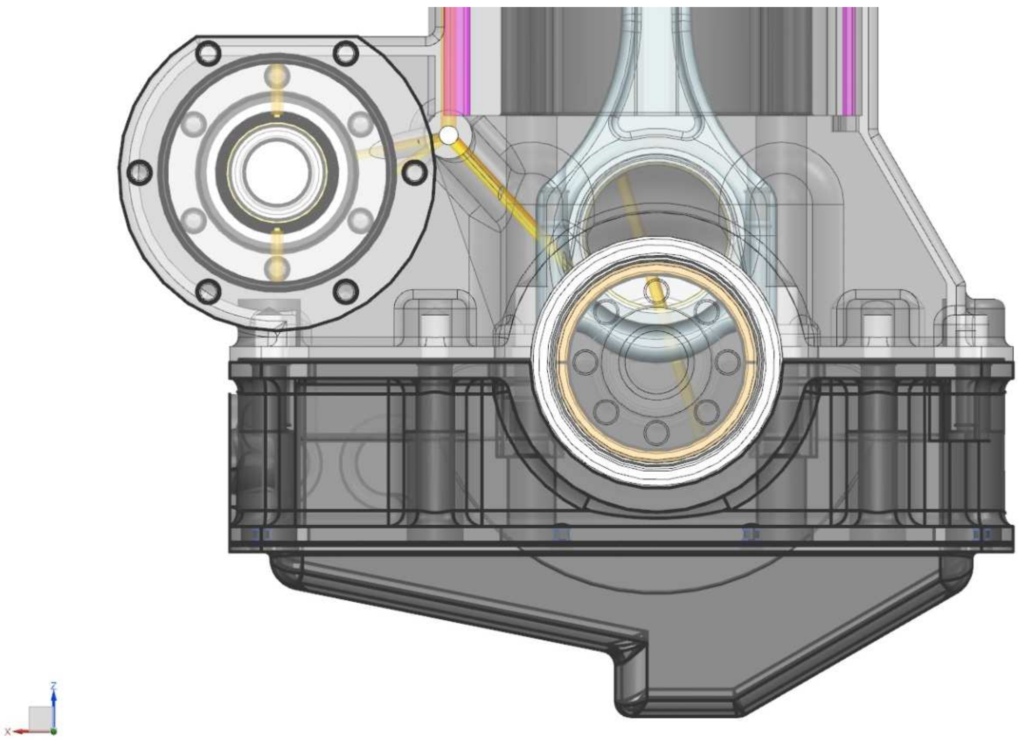

Figure 24 Detail of designed lubrication system - (orange - feedholes, purple- return lines)

6.3 Strategy and scheme of cooling system

In order to avoid thermal overload, combustion of the lubrication oil on the piston's is sliding surface, and to avoid uncontrolled combustion due to high component temperatures, the components neighboring the combustion chamber are intensively cooled. As water has a high specific heat capacity and provides efficient thermal transition between the materials, the designed engine will be water-cooled. More precisely Air/water recirculation cooling system is used in the design concept. It compromises a closed circuit allowing the use of anticorrosion and anti-freezing additives. The coolant is pumped through the engine and through an air/water radiator. The cooling air flows through the radiator in response to vehicle movement and is forced through it by a fan. A thermostatic valve (placed in the cylinder head) regulates the coolant temperatures. Figure 25 shows typical water cooling system with coolant circuit.

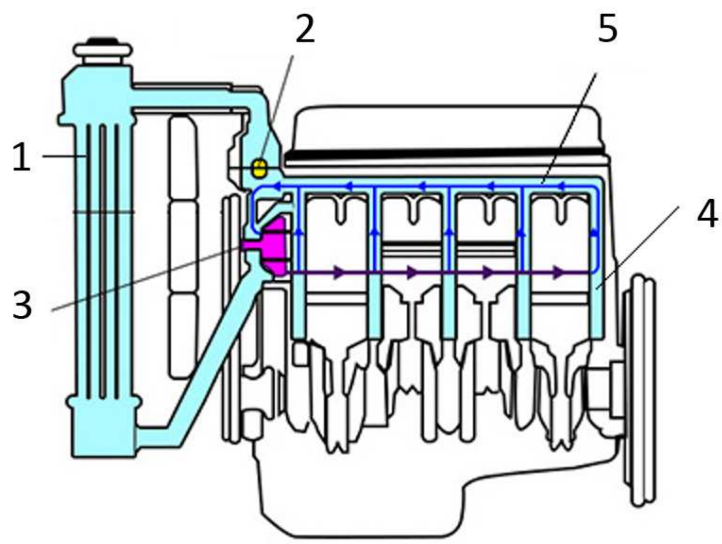

Figure 25 Water cooling system with coolant circuit –

(1- Radiator, 2- Thermostat, 3- Water pump, 4 – Coolant passages in cylinder block, 5- Coolant passage in cylinder head) [25]

Figure 26 and Figure 27 show part of the cooling system of the designed concept.(blue parts of the figures). The outer surfaced of the cylinder and cylinder head are enclosed in a jacket, leaving a space between cylinder and jacket through which coolant is circulated. During its passage through the jacket, the water absorbs heat from the cylinder and cylinder head later, it is cooled by being passed through a radiator (not shown in the figures).

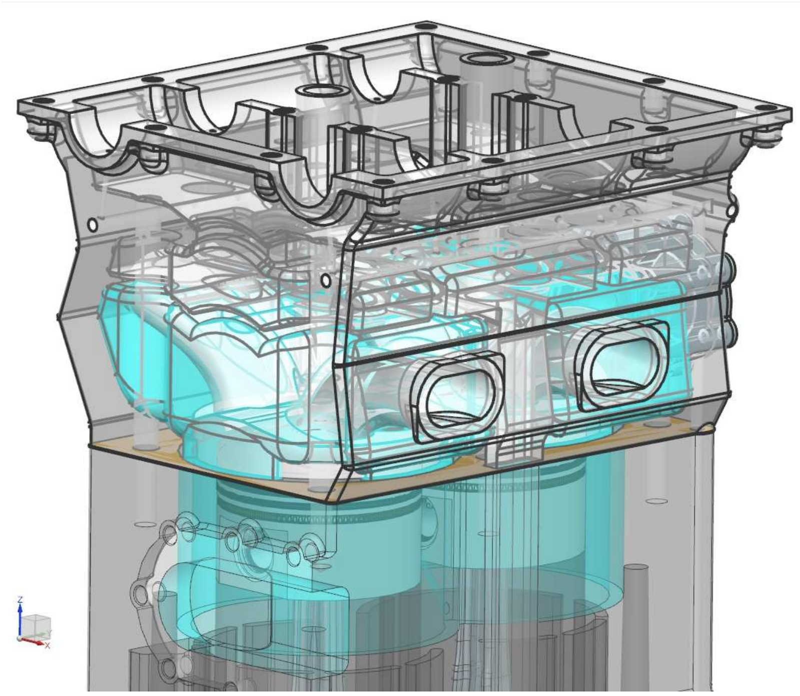

Figure 26 Designed cooling system (blue part)

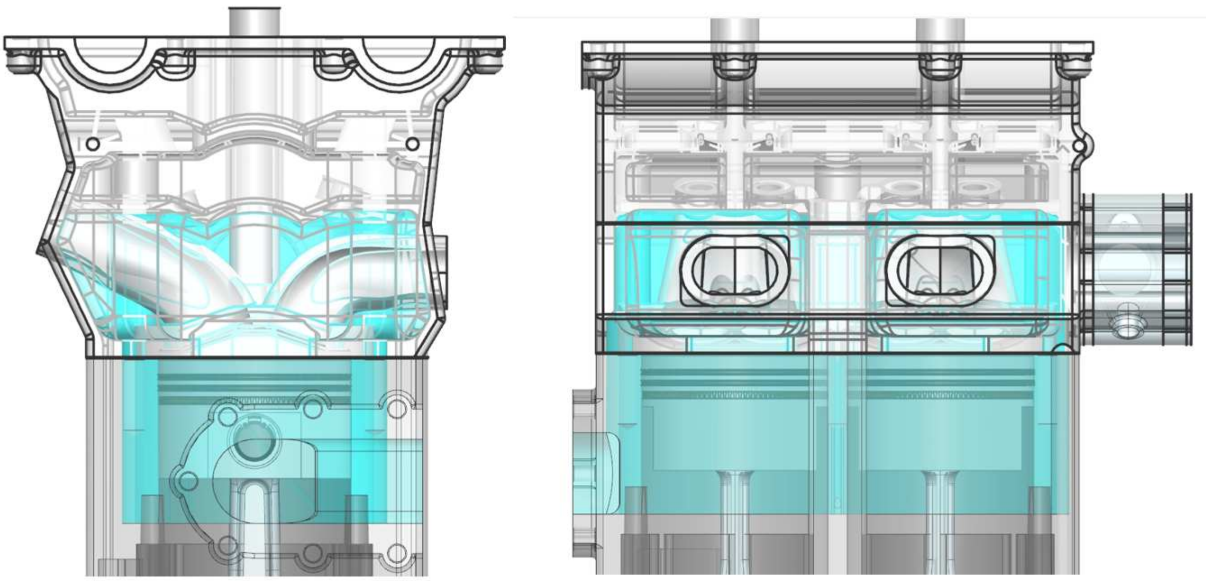

Figure 27 Designed cooling system (blue part)

7 Modeling and design

7.1 Engine layout

The construction of the engine is based on the given parameters. This specification (Table 2) was used to calculate pressure related to crank angle at different engine speed. This data were essential for modeling and design parts of the combustion engine. This chapter is composed of a few subsections provide briefly overview of process modeling. The description of the process modeling isn’t exhaustive due to complexity of each part. This is the reason that some parts are simplified just to show geometry. The purpose of this chapter is to show the basic steps in modeling of the main parts of ICE.

CAD software Siemens NX 10 was used to model all parts.

Specifications	Value
Fuel	Gasoline/CNG
Strokes	4
Engine Type	V2
Displacement	0.9 L
Valves/Cylinder	4
Bore	80.5 mm
Stroke	80 mm
Connecting Rod Length	133.55 mm
Compression Ratio	10
Intake Valve Max. Lift	8.9 mm
Exhaust Valve Max. Lift	8.9 mm
Intake Valve Diameter	29.8 mm
Exhaust Valve Diameter	25.4 mm

Table 2 Engine specification

Figure 28 shows exploded view of conceptual design of the engine. The next chapters describe the design some of the parts.

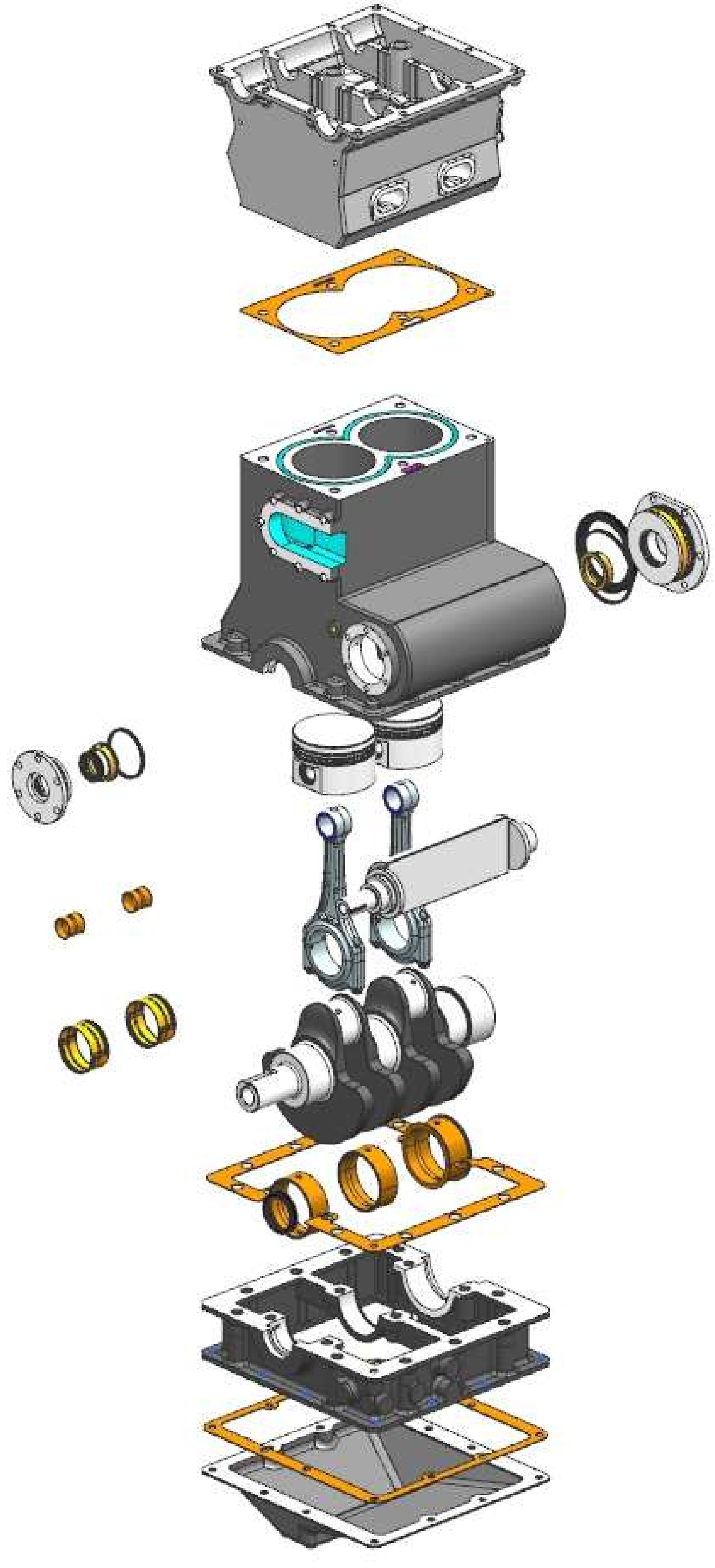

Figure 28 Conceptual design of the engine - exploded view

7.2 Engine block, crankcase and oil pan

Figure 29 shows the engine block, crankcase and oil pan and other parts. The engine block is designed as a monobloc construction. An open-deck construction is used. Since the engine block is designed as aluminum alloy casting, it is necessary to used special coating. The coating called Nikasil was chosen for this application. The weight of the engine block is 8.2kg.

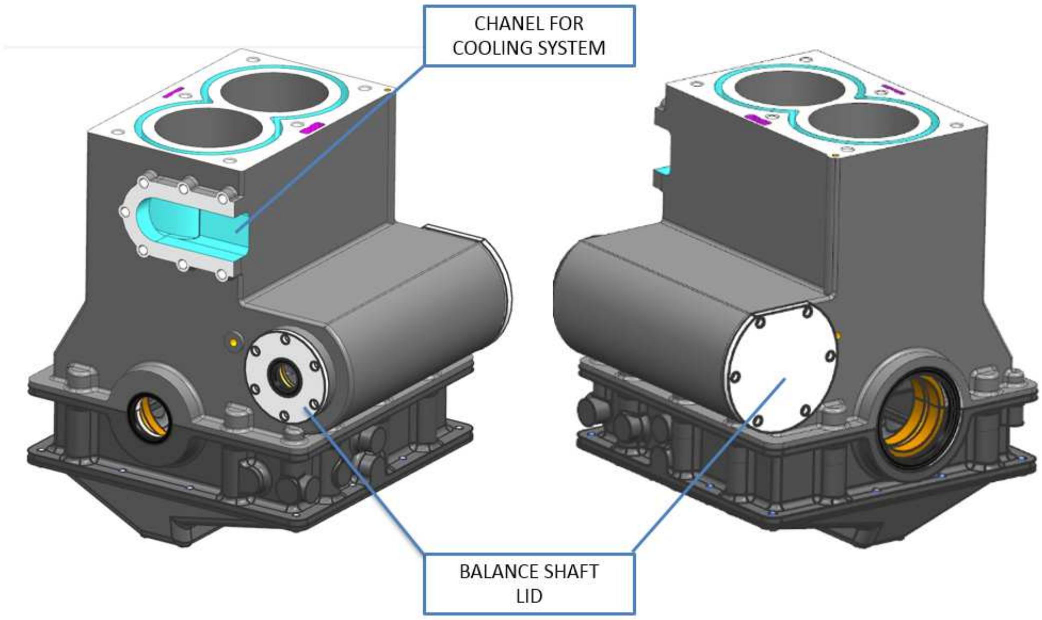

Figure 29 Engine block assembly

The main function of a crankcase and an engine block is to carry crankshaft main bearings. The main bearings are located in webs that lie transversely across the crankcase and the engine block (Figure 30).The webs form the front wall, rear wall the structure. Lower face of the block is level with the center of the main bearing, which helps to simplify the machining of the block. The Figure 29 shows the position of the balance shaft, which is placed into the pair of lids. These lids are bolted to the engine block by 6 screws. Figure 29 shows designed channels for water cooling system where the water pump will be mounted by several screws.

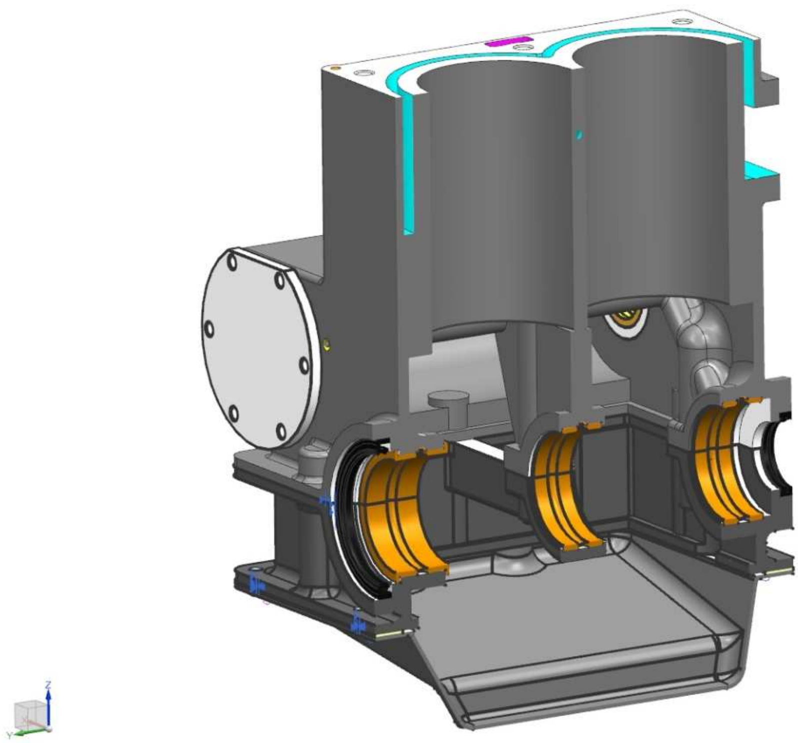

Figure 30 Cross-sectional of the engine block

Figure 30 shows cross-sectional of the engine block. The crankcase is bolted to the engine block by 14 high-strength M12 screws. The crankcase should be possible to assembly in one position only; therefore, a pair of alignment pins is used. The pins are positioned diagonally in order to assembly the crankcase in proper position. (Figure 31).

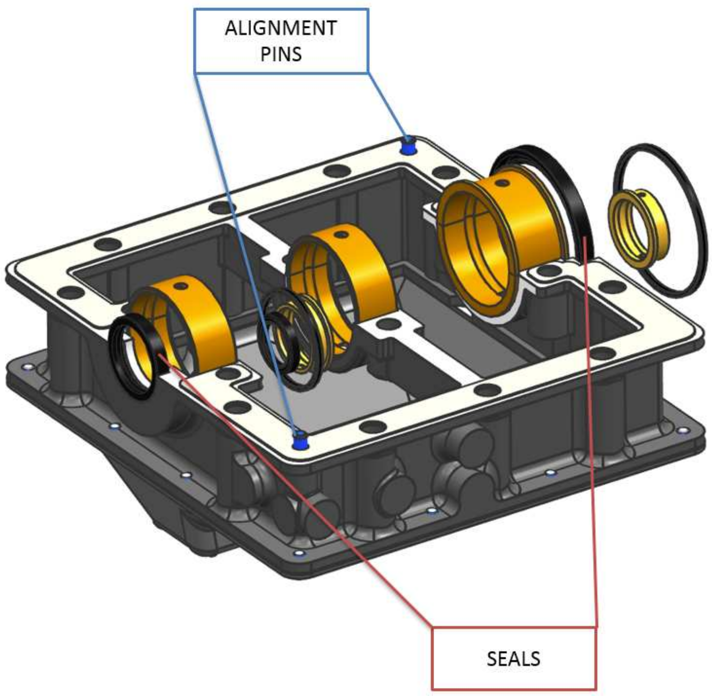

Figure 31 Crankcase with bearings and alignment pins

Lip-type seals are used at both ends of the crankshaft and the balance shaft (Figure 31, Figure 32). This type of seal was selected because it is finding increasing use for this application and they are replacing both the scroll and flinger ring. The seals are press fit in the proper position after assembling of the crankcase and the engine block.

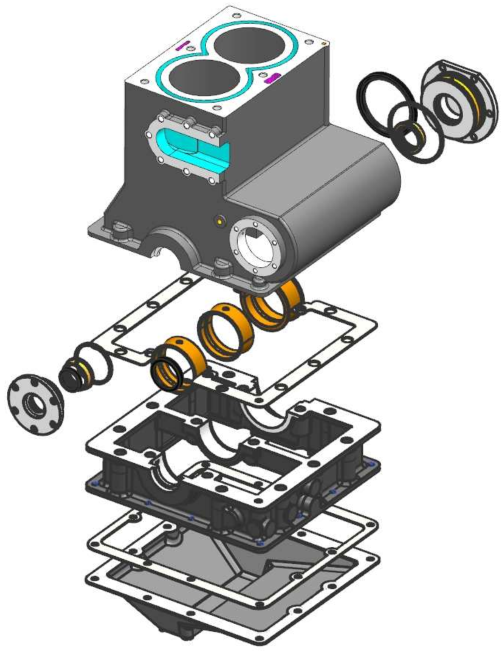

Figure 32 Engine block assembly - exploded view

The designed oil pan, which the main purpose is to collect the supply of oil used of lubrication the engine, is attached to lower part of the crankcase by 12 screws (Figure 33). To make the joint oil-tight the cork gasket is installed between the oil pan and the crankcase. The oil pan is made as a steel pressing.

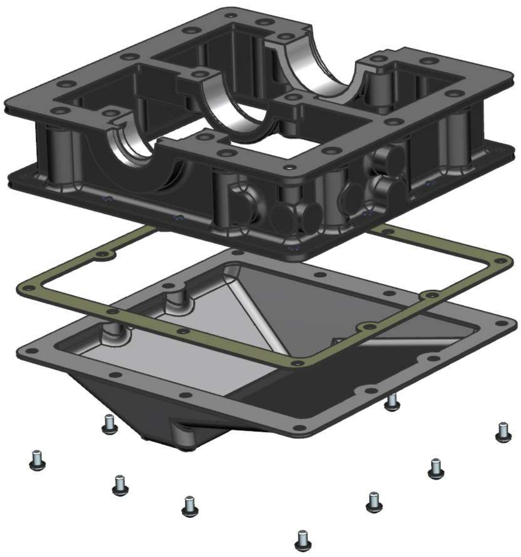

Figure 33 Oil pan and crankcase - exploded view

7.3 Cylinder head

This chapter is focusing on the basic design of a cylinder head. The main functions of the cylinder head are to supply the cylinder with fresh mixture and to discharge the exhaust gas. The cylinder head also absorb the cylinder pressure force. Together with the piston, it also provides the desired combustion chamber shape. In this case, it provides mounting for the entire valve system

The cylinder head is bolted to the engine block by 6 high-strength bolts M10, adjacent cylinders sharing two bolts. The purpose of this, in particular, is to distribute as evenly as possible the pressure force of the cylinder-head gasket. The cylinder head gasket is located between the engine block and the cylinder. Multi layers steel is used as a material for the gasket.

Based on the gas-exchange concept the cylinder head is designed as a crossflow cylinder head. It means that intake and exhaust passage are located on opposite side of the engine.

The cylinder head is cast of aluminum alloy using the lost foam technology.

Valve – timing design significantly affects the concept design of the cylinder head. Double overhead camshaft (DOHC) system was chosen as the most suitable way to control the exchange of gasses in the engine. Therefore, two camshafts are supposed to be located in the cylinder head. This thesis is mainly focusing only on the basic concept of the cylinder head and other parts of the engine. Valve –gear assembly is not design due to lack of time.

Design and production of the cylinder head is the most difficult part of the engine assembly. Generally, the cylinder head is subjected to very height loads. Frequently varying temperatures and the accompanying expansions give rise to stresses, which can only be absorbed by appropriated design

The process design of the cylinder head consists of several steps: The next subchapters describe all of the steps.

7.3.1 Skeleton

Modeling of the cylinder head is very complicated and difficult. It is vital to think over all parts of the cylinder head in advance to reduce number of amendments. Any intervention has heavy impact on the complex model. This is the reason that is necessary to use skeleton. It is group of points, lines, axis, planes and surfaces. These components define the important parts of the cylinder head. Using the skeleton, it is easier to itemize angle of valves, design intake and exhaust ports. The skeleton of the designed cylinder head is in Figure 34.

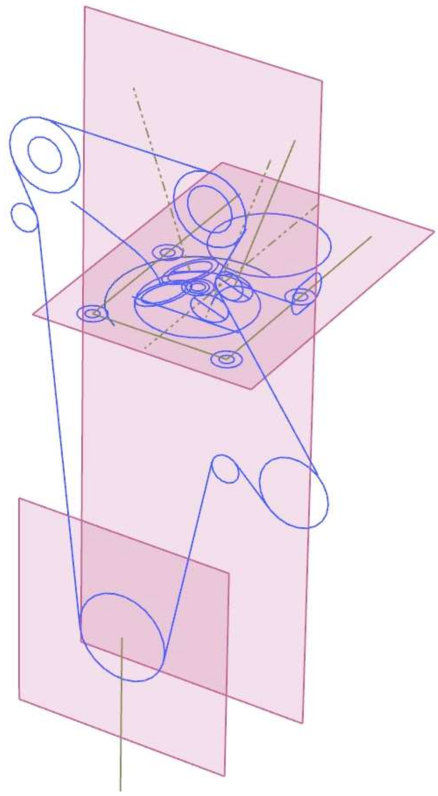

Figure 34 Skeleton of the designed cylinder head

7.3.2 Combustion chamber

Another step is design of a combustion chamber of the cylinder head. The shape of the chamber has a noticeable effect on power output, efficiency and harmful emissions. A pentroof shape of the combustion chamber was chosen as the most suitable for this application. The pentroof head is a cylinder head in which each combustion chamber has its spark plug located close to the center of the combustion chamber. When the spark plug is located in a central position, the flame spreads a minimum distance in all directions allowing for a balanced and clean ignition of the fuel-mix inside the combustion chamber.

According to the simulation data, compression ratio is 10. Using a CAD software, the volume of the proposed combustion chamber was measured. The proposed combustion chamber was modified to the final shape (Figure 35).

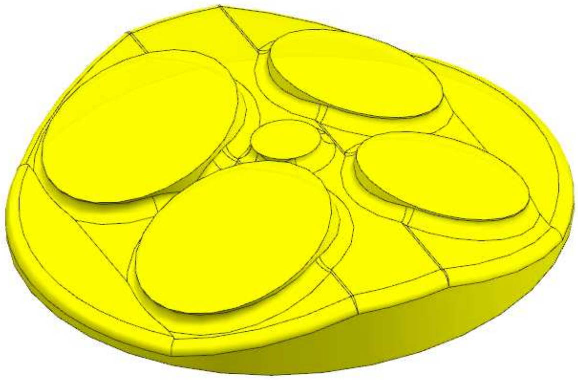

Figure 35 the final shape of the combustion chamber (compression rate - 10)

7.3.3 Inlet and exhaust ports

Intake port (a blue part in Figure 36) function is to distribute the mixture of air and fuel into the combustion chamber. Exhaust port (a red part Figure 36) is a passage in the cylinder head, which connects the exhaust valve and the exhaust manifold. The shape of the exhaust port has significant role on flux of the exhaust gasses, which pass through the port to the exhaust manifold. Generally, the length of the ports must be as short as possible to avoid thermal transfer between the ports and the other parts of the cylinder head. It is vital to pay attention to the shape of the ports, because it plays significant role in the efficiency of an engine.

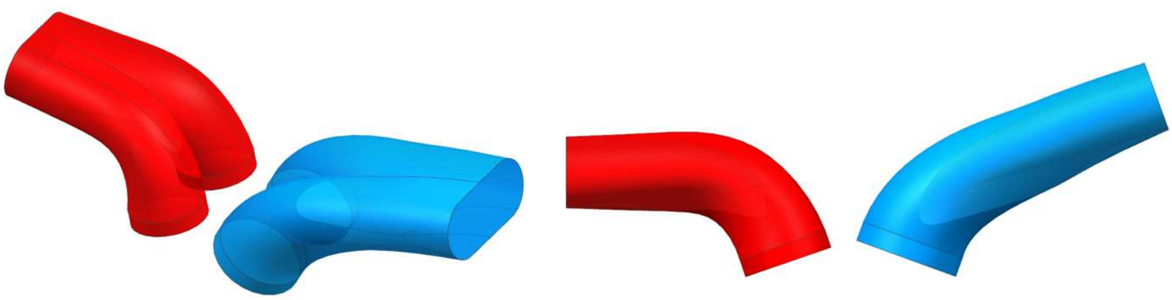

Figure 36 Shape of Intake and exhaust ports

Figure 37 shows connection of the inlet and exhaust ports to the combustion chamber. It also shows cylindrical hole for the spark plug that is located in a central position. A blue translucent body, in the picture, is a proposal water cooling system.

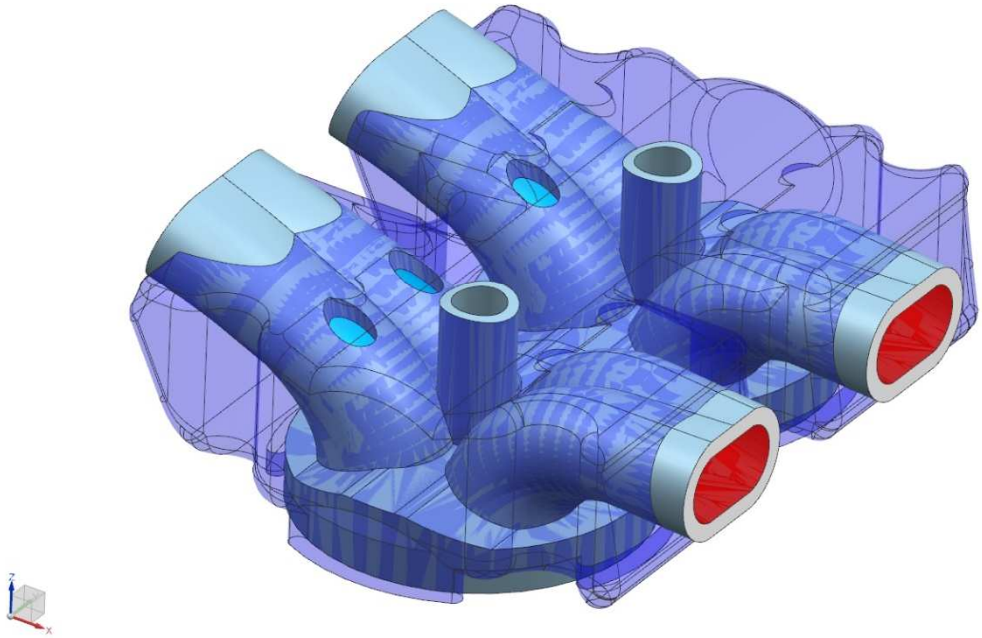

Figure 37 Inlet and exhaust ports

7.3.4 Final concept design

The final concept design is showed in Figure 38 and Figure 39. These figures show part of the lubrication system (orange holes).It is necessary to supplied oil to the camshaft and to the hydraulic lash adjuster. This is provided by holes drilled throught the cylinder head (orange holes in the figures).

After lubricating the camshaft and the related components, the oil flows by gravity back down channels in the head. This is provided by two channels (the purple channels in Figure 38 and Figure 39).

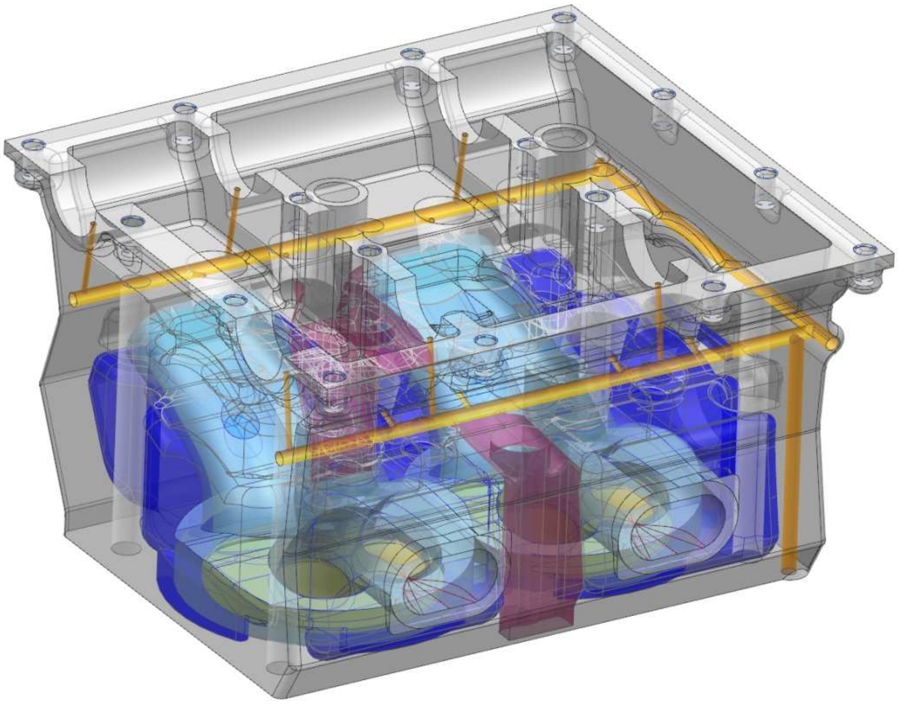

Figure 38 Final concept design of the cylinder head

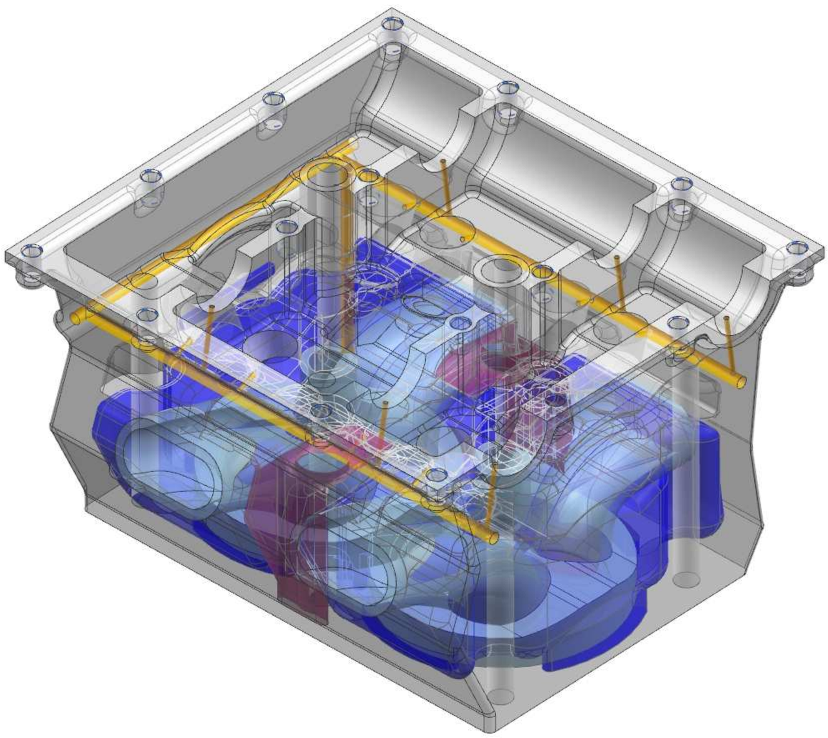

Figure 39 Final concept design of the cylinder head

7.4 Crankshaft mechanism

The crankshaft mechanism is used to convert a reciprocation motion of the piston into a circular motion of the crankshaft. The mechanism is the most important part of a combustion engine. It is subjected to heavy loads and must be precisely and ingeniously designed. Construction of a crankshaft assembly affects all other parts of an engine.

The crankshaft is subjected to end-thrust, which is an axial load in addition to that experienced by the big-end journals and bearings. This axial load is transferred from the crankshaft to the main bearing housing. One main-bearing is designed with trust washers on each side, this bearing takes total axial crankshaft thrust in both direction. Figure 40 shows the crankshaft assembly.On the figure is labeled main bearing and trust bearing of the crankshaft. The thrust bearing is placed next to the connection to the flywheel. These main bearing are split across their diameters to allow assembly of the crankshaft.

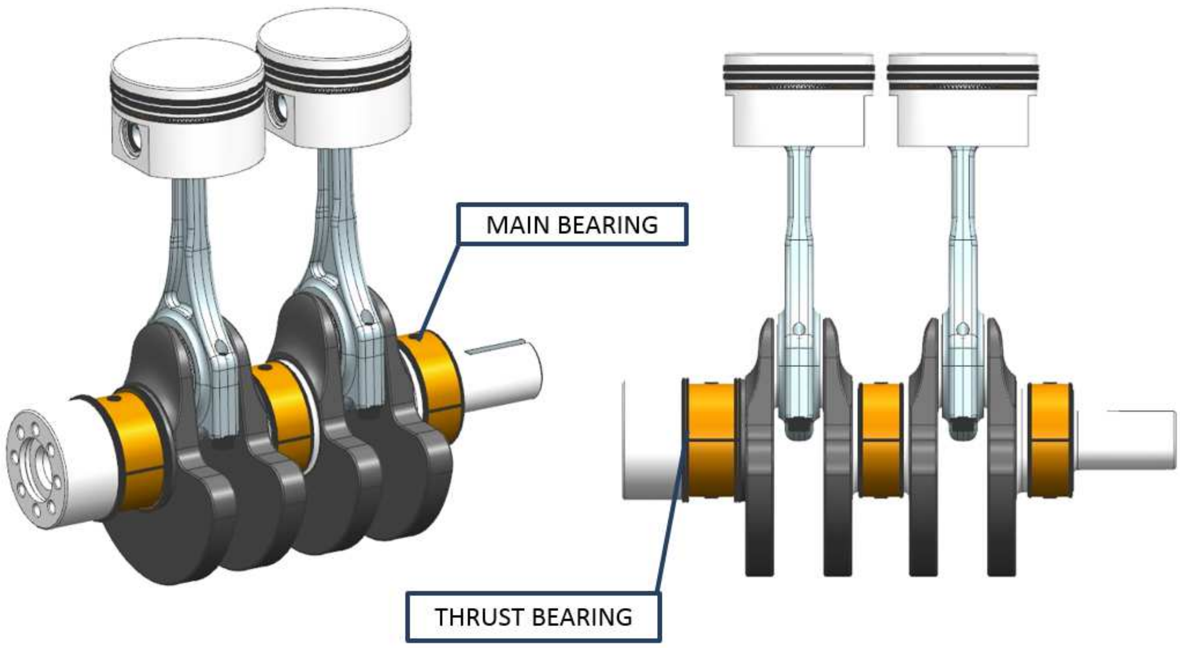

Figure 40 Crankshaft mechanism

7.4.1 Crankshaft

The dimensions of a crankshaft are given by bore diameter, thickness of the cylinder and by the bearing dimensions. Design process consists of few steps including choosing the main dimensions according to literature [26], balancing of the rotation and reciprocation masses and dealing with an engine lubrication system. The crankshaft is one of the most stressed parts in the ICE. This is the reason that material with excellent mechanical properties is needed. The material of the crankshaft is cast-iron EN-GJS-1000-5. Table 3 shows properties of the crankshaft material.

Name	Abbreviation	Value	Unit
Tensile Yield Strength	R_e	700	MPa
Tensile Ultimate Strength	R_m	1000	MPa
Poisson Ratio	ν	0,27	-
Density	ρ	7 100	kg/m^3
Young's Modulus	E	168 000	MPa

Table 3 Properties of the crankshaft material (EN-GJS-1000-5)

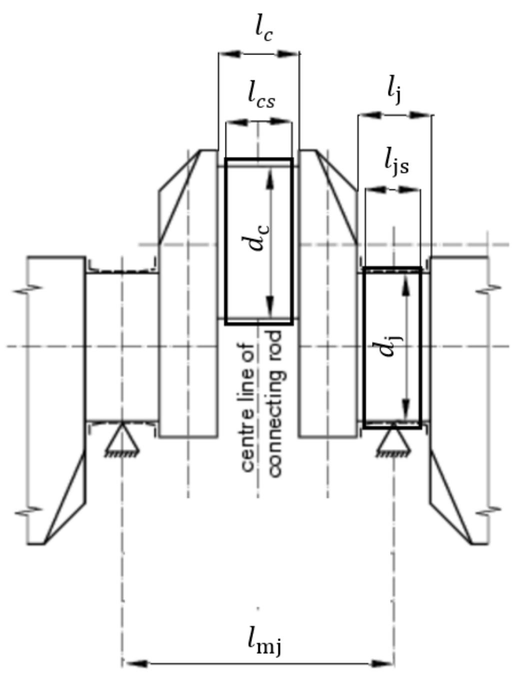

Figure 41 Scheme of crankshaft with the main dimensions for design

Calculation of the main dimensions of the designed crankshaft according literature [26]:

Main journal diameter (d_j):

$$d_j = 0,7 \cdot D \cong 56\ mm \tag{1}$$

Main journal width (l_j):

$$l_j = 0,39 \cdot D \cong 31\ mm \tag{2}$$

Main bearing width (l_{js}):

$$l_{js} = 0,28 \cdot D \cong 22,5\ mm \tag{3}$$

Crankpin diameter (d_c):

$$d_c = 0,56 \cdot D \cong 45\ mm \tag{4}$$

Crankpin width (l_c):

$$l_{\mathrm{c}} = 0{,}34 \cdot D \cong \ 27\ mm \tag{5}$$

Big- end bearing width (l_{cs}):

$$l_{\mathrm{cs}} = 0{,}27 \cdot D \cong \ 22\ mm \tag{6}$$

Main journal distance (l_{mj}):

$$l_{\mathrm{mj}} = 1{,}1 \cdot D \cong \ 88\ mm \tag{7}$$

The design of the crankshaft is shown in Figure 42 and Figure 43. The main dimensions are calculated above and they are implemented in the model. The shape and size of the web and counterweights are calculated in the chapter Engine balancing.

Figure 42 Crankshaft - isometric view (left) translucent isometric view (right)

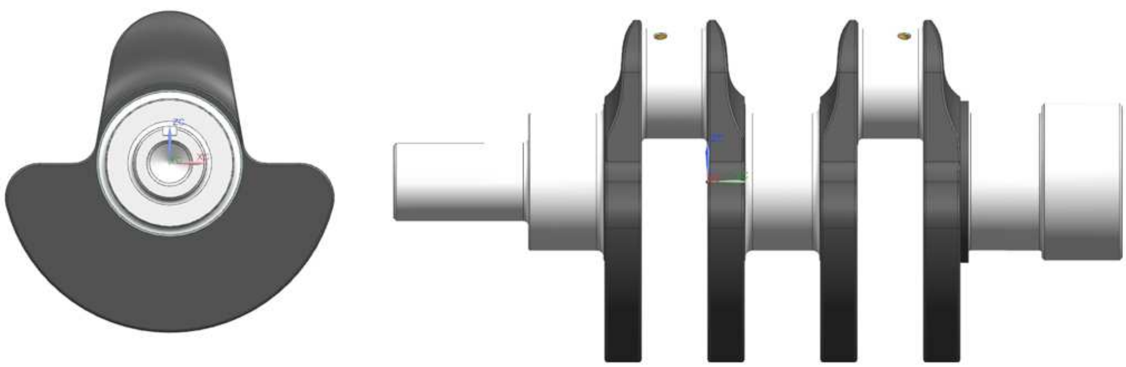

Figure 43 Crankshaft - front and side view

Preliminary design of the flywheel attachment is shown in Figure 44. The flywheel is attached to the rear end of the crankshaft. The attachment must be perfectly secure; therefore, eight bolts M8 are used. The flywheel should be possible to assembly in one position only, partly because the flywheel is marked to indicate to particular position, but more because the crankshaft and flywheel are balanced as an assembly. Misalignment position one of the holes for bolts is used to secure one assembly position.

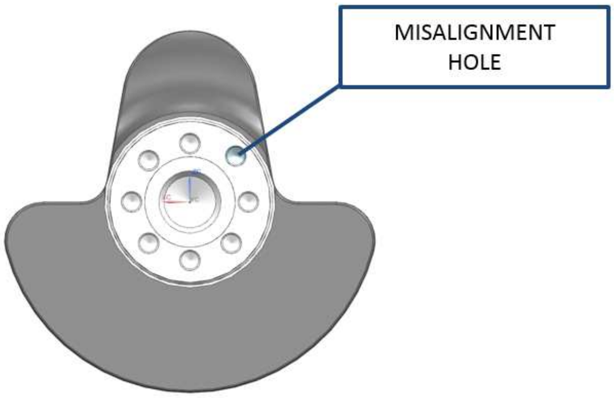

Figure 44 Preliminary design of the flywheel attachment

It is necessary to supplied oil to the crank pins. This is provided by two holes drilled throught the crankshaft running from the main journal, throught the web to the surface of the crankpin (Figure 45). Oil is delivered under pressure to the main bearing, where it is fed into a groove running around the bearing at about the middle of its length. The main-journal end of the hole moves around the groove in the main bearing while the crankshaft rotates. This allows a continuous supply of to pass to the crank pin.

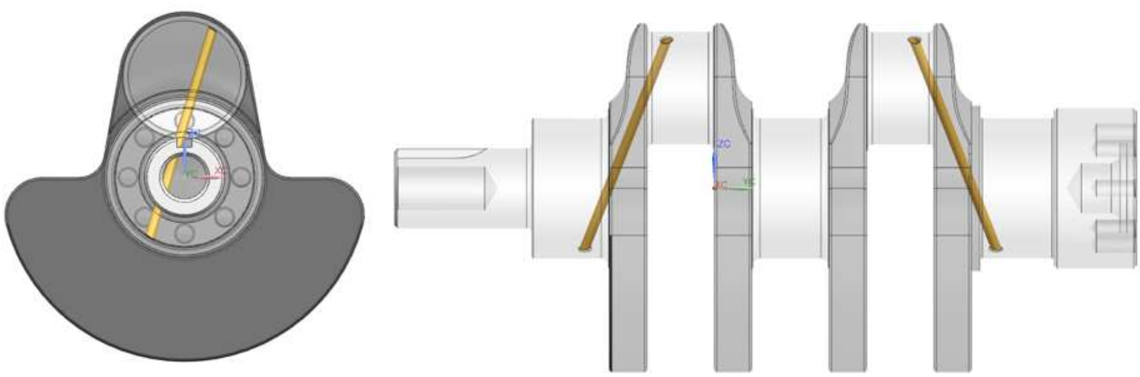

Figure 45 Crankshaft - front and side view - lubrication hole

7.4.2 Connection rod

The main design of the connection rod is shown in Figure 46. This figure shows also the rod bolts, big and small end bearings. The connection rod is made by die forging and accurately machined. For this application and the design is suitable to use alloy steel. The connection rod is made from steel C70S6. The big end diameter is $D_d = 47mm$ and width is $l_{cs} = 22mm$. The dimensions were designed according crankshaft design. The small end diameter is $D_h = 21mm$, and width $H_h = 20{,}6mm$. The width of the rod is from 15 mm (close to big end) to 12mm close to the small end rod. The shank of the rod is made of H section, which generally gives the better possible resistance to sideway buckling without excessive weight. The oil hole is drilled into small end to provide lubrication of a gudgeon pin. The distance between the small end and big end so called center distance is $L_{oj} = 133{,}55mm$.

The big end is split by fracture-split technique. This method has a lot of advantages. The first comes a 30-percent manufacturing cost reduction from not having to machine and dowel the mating surfaces of rod and cap. The second advantage is greater roundness and more accurate, longer lasting registration of the two pieces, which brings benefits in bearing capacity and life. Two screws M8 are used to fasten a big-end cap. Total weight of the connection rod assembly is $m_{oj} = 0{,}540kg$. Drawing of the connection rod is attached.

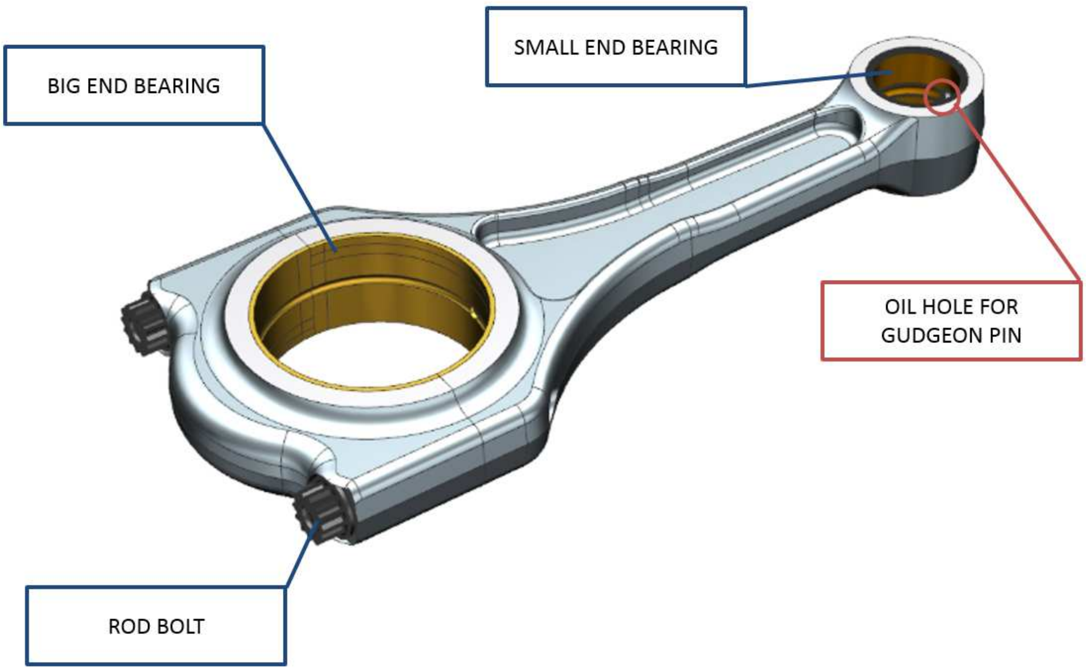

Figure 46 Connection rod assembly

7.4.3 Piston

The main dimensions of the piston were designed according to literature [26]. The scheme of a piston with the main dimensions for design could be seen Figure 47.

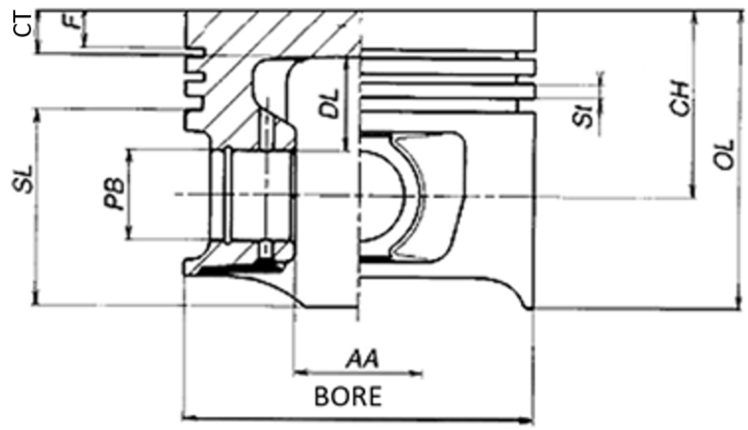

Figure 47 Scheme of a piston with the main dimensions for design [26]

Calculation of the main dimension according literature:

Overall length:

$$OL = 0{,}62 \cdot \mathrm{BORE} = 0{,}60 * 80{,}5 \cong 48{,}3 \xRightarrow{Designed} 50mm \tag{8}$$

Compression height:

$$CH = 0{,}43 \cdot \mathrm{BORE} = 0{,}4 \cdot 80{,}5 \cong 34{,}65 \xRightarrow{Designed} 34{,}5mm \tag{9}$$

Skirt length:

$$SL = 0{,}37 \cdot \mathrm{BORE} = 0{,}37 \cdot 80{,}5 \cong 29{,}79 \xRightarrow{Designed} 30mm \tag{10}$$

Distance between bosses:

$$AA = 0{,}28 \cdot \mathrm{BORE} = 0{,}28 \cdot 80{,}5 \cong 22{,}54 \xRightarrow{Designed} 22mm \tag{11}$$

Pin hole diameters:

$$PB = 0{,}26 \cdot \mathrm{BORE} = 0{,}26 \cdot 80{,}5 \cong 21 \xRightarrow{Designed} 21mm \tag{12}$$

Crown thickness:

$$CT = 0{,}09 \cdot \mathrm{BORE} = 0{,}09 \cdot 80{,}5 \cong 7{,}25 \xRightarrow{Designed} 7mm \tag{13}$$

Crown underside to pin hole

$$DL = 0{,}20 \cdot \mathrm{BORE} = 0{,}20 \cdot 80{,}5 \cong 16{,}1 \xrightarrow{Designed} 17mm \tag{14}$$

Top land width:

$$F = 0{,}09 \cdot \mathrm{BORE} = 0{,}09 \cdot 80{,}5 \cong 7{,}25 \xrightarrow{Designed} 7mm \tag{15}$$

Ring land width:

$$St = 0{,}035 \cdot \mathrm{BORE} = 0{,}035 \cdot 80{,}5 \cong 2{,}82 \xrightarrow{Designed} 2{,}8mm \tag{16}$$

In the following figure (Figure 48) is shown the piston assembly designed according calculation above. The assembly consists of three piston rings (two compression rings, one oil control ring) and gudgeon pin. The location of a gudgeon pin is by two circlips. The overall weight of the piston assembly is 0,468g. The main dimensions are shown in Table 4. Material for piston is aluminum alloy 2618.

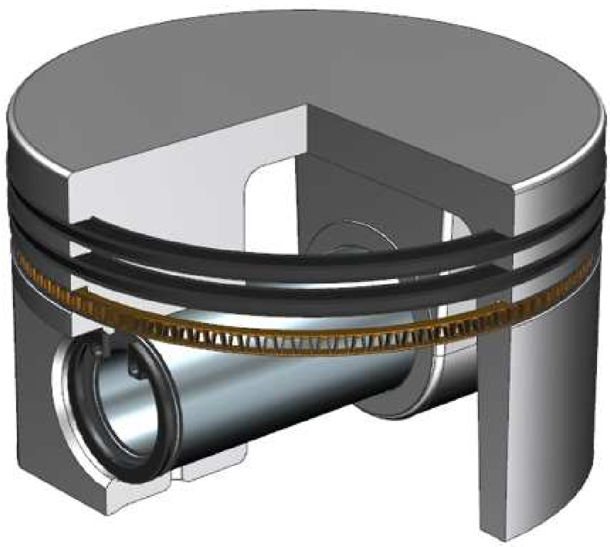

Figure 48 Part section of the piston assembly

Name	Abbrevation	Value	Unit
Overall length	OL	50	mm
Compression height	CH	34,5	mm
Skirt length	SL	30	mm
Distance between bosses	AA	22	mm
Pin hole diameters	PB	21	mm
Crown thickness	CT	7	mm
Crown underside to pin hole	DL	17	mm
Top land width	F	7	mm
Ring land width	St	2,8	mm

Table 4 Piston assembly - main dimensions

7.5 Design of the balance shaft

Minimizing of the vibration consists of balancing all components that have to rotate at high speed and balancing reciprocating masses as well. To achieve good primary balance is essential to selected all parts that move in the same manner so that they are all nearly equal in weight. The chapter called Engine balancing covers all parts of the calculation of reciprocating masses, rotating masses and first order balancing.

When a piston passes through TDC and BDC the change of the direction produces an inertia force with attempts to keep the piston moving in the same direction in which it went before the change. This force, called the primary force, increases as the engine speed is raised.

In order to balance primary inertia forces of the reciprocating masses one balance shaft and counterweights, which are attached to the crankshaft, were designed.

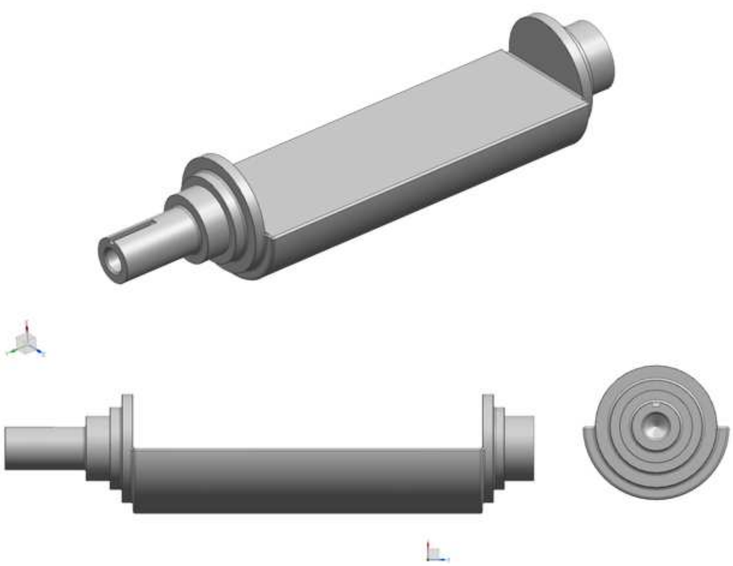

Figure 49 Design of the balance shaft

This chapter describes only basic design of the balance shaft; all calculations are performed in later chapter. The basic design of the balance shaft is in Figure 49. The balance shaft is mounted by two sliding bearings. (see Figure 50) . This figure is cross-section view of the position of the balance shaft; it shows also seals, lids and parts of the lubrication system. Oil is delivered under pressure to the balance shaft bearings, where it is fed into a groove running around the bearing at about the middle of its length. The drilled hole for the bearing in the closed lid (righ side) is not visible, because it is drilled in different angle.

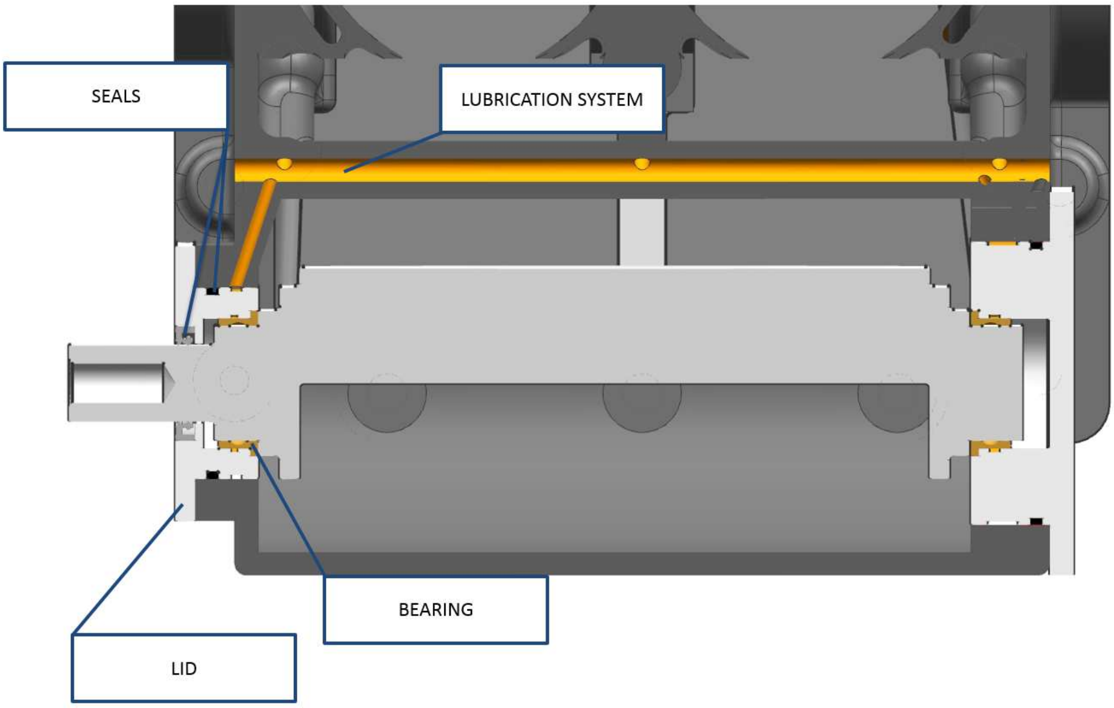

Figure 50 Cross –section view of the position of the balance shaft

The location of the balance shaft is shown in Figure 51.

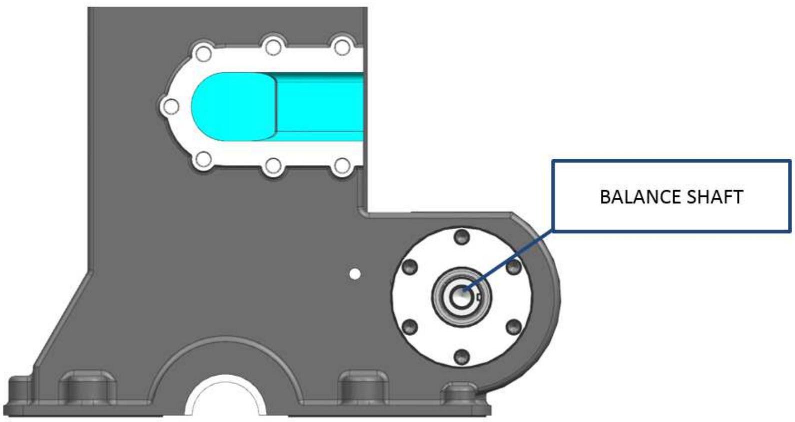

Figure 51 Balance shaft location

8 Calculations and Simulations

8.1 Structural analysis of a connection rod

Structural analysis was performed by Siemens NX 10. The NX 10 contains a special module for Finite element analysis called *Advanced Simulation*. The software of a FEM analysis consists of a preprocessor, a postprocessor and actual FEM solver. Network creation (breakdown into finite number of elements) is performed in the preprocessor on the basis of a design CAD geometry. The FEM solver calculates the computing model formulated in this way. The result found is then shown in graphic form in the postprocessor. For example, strain or stress distribution by means of isocolors or as motion animation. *Advance Simulation* module consists lots of different solvers for various problems (structural, dynamics, thermal etc.). NX Nastran was used as a solver for structural analysis of the connection rod. Typical calculation procedure of Finite element method is:

1. PREPROCESSING
    - Import of a CAD model
    - Meshing (choosing proper element)
    - Definition of material properties
2. FEM solver:
    - Definition of boundary conditions
    - Definition of loads
    - Computing of system of equations
3. POSTPROCESSING
    - Results display

8.1.1 Connection rod load calculation

Crank mechanism of an internal combustion engine is exposed to two types of forces. Gas pressure acts on the upper surface of the piston. The force (F_g) due to this pressure is then equal to the cross-sectional area of the cylinder multiplied by the gas pressure. This force, which acts along the center-line of the cylinder, is then transmitted through the piston structure to the gudgeon pin bosses and thence through the gudgeon pin to the connection rod. The other force is inertial force (F_{IS}) of the moving parts of a crank mechanism.

The first step of the calculation of the connection rod load is calculation of the basic crank mechanism quantities (crank radius, angular velocity, connection rod ratio). The second step is the calculation of crankshaft drive kinematics; this step consists of enumeration of piston acceleration, angular velocity and angular acceleration of the connection rod etc. The last step is calculation of crankshaft – assembly kinetics.

8.1.1.1 Basic crank mechanism quantities

Table 5 shows given parameters for the calculation of basic crank mechanism parameters.

Some of basic crank mechanism quantities are shown Figure 52.

Name	Abbrevation	Value	Unit
Piston stroke	s	80,5	mm
Engine speed	n	4000	rpm
Connection rod length	L_{oj}	133,55	mm

Table 5 Basic crank mechanism qualities - input data

Crank radius:

$$r_k = \frac{s}{2} = \frac{80{,}5}{2} = [40{,}25\ mm] \tag{17}$$

Angular velocity of the crankshaft:

$$\omega = \frac{2 \cdot \pi \cdot n}{60} = \frac{2 \cdot \pi \cdot 5500}{60} \cong 576\ [rad \cdot s^{-1}] \tag{18}$$

Connection rod ratio:

$$\lambda = \frac{r_k}{L_{oj}} = \frac{40{,}25}{133{,}55} \cong 0{,}301[-] \tag{19}$$

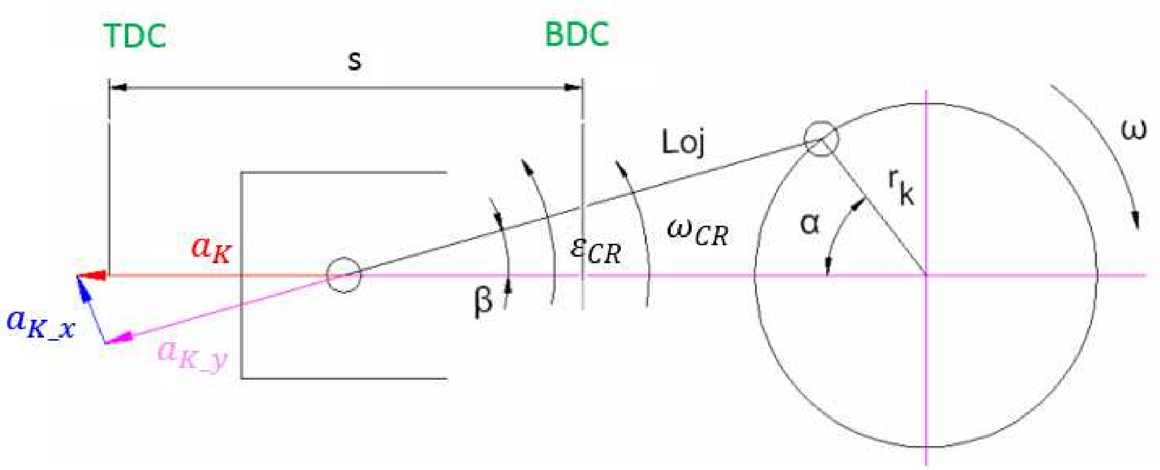

Figure 52 Scheme of crank mechanism

8.1.1.2 Crankshaft- drive kinematics

8.1.1.2.1 Piston

Piston- travel function f=s(α):

$$s(\alpha) = r_k \cdot \left[1 - \cos(\alpha) + \frac{\lambda}{4}(1 - \cos(2\alpha))\right] \tag{20}$$

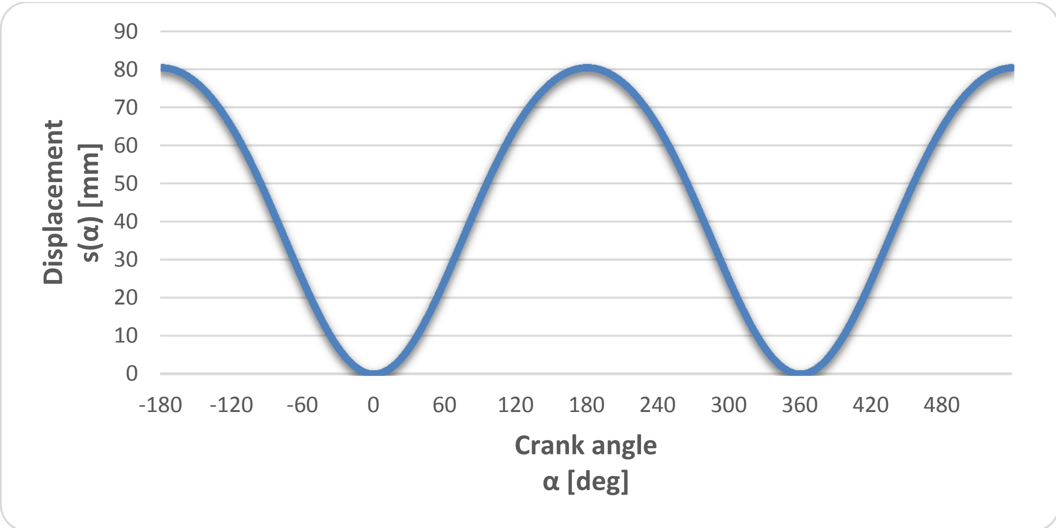

Figure 53 Graph - Piston- travel function

Piston- velocity function f=v(α):

$$v(\alpha) = \omega \cdot r_k \cdot \left[\sin(\alpha) + \frac{\lambda}{2} sin(2\alpha)\right] \tag{21}$$

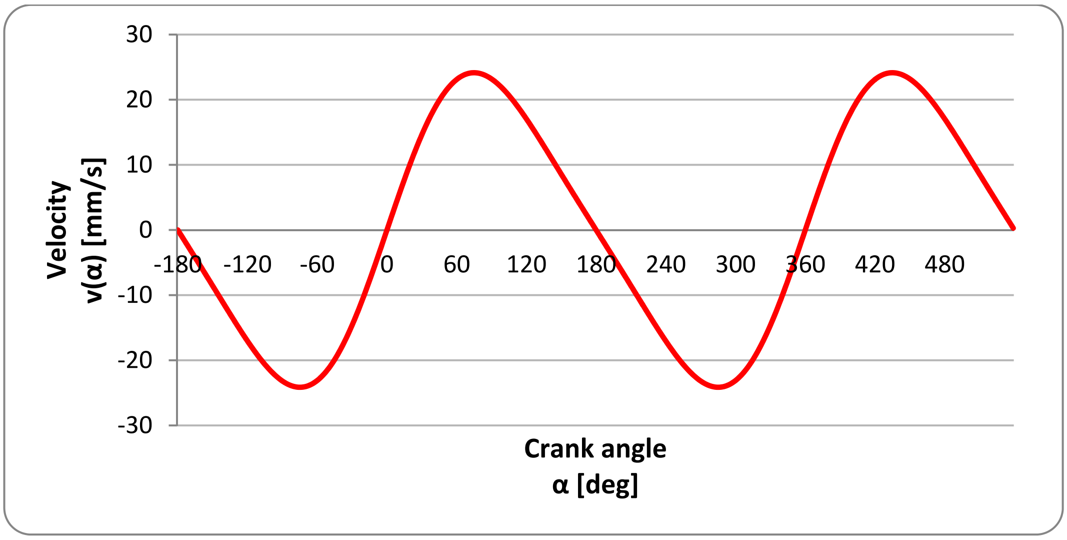

Figure 54 Graph - Piston- velocity function

Piston- acceleration function f=$a_k(\alpha)$

$$a_K(\alpha) = \omega^2 \cdot r_k \cdot [\cos(\alpha) + \lambda \cdot cos(2\alpha)] \quad (22)$$

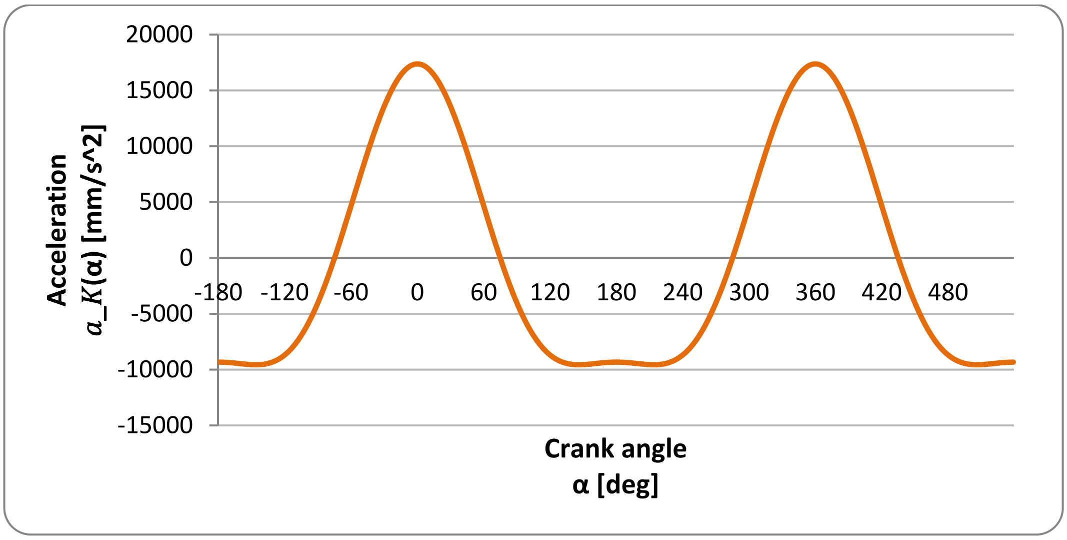

Figure 55 Graph - Piston- acceleration function

The last equation describes piston acceleration, which is calculate along the centerline of the cylinder. For further analysis, is suitable to calculate piston acceleration function in two perpendicular components $a_{K\_x}(\alpha)$ and $a_{K\_y}(\alpha)$ (see Figure 52).

$$a_{K\_x}(\alpha) = a_K \cdot sin(\beta) \quad (23)$$

$$a_{K\_y}(\alpha) = a_K \cdot cos(\beta) \quad (24)$$

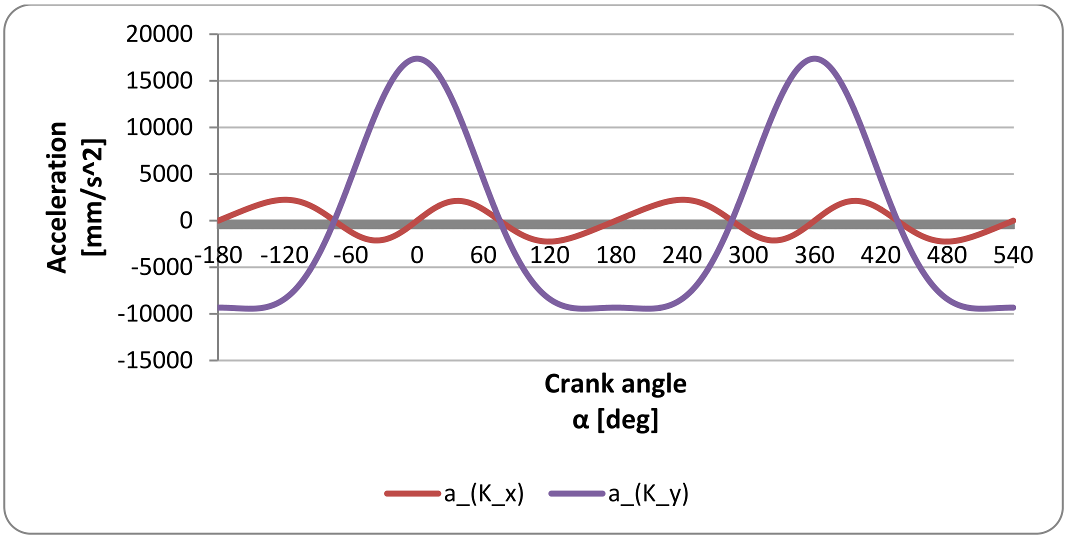

Figure 56 Piston- acceleration function in two perpendicular components

Maximum piston acceleration in X component is deducted from the graph (Figure 56):

$$\text{Max}(a_{K\_x}) \cong 2242 mm/s^2$$

Maximum piston acceleration in Y component is deducted from the graph (Figure 56):

$$\text{Max}(a_{K\_y}) \cong 17376 mm/s^2$$

8.1.1.2.2 Connection rod

Connection rod – pivoting angle function

$$\beta(\alpha) = \lambda \cdot \sin(\alpha) \tag{25}$$

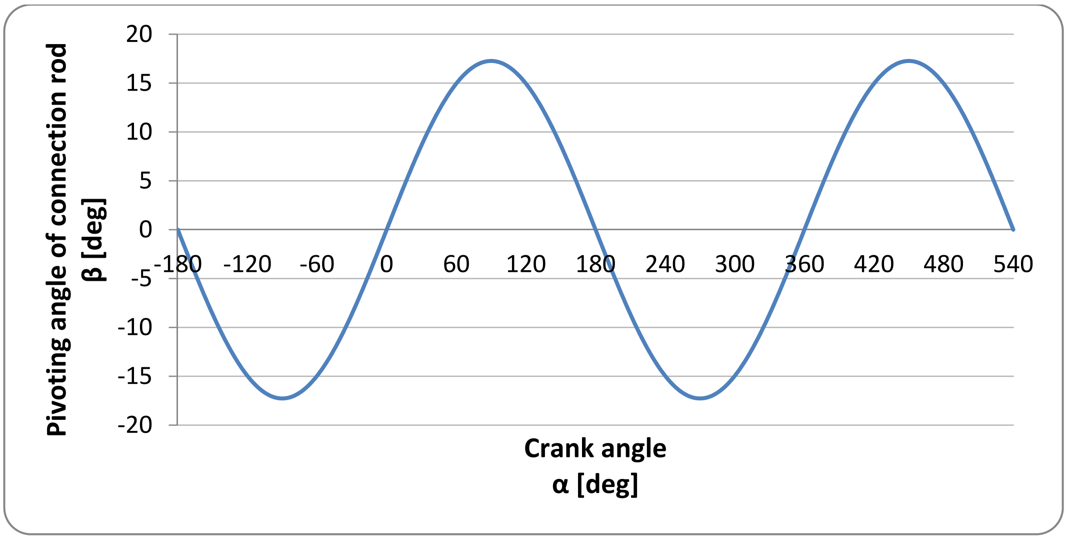

Figure 57 Graph- pivoting angle function

Connection rod – angular velocity function

$$\omega_{CR}(\alpha) = \lambda \cdot \omega \cdot \cos(\alpha) \tag{26}$$

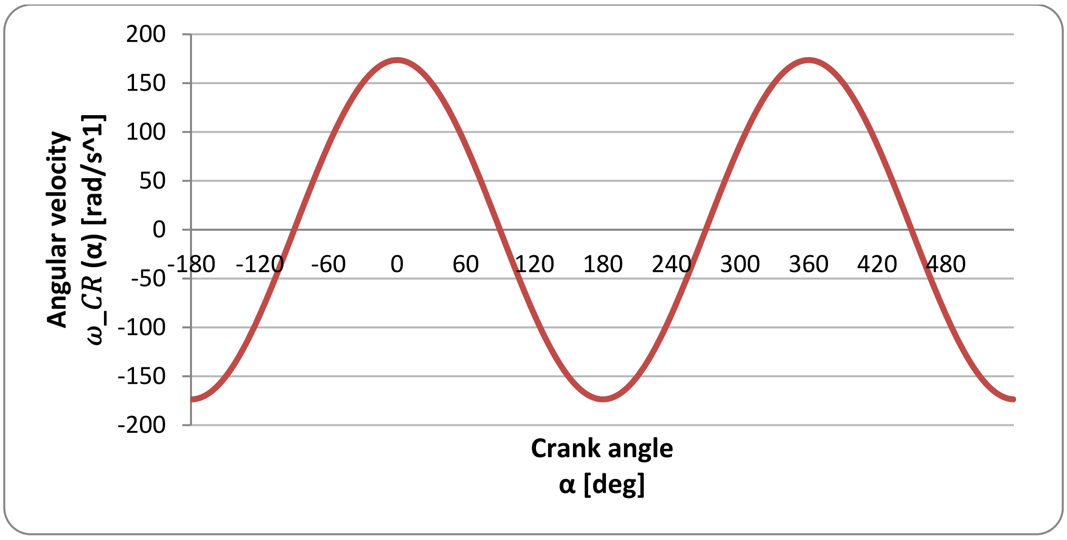

Figure 58 Graph -connection rod – angular velocity function

Maximum angular velocity is deducted from the graph (Figure 58): Max(ω_{CR}) $\cong 174 rad/s$

Connection rod – angular acceleration function

$$\varepsilon_{CR}(\alpha) = -\lambda \cdot \omega^2 \cdot \sin(\alpha) \tag{27}$$

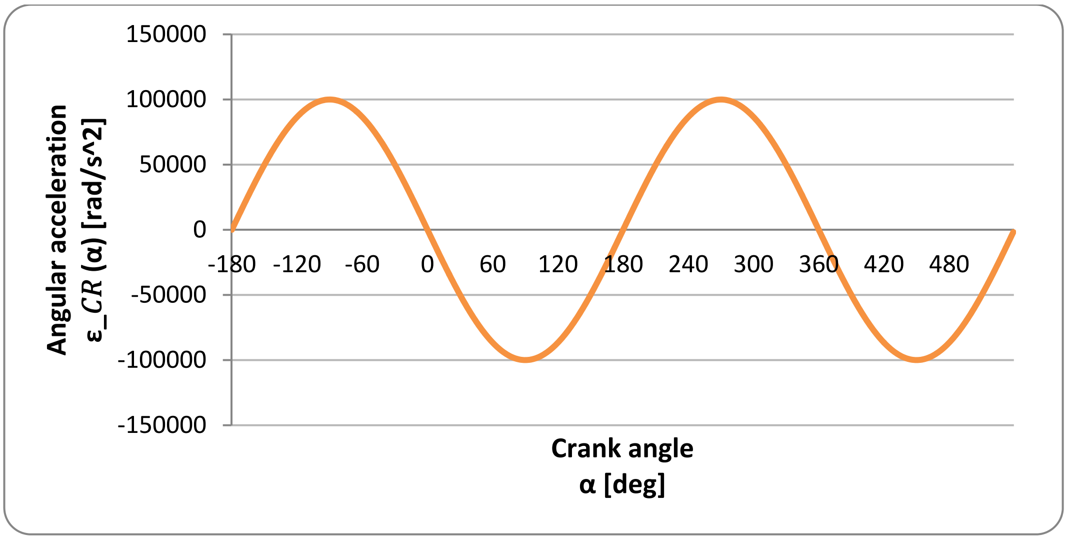

Figure 59 Graph -connection rod – angular acceleration function

Maximum angular acceleration is deducted from the graph (Figure 59): Max(ε_{CR}) $\cong 99978 rad/s^2$

8.1.1.3 Crankshaft – assembly kinetics

The force acting on the crankshaft assembly and the resulting moments can initially be derived as follows (see Figure 60). The figure includes gas force (F_g) from the combustion-chamber pressure, connection – rod force(F_S), piston normal force(F_N), tangential force at the crankshaft(F_T), radial force at the crankshaft(F_R) and inertia force of the reciprocating mass of the crankshaft assembly for one cylinder$(F_{S_{cylinder}})$. [21]

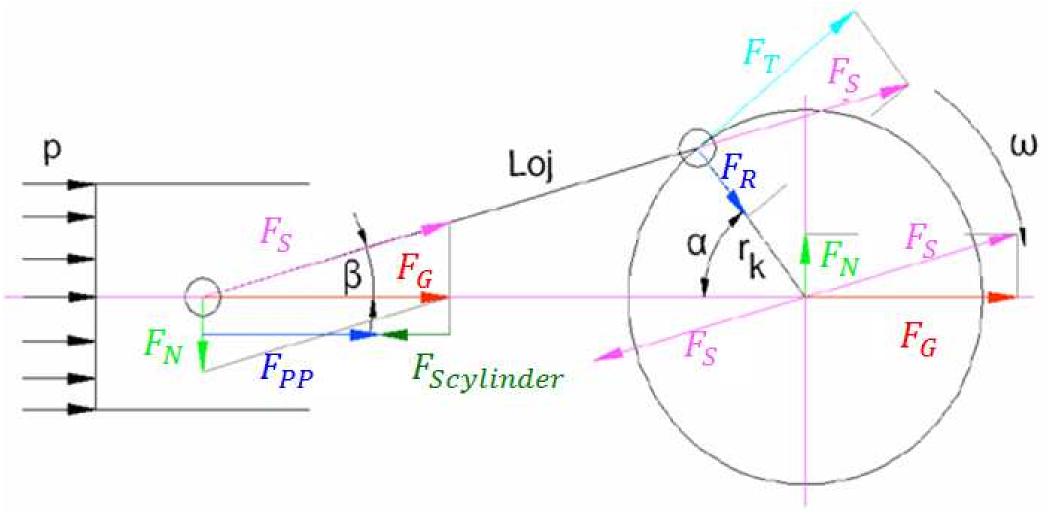

Figure 60 Gas- force components shown on a basic crankshaft drive

For further calculation is necessary to know indicator diagram known as Pressure – crank angle diagram. These data were obtained from 1D engine simulation. The simulation was performed in the company Ricardo Prague using simulation software package WAVE. The Diagram (Figure 61) was compiled for engine speed 4000 rpm and 5500 rpm that correspond to maximum torque and maximum power respectively. Maximum pressure for 4000 rpm is 7,6 MPa and maximum pressure for 5500 rpm is 7,2 MPa.

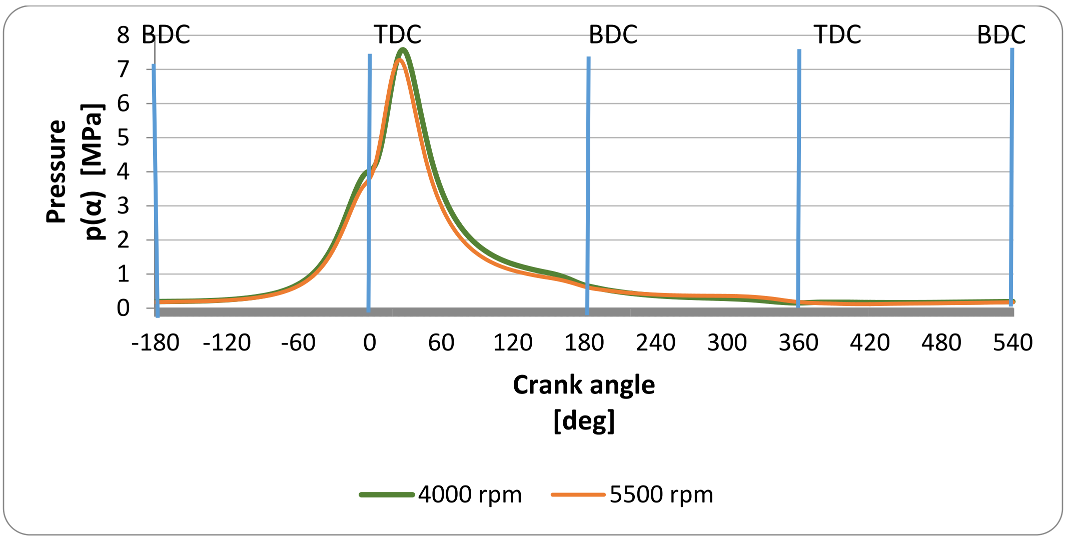

Figure 61 Pressure - crank angle diagram - 4000 rpm and 5500 rpm

The piston-pin force results as gas force from the combustion-chamber pressure multiplied by the piston area(A_{piston}).

Piston area A_{piston}

$$A_{piston} = \frac{\pi \cdot BORE^2}{4} = \frac{\pi \cdot 80{,}5^2}{4} = 5090mm^2 \tag{28}$$

$$F_g(\alpha) = [p(\alpha) - p_{atmospheric}] \cdot A_{piston} \tag{29}$$

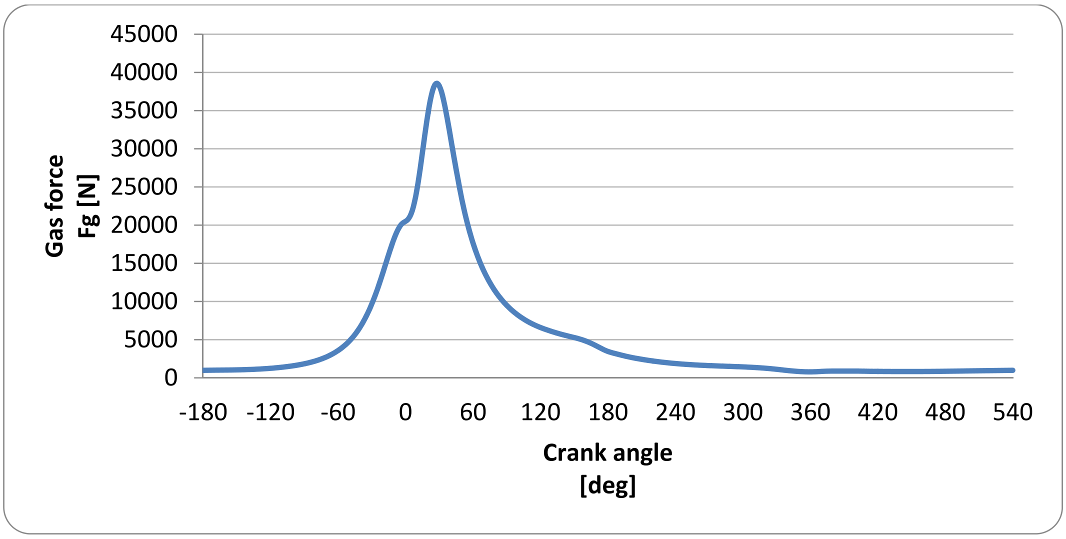

Figure 62 Graph - Gas force - crank angle

Maximum pressure force is deducted from the graph (Figure 62): Max$(F_g) \cong 38{,}6kN$

The inertia force of the reciprocating masses of the crankshaft assembly for one cylinder is acceleration of the piston multiplied by all reciprocating masses.

$$F_{S_{cylinder}}(\alpha) = -(m_s + m_p) \cdot a(\alpha) \tag{30}$$

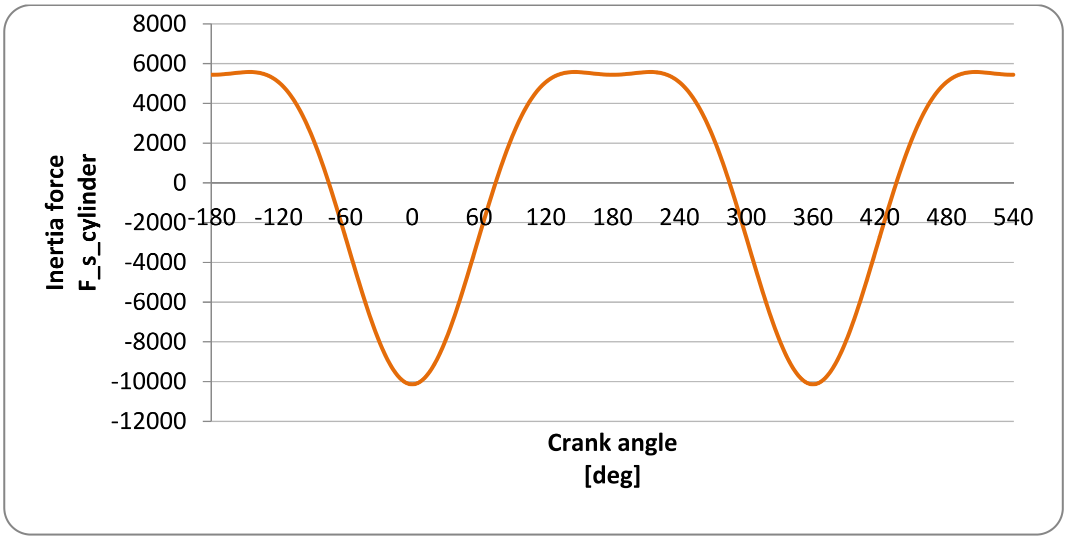

Figure 63 Graph - Inertia force - crank angle

Maximum inertia force of the reciprocating mass of the crankshaft assembly is deducted from the graph (Figure 63): Max $(F_{S_{cylinder}}) \cong -10{,}1kN$

The overall force acting on the piston pin is:

$$F_{PP}(\alpha) = F_g(\alpha) + F_{S_{cylinder}}(\alpha) \tag{31}$$

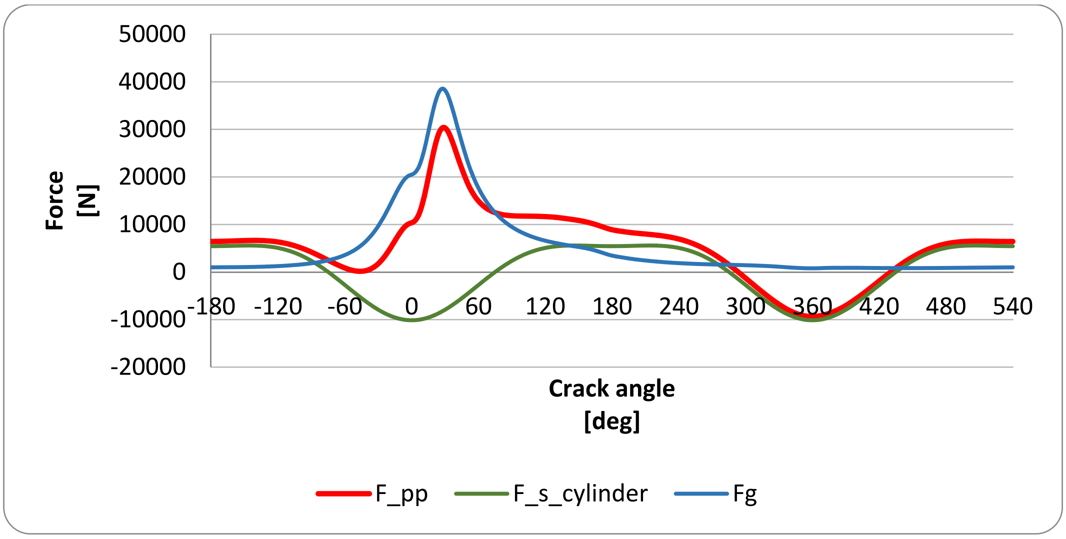

Figure 64 Graph – Piston pin force - crank angle

Maximum overall force acting on the piston pin is deducted from the graph (Figure 64): Max $(F_{PP}) \cong 30{,}4kN$.

The connecting –rod force is obtained from the vectorial analysis of the overall piston-pin force in the direction of the connecting rod. The following applies:

$$F_S(\alpha) = \frac{F_{pp}(\alpha)}{\cos(\beta)} \tag{32}$$

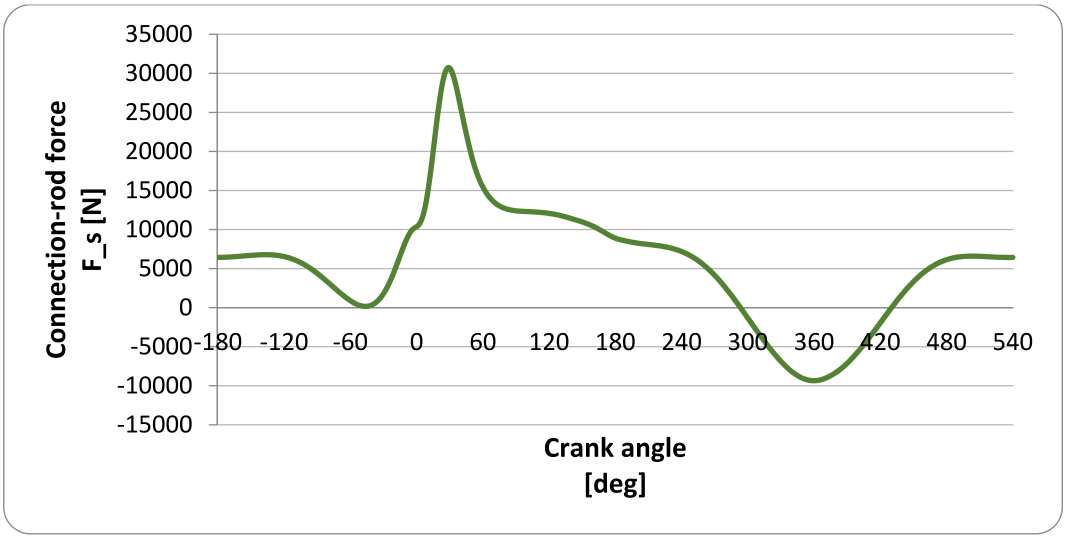

Figure 65 Graph - Connecting-rod force

Maximum the connecting –rod force is is deducted from the graph (Figure 64): Max $(F_S) \cong 30{,}7kN$

The piston normal force $F_N$is the vectorial component of the piston-pin force normal to the cylinder wall and for balancing the connection-rod force (see Figure 60)

$$F_N(\alpha) = F_{pp}(\alpha) \cdot \tan(\beta) \tag{33}$$

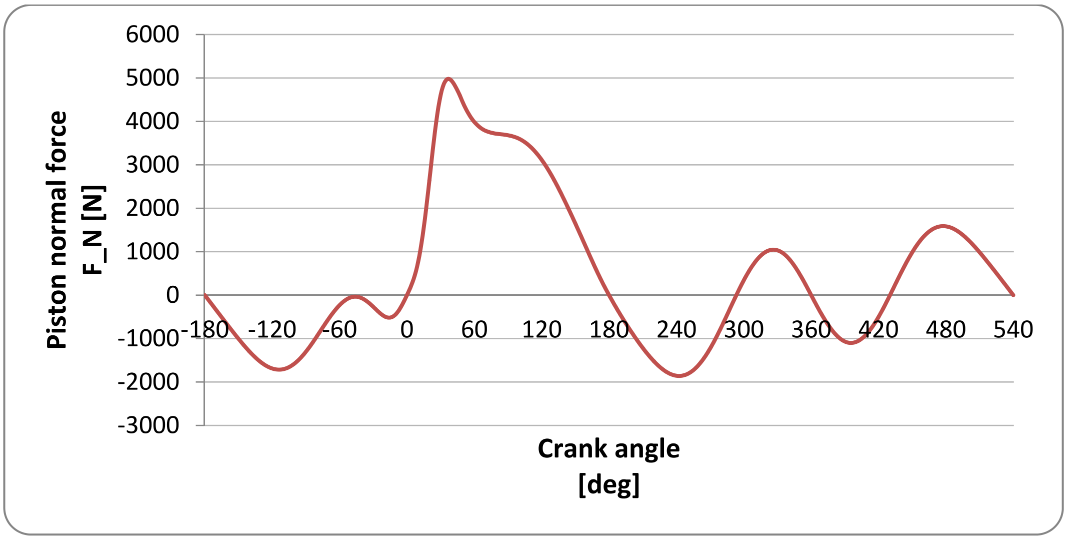

Figure 66 Graph - Piston normal force

The tangential force at the crankshaft crank pin contributes to an acceleration of the crankshaft and thus to be build-up of torque at the crankshaft. It is created from the vectorial analysis of the connection rod force. Simplified equations is:

$$F_T(\alpha) \approx F_{pp}(\alpha) \cdot [\sin(\alpha) + \frac{\lambda}{2}\sin(2\alpha)] \tag{34}$$

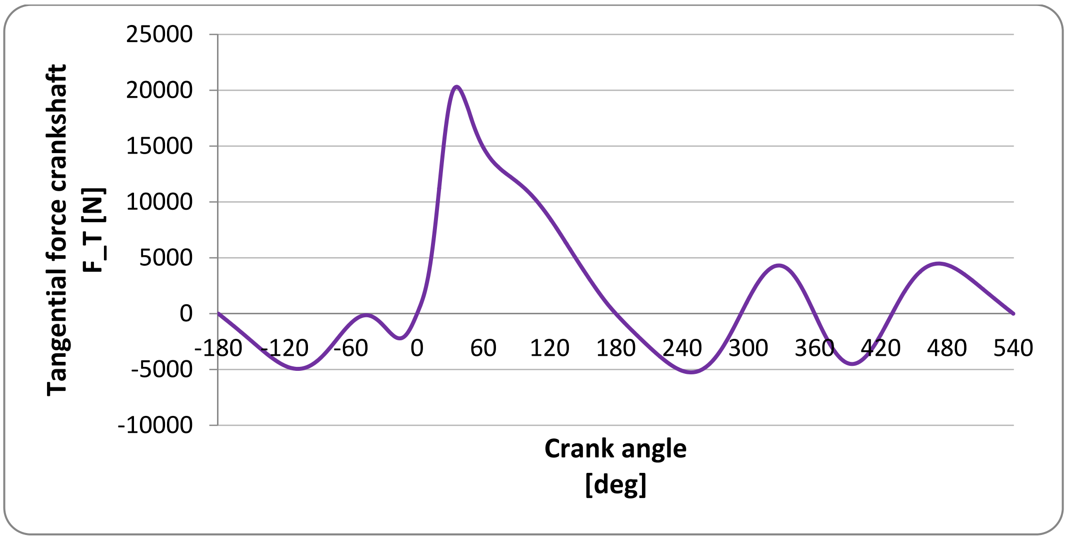

Figure 67 Graph - Tangential force at the crankshaft crank pin

Simplified calculation of the radial force F_R at the crankshaft crank pin is:

$$F_R(\alpha) \approx F_{pp}(\alpha) \cdot [\cos(\alpha) - \frac{\lambda}{2} + \frac{\lambda}{2}\cos(2\alpha)] \tag{35}$$

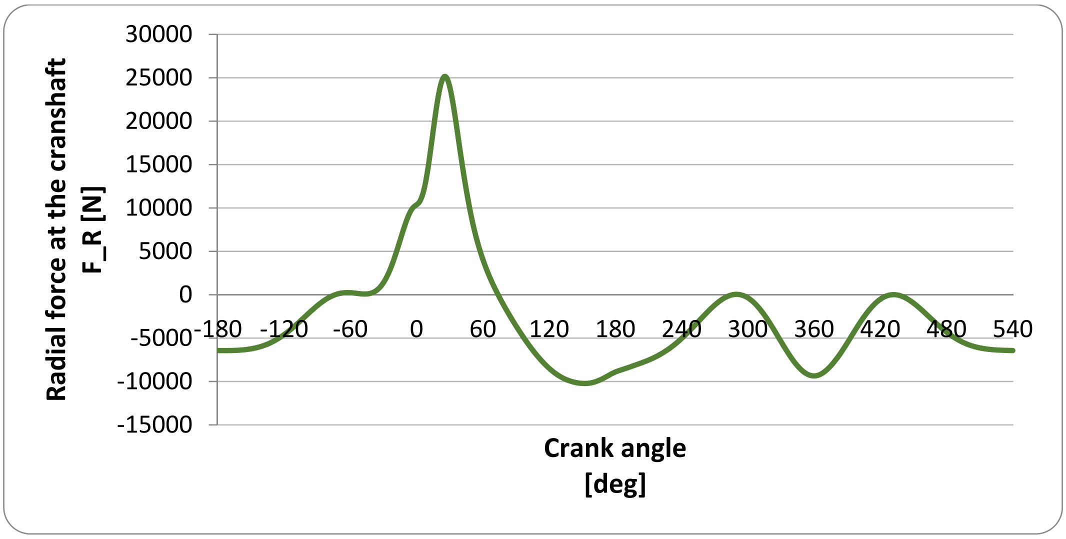

Figure 68 Graph - Radial force at the crankshaft crank pin

8.1.2 Description of the FEM Analysis model

The construction of the connection rod was simplified in order to mesh the model. That involves deleting some faces and the connection rod was united in one solid body. The simplified geometry is shown in Figure 69.

Figure 69 – Simplified geometry of the connection rod

The next step in the calculation involved a choosing an element type and determining a finesses of the mesh. The finite element mesh was generated using parabolic tetrahedral elements CTETRA (10), the size of the element is 2mm. The Crankpin journal and the piston pin were substituted by 1D rigid connection between cylindrical face and the midpoint (see Figure 70). Using this 1D rigid element a bearing rigidity has been neglected.

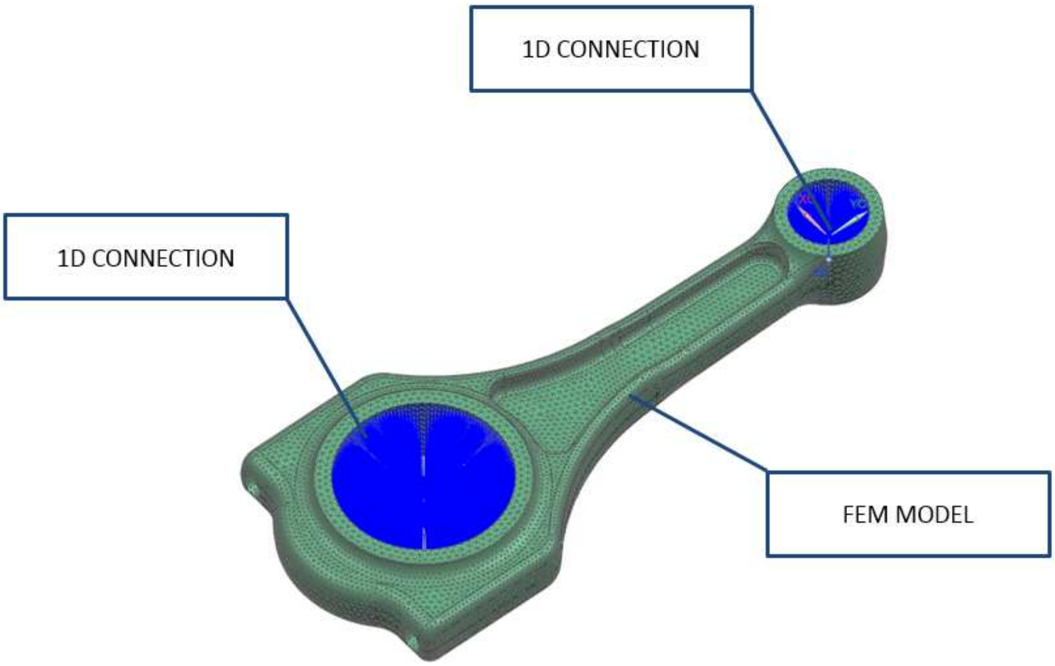

Figure 70 FEM model of the connection rod

A further step is involved a defining the properties. It is necessary to define elastic material properties for structural analysis. Elastic properties for steel are relatively consistent between steel grades (similar Young's modulus, E, and Poisson's ratio, ν) .Typical steel values with an E of 210,000 MPa and ν of 0.3 were considered in the analysis. Table 6 describes properties of the connection rod material (C 70S6).

Name	Abbreviation	Value	Unit
Tensile Yield Strength	R_e	550	MPa
Tensile Ultimate Strength	R_m	900	MPa
Poisson Ratio	ν	0,3	-
Density	ρ	7850	kg/m^3
Young's Modulus	E	210 000	MPa

Table 6 Properties of the connection rod material (C70S6)

The final step involved a determining the support conditions and the loads.

Support condition:

The midpoint of the 1D connection in the big end is fixed (see Figure 71) in all three directions.

.

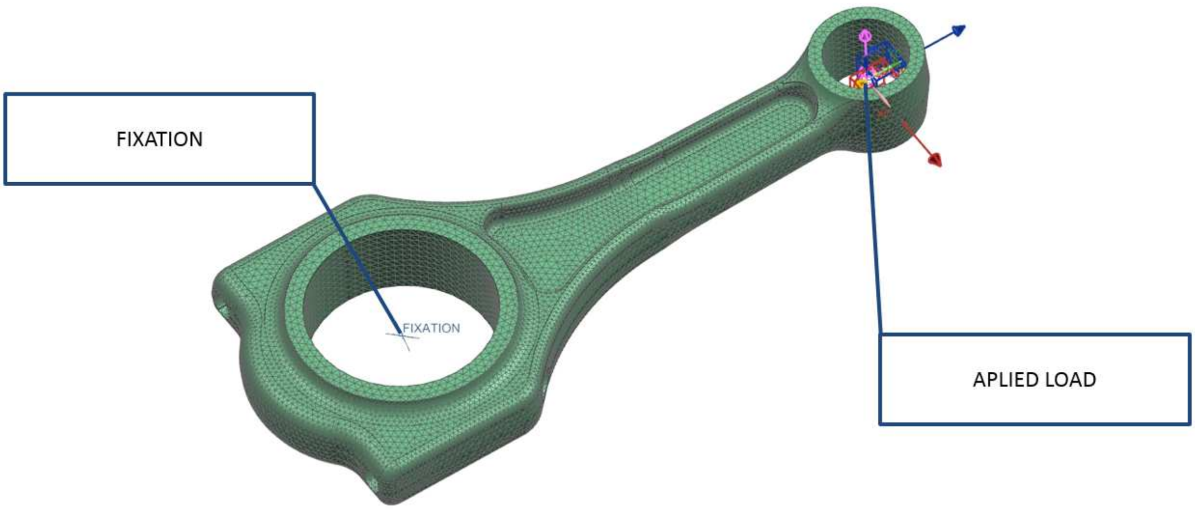

Figure 71 FEM model - boundary condition

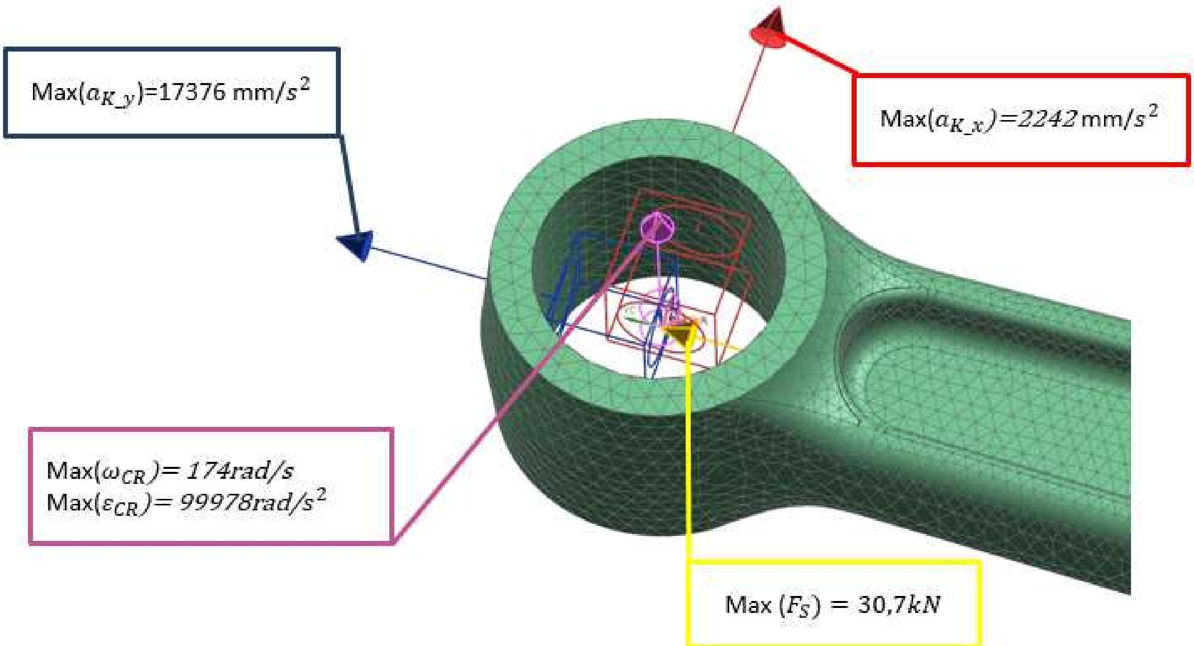

Figure 72 FEM model - Applied loads

Applied loads:

Figure 72 describes all applied loads. These loads were calculated in the previous chapter. The analysis used the maximums of these loads even thought that were deduced for different crank angle.

8.1.3 Results of FEM Analysis

In this chapter, results are obtained for static stress analysis in the form of Von-Misses stresses. Figure 73 to Figure 80 show results in terms of Von Misses stresses of the connecting rod under the static loading with stress intensity as a colors representation. The analysis shows that the shank of the rod is the part with the highest stress intensity. According to the legend on the left side, the stress in this area is between 160 MPa and 300 MPa, and the loads are evenly distributed over the beam section. The maximum value of the stress is 387MPa The maximum stress is between small-end and rod-linkage (Figure 76).

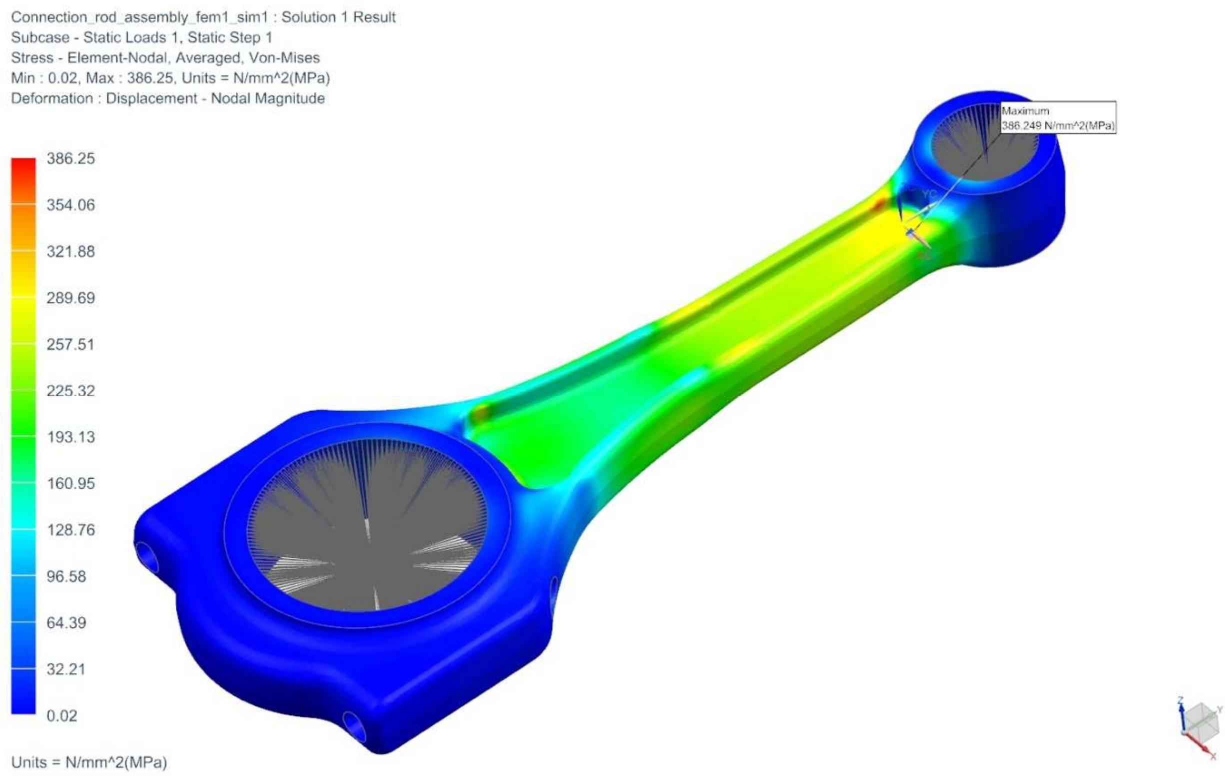

Figure 73 Connecting rod Von misses Stress Distribution

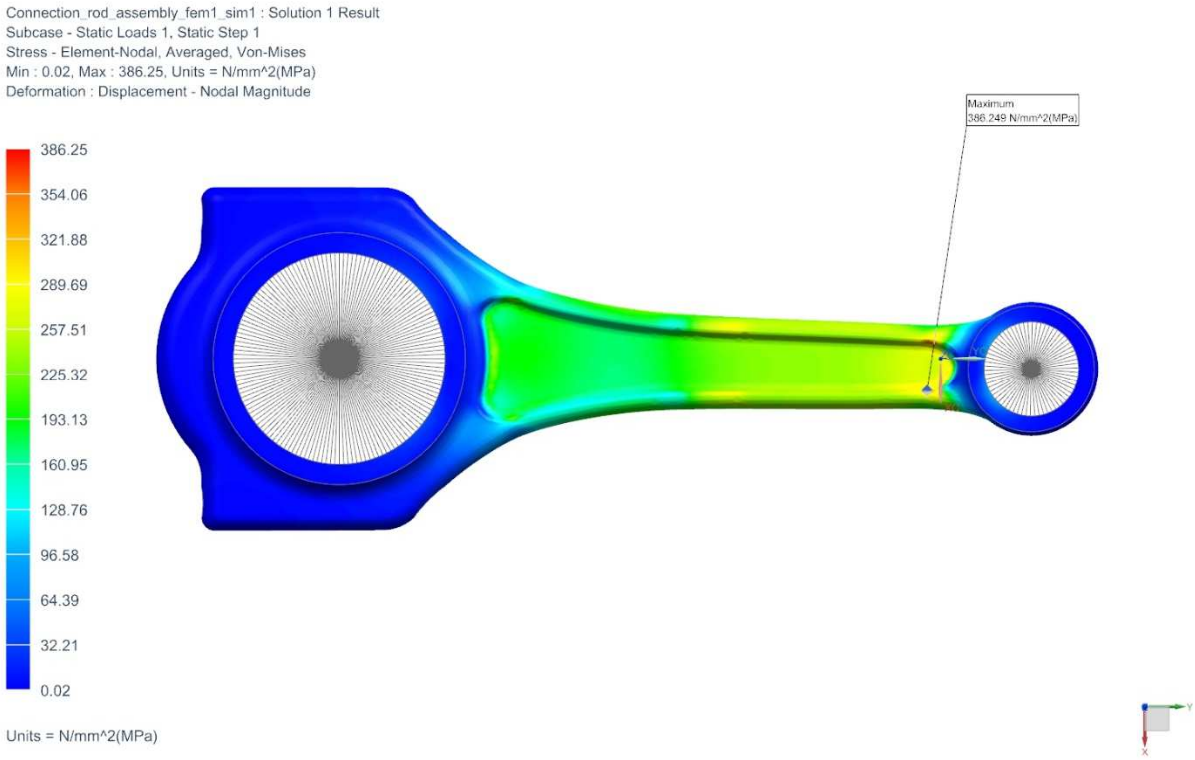

Figure 74 Connecting rod Von misses Stress Distribution

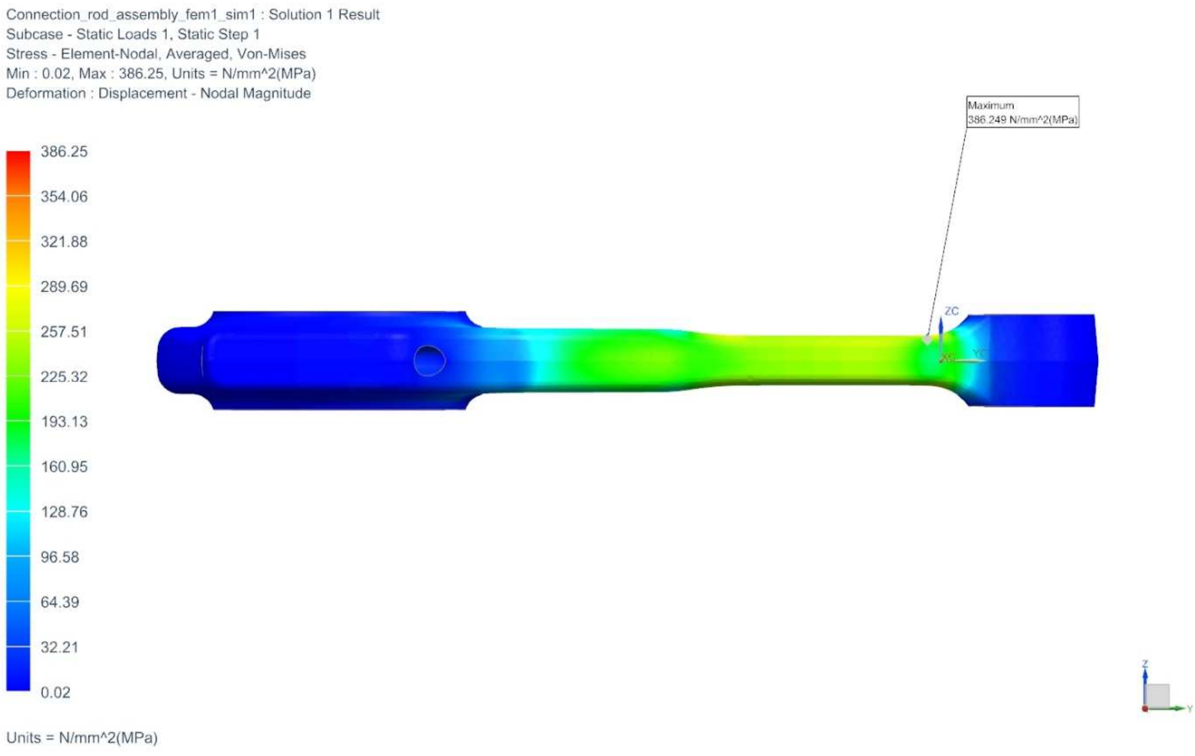

Figure 75 Connecting rod Von misses Stress Distribution

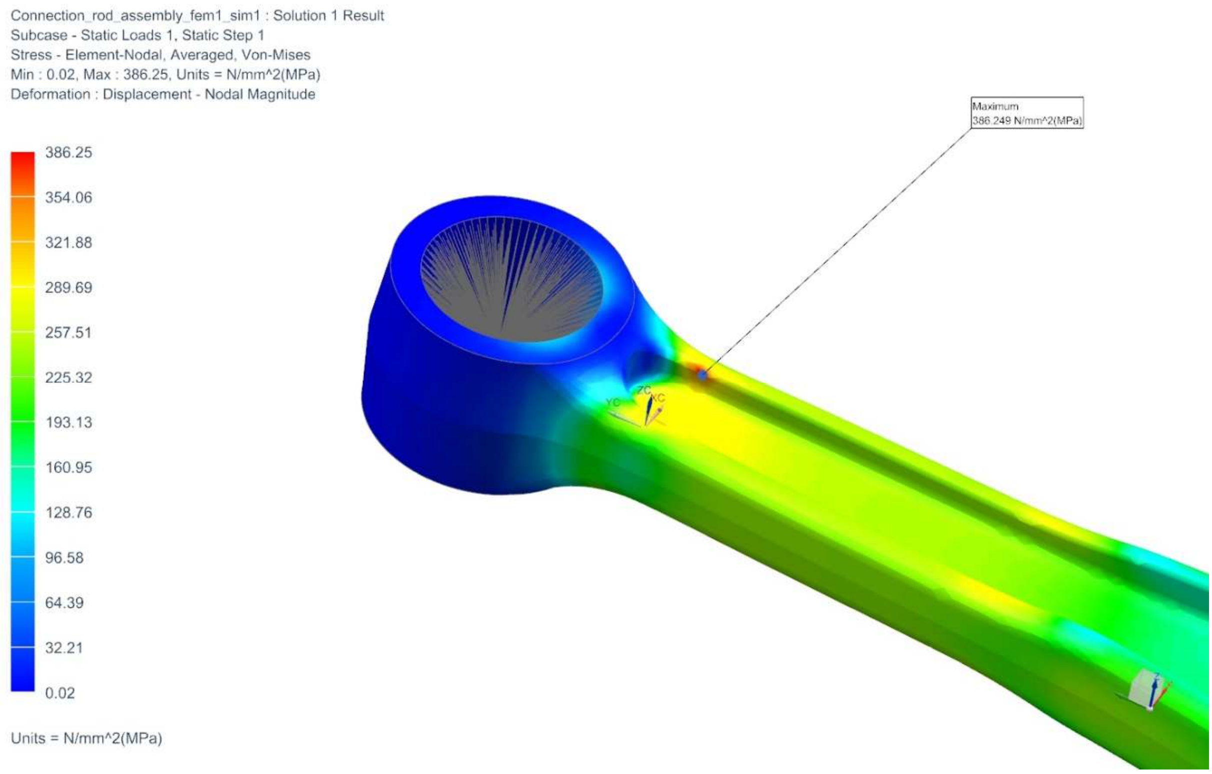

Figure 76Connecting rod Von misses Stress Distribution - Detail of the most loaded part

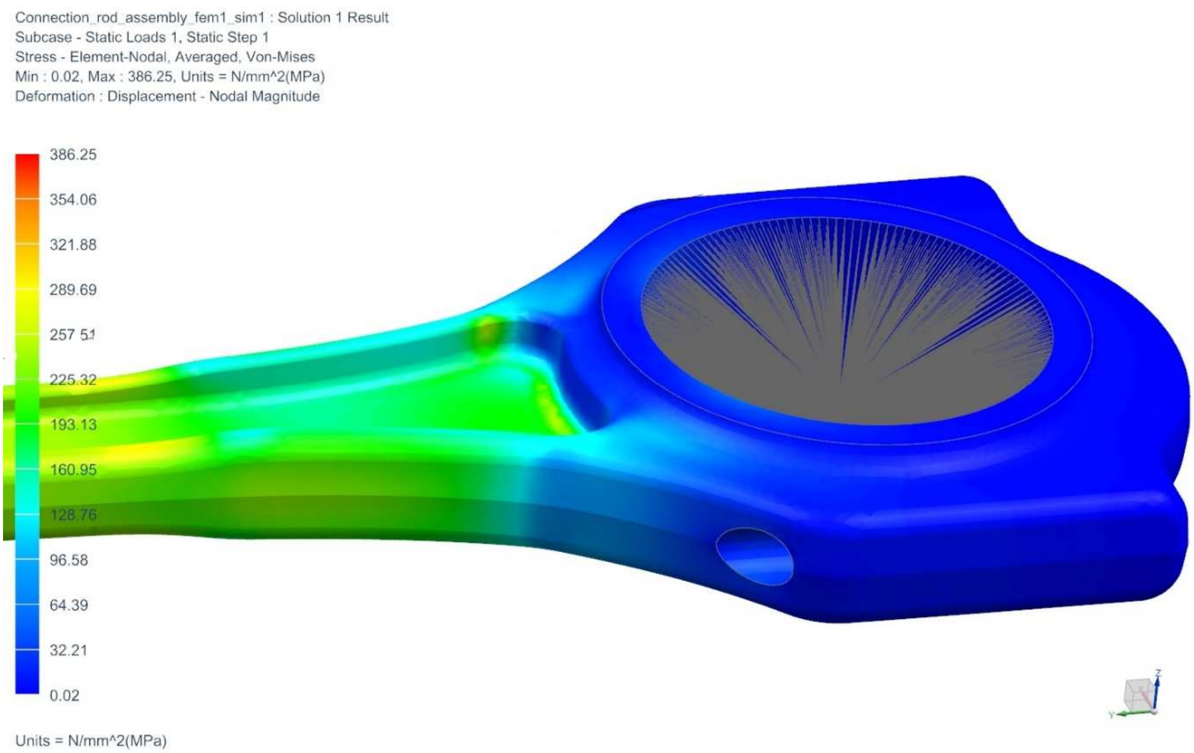

Figure 77Connecting rod Von misses Stress Distribution

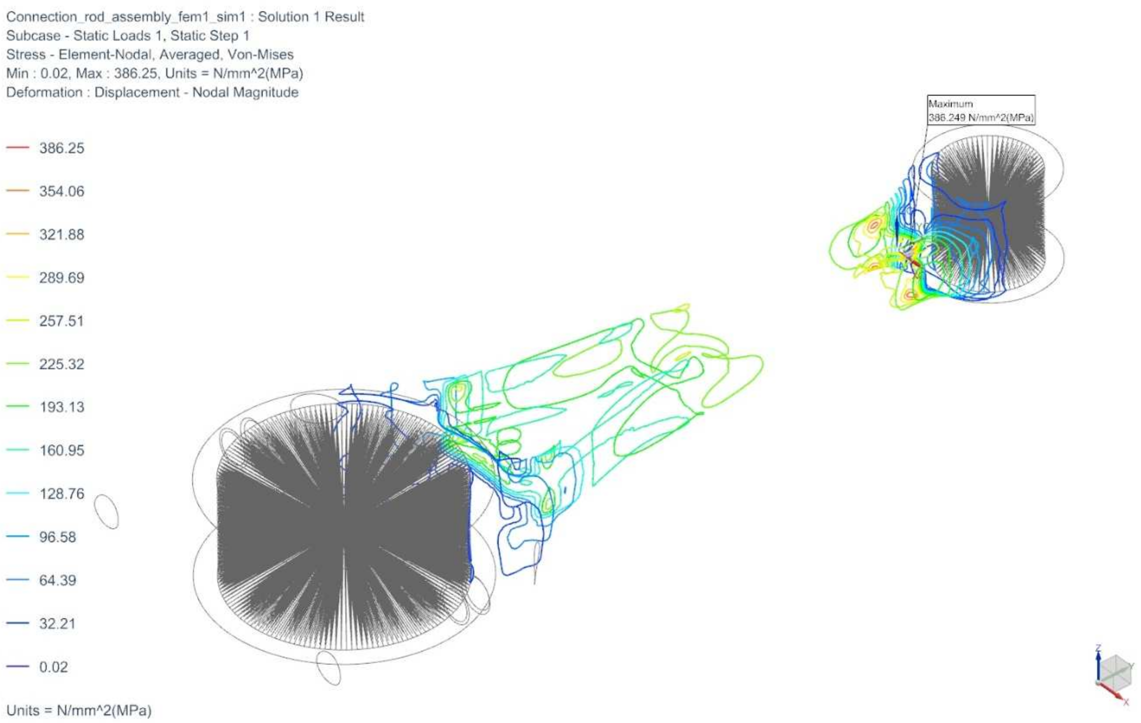

Figure 78 Connecting rod Von misses Stress Distribution - ISO – Lines

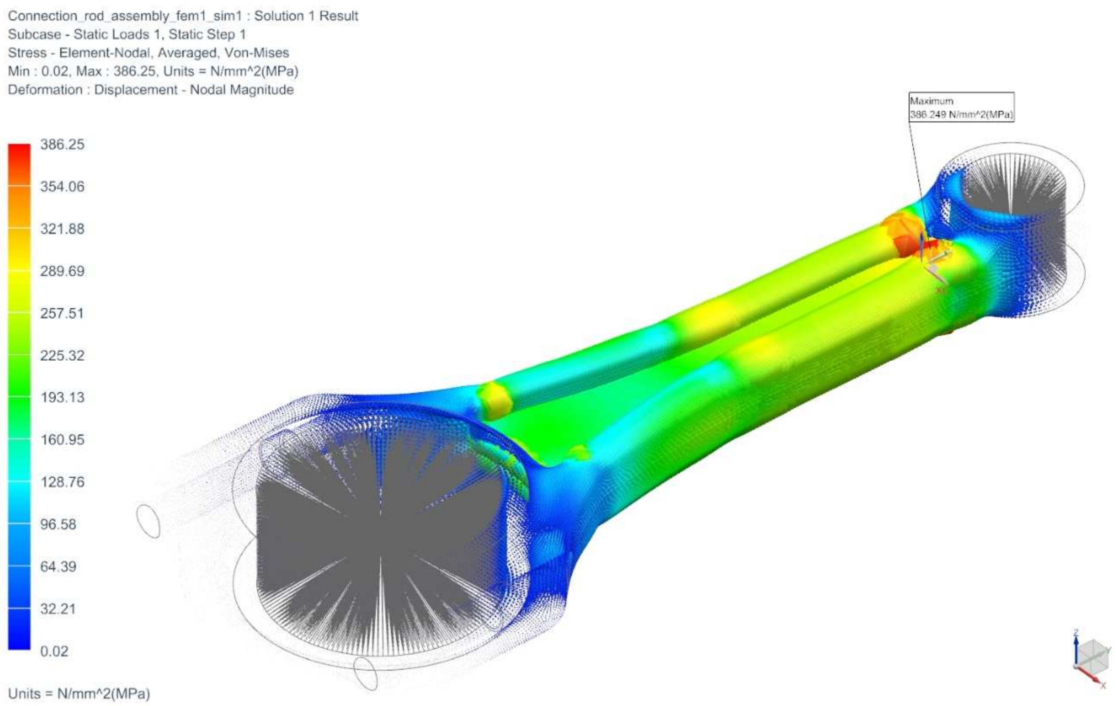

Figure 79 Connecting rod Von misses Stress Distribution - Spheres

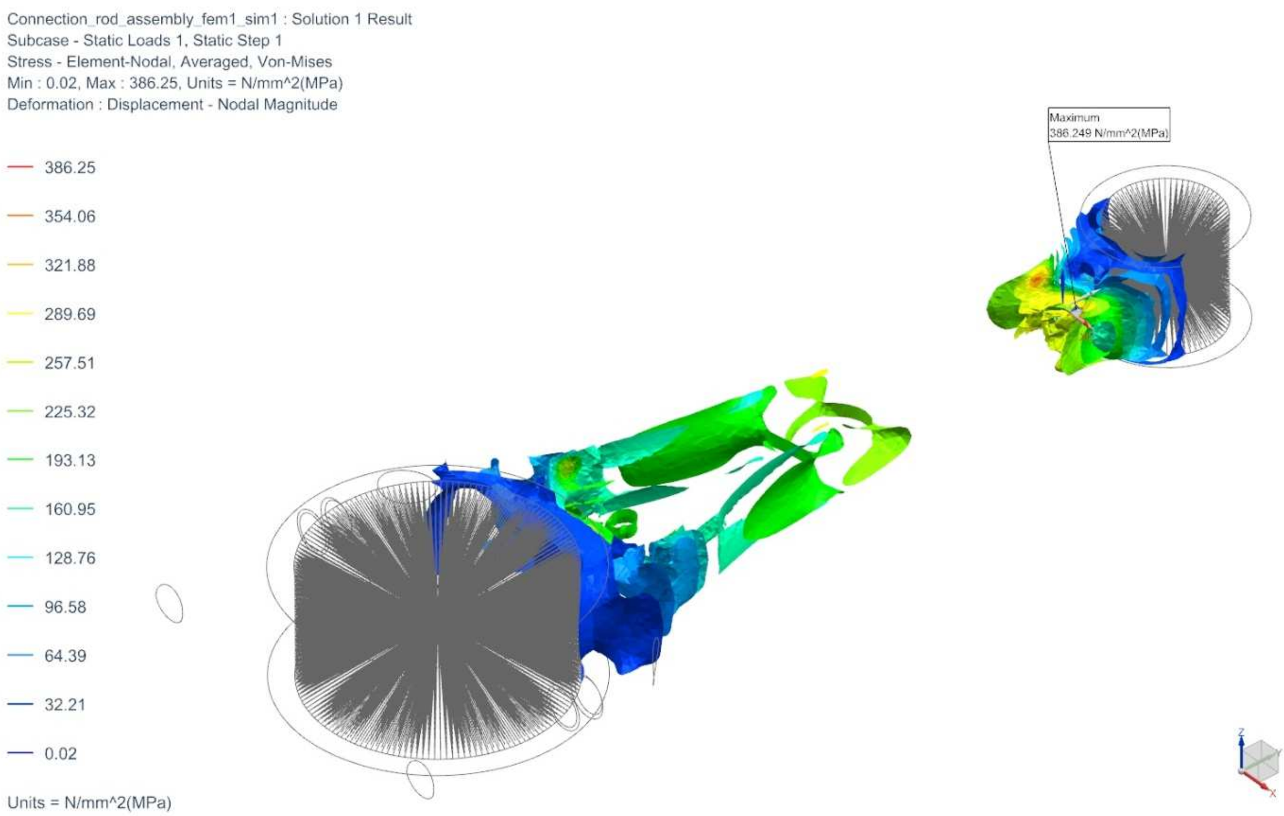

Figure 80 Connecting rod Von misses Stress Distribution - ISO - Surface

Value of Factor of Safety of the connecting rod is around 1.5, which indicates Safe Design of the Connecting Rod.

The main purpose of the analysis is to demonstrate the using of a FEM in a design of the combustion engine.

8.2 Calculation of connection rod bolts

The connection rod bolts are designed as a prestressed bolt connection. The static and the dynamic forces acting on the connection rod bolt. The static force results from preload F_i of the connection. The dynamic force comes from the inertia force of the rotating masses of the crankshaft assembly $F_{S_{cylinder}}$. This connection is loaded with great internal axis force (mounting prestressing) during assembly to provide the necessary force to bond contact surfaces of the divided big end of the connection rod. The scheme of a bolted connection is seen Figure 81. Parameters for a calculation is in Table 7.

Name	Abbrevation	Value	Unit
Material of the bolt	15 230.7	-	-
Yield Strength	R_e	835	MPa
Head diameter	D_1	12	mm
Hole diameter	D_0	8,5	mm
Hole lenght	L_0	44,5	mm
Nominal thread diameter	d_0	8	kg
Thread root diameter	d_3	6,2	mm
Threated lenght	L_1	11	mm
Pitch	P	1,5	mm
Under-head friction	f_H	0,2	-
Thread friction	f_T	0,15-	-
Shank diameter	d_2	7	mm
Shank length	L_2	31	mm
Contact surfaces (one bolt)	S_0	$1{,}956 \cdot 10^{-4}$	m^2
Tightening torque	T_T	35,5	Nm
Number of bolts of connection rod	i	2	-
Young module	E	$2{,}1 \cdot 10^{11}$	Pa
Stress concentrator factor	C_σ	4	-
Surface finish Factor	C_f	0,8	-
Size factor	C_S	1	-

Table 7 Calculation of the connection rod bolts - input data

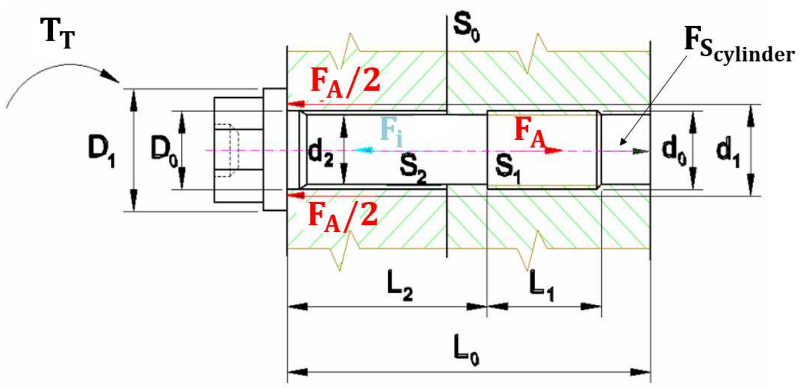

Figure 81 Scheme of a bolted connection

Tightening the bolts:

Diameter $d_1$for calculation of internal axis force:

$$d_1 = \frac{D_1+D_0}{2} = \frac{12+8,5}{2} = 10,25\text{mm} \tag{36}$$

Thread angle:

$$\varphi_z = arctg\frac{P}{\pi \cdot D_0} = arctg\frac{1,5}{\pi \cdot 8,5} = 3,22° \tag{37}$$

Axial operating force:

$$F_A = \frac{T_T}{tg\varphi_z \cdot \frac{D_0}{2} + f_T \cdot \frac{D_0}{2} + f_H \cdot \frac{d_1}{2}} \tag{38}$$

$$F_A = \frac{35,5}{tg\ 2,9° \cdot \frac{0,0085}{2} + 0,15 \cdot \frac{0,0085}{2} + 0,2 \cdot \frac{0,01025}{2}}$$

$$F_A = 18\,905\text{N}$$

Tensile stress in the shank of the bolt:

$$\sigma_T = \frac{F_A}{S_2} = \frac{29\ 805}{\frac{\pi \cdot 7^2}{4}} = 491MPa \tag{39}$$

Preload:

Condition to maintain a contact between the surfaces of the divided big end of the connection rod:

$$F_i > \frac{F_{S_{cylinder}}}{i} \tag{40}$$

Proposal of the preload force:

$$F_i = 2,5 \cdot \frac{F_{S_{cylinder}}}{i} = 2,5 \cdot \frac{10\ 100}{2} = 12625N \tag{41}$$

The coefficient of flexibility of the connecting rod bolt:

$$\kappa_B = \sum_{j}^{n} \frac{L_j}{E \cdot S_j} = \frac{L_1}{E \cdot S_1} + \frac{L_2}{E \cdot S_2} \tag{42}$$

$$= \frac{0{,}011}{2{,}1 \cdot 10^{11} \cdot \frac{\pi \cdot 0.008^2}{4}} + \frac{0{,}031}{2{,}1 \cdot 10^{11} \cdot \frac{\pi \cdot 0.007^2}{4}} = \underline{4{,}88 \cdot 10^{-9} Nm^{-1}}$$

The flexibility coefficient of the connection rod:

$$\kappa_S = \frac{L_o}{E \cdot S_o} = \frac{0{,}0445}{2{,}1 \cdot 10^{11} \cdot 1{,}956 \cdot 10^{-4}} = \underline{1{,}083 \cdot 10^{-9} Nm^{-1}} \tag{43}$$

Overall flexibility coefficient of the connection:

$$\kappa = \frac{\kappa_S}{\kappa_B \cdot \kappa_S} = \frac{1{,}083 \cdot 10^{-9}}{4{,}88 \cdot 10^{-9} \cdot 1{,}083 \cdot 10^{-9}} = 0{,}205 \tag{44}$$

Maximal tensile force acting on the bolt:

$$F_{Tmax} = F_i + \kappa \cdot \frac{F_{S_{cylinder}}}{2} = \tag{45}$$

$$12625 + \left(0{,}205 \cdot \frac{10\ 100}{2}\right) = \underline{13660\ N}$$

Fatigue analysis:

A. Screw shank:

Maximum stress in the cycle:

$$\sigma_{MAX}^{S} = \frac{F_{Tmax}}{S_2} = \frac{13660}{\frac{\pi \cdot 7^2}{4}} \cong 355MPa \tag{46}$$

Minimum stress in the cycle:

$$\sigma_{MIM}^{S} = \frac{F_i}{S_2} = \frac{12625}{\frac{\pi \cdot 7^2}{4}} \cong 328MPa \tag{47}$$

Mean stress in the cycle:

$$\sigma_{m}^{S} = \frac{\sigma_{MAX}^{S} + \sigma_{MIM}^{S}}{2} = \frac{355 + 328}{2} \cong 341{,}5MPa \tag{48}$$

Stress amplitude:

$$\sigma_{a}^{S} = \frac{\sigma_{MAX}^{S} - \sigma_{MIM}^{S}}{2} = \frac{355 - 328}{2} \cong 13{,}5MPa \tag{49}$$

Maximum stress:

$$\sigma_{max}^{S} = \frac{C_\sigma}{C_s \cdot C_f} \cdot \sigma_a^S + \sigma_m^S \tag{50}$$

$$= \frac{4}{1 \cdot 0{,}8} \cdot 13{,}5 + 341{,}5 \cong 409MPa$$

Safety factor:

$$f_s^S = \frac{R_e}{\sigma_{max}^{S}} = \frac{835}{409} \cong 2{,}04 \tag{51}$$

B. Cross-section of the screw core:

Maximum stress in the cycle:

$$\sigma_{MAX}^{C} = \frac{F_{Tmax}}{S_3} = \frac{13660}{\frac{\pi \cdot 6{,}2^2}{4}} \cong 452MPa \tag{52}$$

Minimum stress in the cycle:

$$\sigma_{MIM}^{C} = \frac{F_i}{S_3} = \frac{12625}{\frac{\pi \cdot 6{,}2^2}{4}} \cong 418MPa \tag{53}$$

Mean stress in the cycle:

$$\sigma_m^C = \frac{\sigma_{MAX}^C + \sigma_{MIM}^C}{2} = \frac{452 + 418}{2} \cong 435MPa \tag{54}$$

Stress amplitude:

$$\sigma_a^C = \frac{\sigma_{MAX}^C - \sigma_{MIM}^C}{2} = \frac{452 - 418}{2} \cong 17MPa \tag{55}$$

Maximum stress:

$$\sigma_{max}^C = \frac{C_\sigma}{C_s \cdot C_f} \cdot \sigma_a^C + \sigma_m^C \tag{56}$$

$$= \frac{4}{1 \cdot 0{,}8} \cdot 17 + 435 \cong 520MPa$$

Safety factor:

$$f_s^C = \frac{R_e}{\sigma_{max}^C} = \frac{835}{520} \cong 1{,}6 \tag{57}$$

Fatigue safety coefficient for the bolt must be $f_s = 1{,}5 \div 2{,}5$. This condition is satisfied for the both cases (see above)

8.3 Engine balancing

8.3.1 Calculation of the rotating and reciprocating masses of the connection rod

First will be explained some concepts in dynamics. Two systems of bodies are said to be dynamically equivalent if their motions are the same under the same sets of forces and moments. This can be seen in Figure 82 where a real connection rod is idealized by its dynamically equivalent system consisting of two masses m_S and m_R connected by a rigid massless rod. This concept of the equivalent system is useful especially in solving complex problems. To be more precise, it is necessary to mathematically satisfy the following equations in order to ensure dynamic equivalency:

$$m_S + m_R = m_{oj} \tag{58}$$

$$m_S L_S - m_R L_R = 0 \tag{59}$$

$$m_S L_S^2 + m_R L_R^2 = I_G \tag{60}$$

The first equation (58) is the sum of the mass of an ideal system = mass of the real object.

Equation (59) identifies location of the center of mass for the ideal object. Equation (60) describes that moment of inertia of the real object and the ideal system is balanced.

The following table (Table 8) contains data, which are essential for further calculation. The data were provided by NX 10 from CAD model of the connection rod.

Name	Abbreviation	Value	Unit
Distance between center of gravity and center of big end	L_R	28,55	mm
Distance between center of gravity and center of small end	L_S	105	mm
Distance between center of small end and big end	L_{oj}	133,55	mm
Connection rod total weight	m_{oj}	0,540	kg

Table 8 Calculation of the connection rod masses - input data

Typically, for static balancing equation (60) can be omitted. Using just the first two equations calculation of rotating and reciprocation masses of the connection rod will be performed.

$$m_S = m_{oj} \frac{L_R}{L_{oj}} = 0{,}540 \frac{28{,}55}{133{,}55} \cong 0{,}115\ [kg] \tag{61}$$

$$m_R = m_{oj} \frac{L_S}{L_{oj}} = 0{,}540 \frac{105}{133{,}55} \cong 0{,}425\ [kg] \tag{62}$$

Table 9 shows enumeration of the output data.

Name	Abbreviation	Value	Unit
Reciprocation mass of the connection rod	m_S	0,115	kg
Rotation mass of the connection rod	m_R	0,425	kg

Table 9 Calculation of the connection rod masses - output data

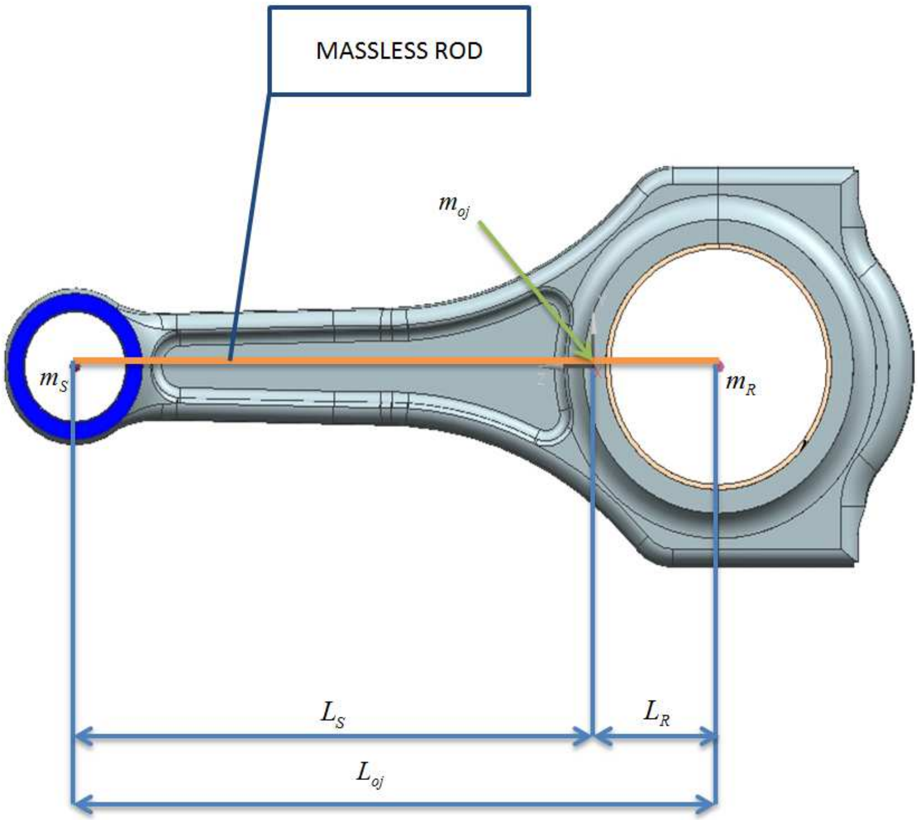

Figure 82 Dumbbell-shaped equivalent of a real connection rod. Center of mass is the same for both

8.3.2 Calculation of the rotating and reciprocating masses for one cylinder

Firstly, it is necessary to find out the mass and the center of mass of the crank arm. These data were provided by NX 10 from the CAD model of the crankshaft shows in Figure 83.

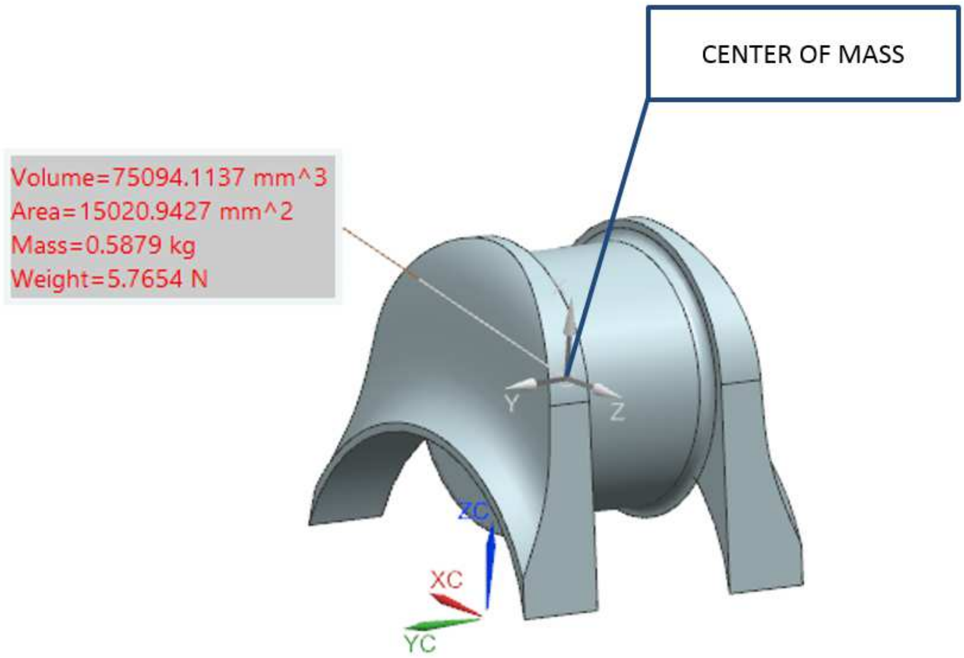

Figure 83 CAD model of the crank arm

Name	Abbreviation	Value	Unit
Mass of the crank arm	m_{zal}	0,588	kg
Distance between crankshaft axis and center of mass of the crank arm	r_{Tzal}	40,44	mm
Crank radius	r_K	40,25	mm
Piston assembly weight	m_p	0,468	kg

Table 10 Calculation of rotating and reciprocating masses - input data

Secondary, it is a calculation of an equivalent mass of the crank arm, which is moved to crankpin axis showed in Figure 82

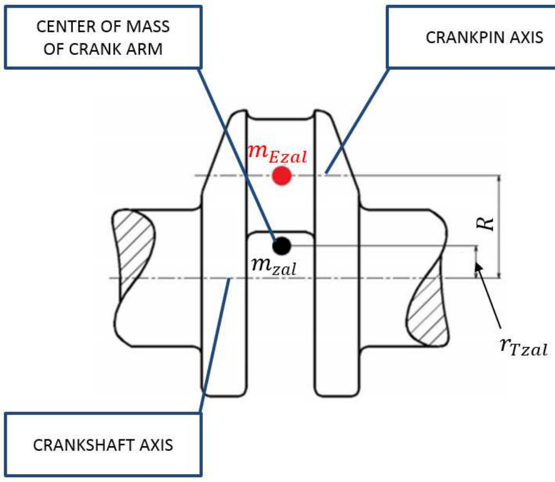

Figure 84 Equivalent of mass of the crank pin

$$m_{Ezal} = m_{zal}\frac{r_{Tzal}}{r_K} = 0{,}588\frac{40{,}44}{40{,}25} = 0{,}591[kg] \tag{63}$$

Thirdly, rotating mass of the crankshaft assembly is:

$$m_{R\_cylinder} = m_{Ezal} + m_R = 0{,}591 + 0{,}425 = 1{,}016\ [kg] \tag{64}$$

Finally, reciprocating mass of the crankshaft assembly is:

$$m_{S\_cylinder} = m_S + m_p = 0{,}115 + 0{,}468 = 0{,}583[kg] \tag{65}$$

Name	Abbreviation	Value	Unit
Rotating mass of the crankshaft assembly for one cylinder	$m_{R\_cylinder}$	1,016	kg
Reciprocating mass of the crankshaft assembly for one cylinder	$m_{S\_cylinder}$	0,583	kg

Table 11 Calculation of rotating and reciprocating masses - output data

8.3.3 Balancing of rotating system

Generally speaking, the goal is that center of gravity of the crankshaft must be on the axis of a rotation.

In order to balance the rotational inertia force, the counterweights are attached to the crankshaft. The counterweights are attached to the both webs for each crank arm as could be seen in Figure 85. This design provides static balance and dynamic as well.

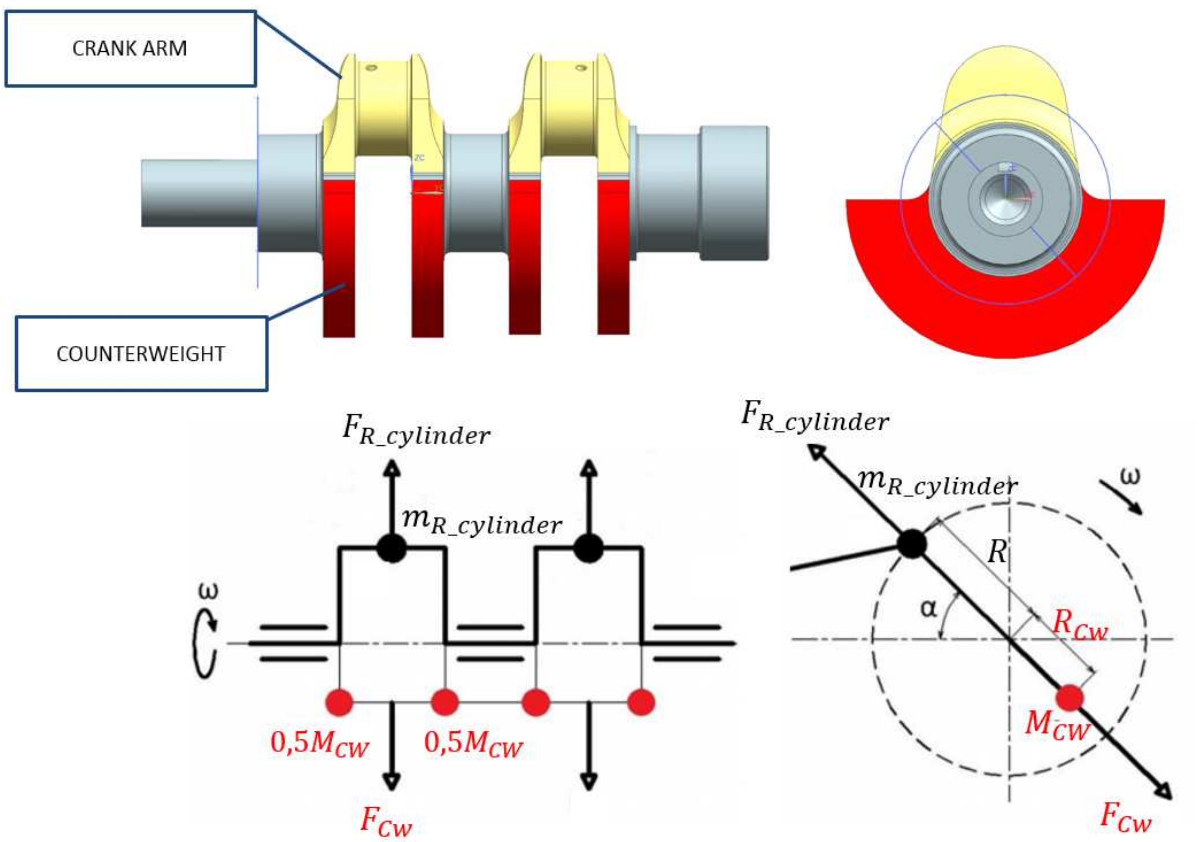

Figure 85 CAD model and scheme of the balancing of the rotating inertia forces

The overall rotational inertia force for one cylinder of an in-line two cylinder engine is:

$$F_{R\_cylinder} = m_{R\_cylinder} \cdot r_K \cdot \omega^2 \tag{66}$$

The goal is balance rotation inertia force and centrifugal force of the counterweights for each crank arm.

$$F_{R\_cylinder} = F_{CW} \tag{67}$$

$$m_{R\_cylinder} \cdot r_K \cdot \omega^2 \cdot = m_{CW} \cdot R_{CW} \cdot \omega^2 \tag{68}$$

An effective counterweight radius R_{CW} was obtained by Siemens NX 10 from CAD model of the counterweights

Name	Abbreviation	Value	Unit
Effective counterweight radius	R_{CW}	33,5	mm

Table 12 Rotation balancing - input data

$$m_{CW} = \frac{m_{R\_cylinder} \cdot r_K}{R_{CW}} = \frac{1{,}016 \cdot 40.25}{33.5} = 1{,}221[kg] \tag{69}$$

The design of the counterweights is shown in Figure 85.

8.3.4 Balancing of reciprocation system (first order)

For an in-line, two-cylinder engine is common to balance just primary inertia forces and moments. Primary moments of the reciprocating masses are naturally balanced due to crankshaft design

In order to balance primary inertia forces of the reciprocating masses, one balance shaft and counterweights, which are attached to the crankshaft, were designed.

The basic design of the balance shaft is shown in Figure 86. The half-cylinder shaped counterbalance (the green part) is used to balance half of the reciprocating mass of two cylinders.

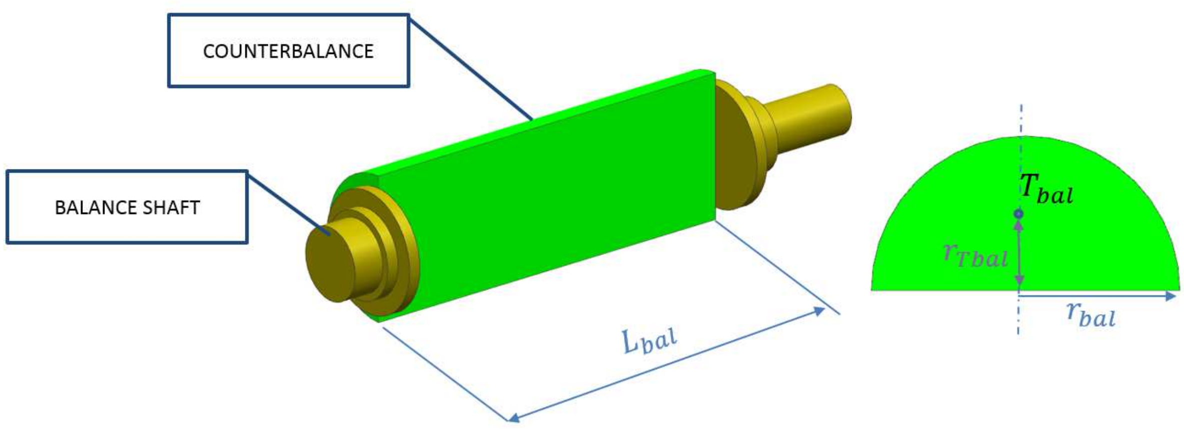

Figure 86 Basic design of the balance shaft with half cylinder shaped counterbalance

Primary inertia force for two cylinders of an in-line two cylinder engine is:

$$F_S^1 = F_{S_{cylinder}}^1 + F_{S_{cylinder}}^1 \quad (70)$$

$$= 2 \cdot m_{S\_cylinder} \cdot r_K \cdot \omega^2 \cdot cos\alpha$$

The first step is to balance centrifugal force of the balance shaft and half of the primary inertia force. The second step is to balance centrifugal force of the crankshaft counterweight (the blue part in Figure 87) and half of primary inertia force.

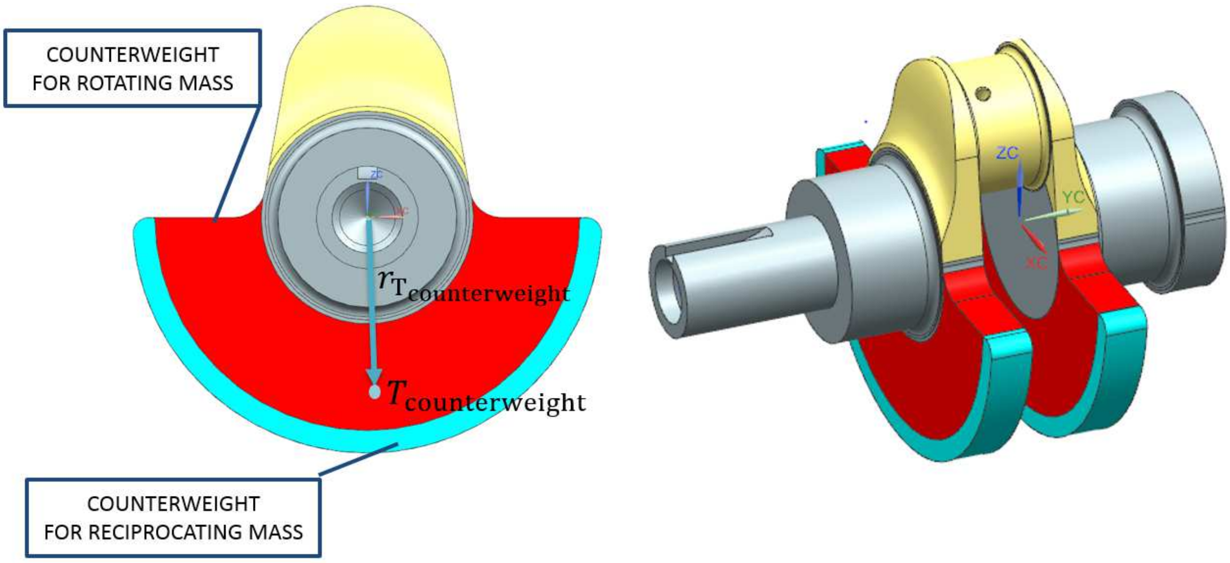

Figure 87 Basic design of the crankshaft with counterweight for rotating and reciprocatinng masses

First step - Balance shaft calculation:

$$F_{counterbal}^1 = \frac{1}{2} \cdot F_S^1 \quad (71)$$

$$m_{counterbal} \cdot r_{\mathrm{T_{bal}}} = \frac{1}{2}(2 \cdot m_{S_{cylinder}} \cdot r_K) \quad (72)$$

The mass of the half-cylinder shaped counterbalance is:

$$m_{counterbal} = \frac{1}{2} \cdot \pi \cdot r_{bal}^2 \cdot \rho \cdot L_{bal} \quad (73)$$

The center of the mass for a half-cylinder shaped counterbalance is:

$$r_{\mathrm{T_{bal}}} = \frac{4}{3 \cdot \pi} \cdot r_{\mathrm{bal}} \quad (74)$$

Name	Abbreviation	Value	Unit
Length of the counterbalance	L_{bal}	165	mm
Distance between balance shaft axis and center of mass of the counterbalance	$r_{\mathrm{T}_{\mathrm{bal}}}$	$\frac{4}{3\cdot\pi}\cdot r_{\mathrm{bal}}$	mm-
Density of steel	ρ	7850	$\frac{kg}{m^3}$

Table 13 Calculation of the counterbalance - input data

Using equations (73) and (74) in equation (72):

$$\frac{1}{2}\cdot\pi\cdot r_{bal}^2\cdot\rho\cdot L_{bal}\cdot\frac{4}{3\cdot\pi}\cdot r_{\mathrm{bal}} = \frac{1}{2}(2\cdot m_{S_{cylinder}}\cdot r_K) \tag{75}$$

then:

$$r_{\mathrm{bal}} = \sqrt[3]{\frac{3\cdot m_{S_{cylinder}}\cdot r_K}{2\cdot\rho\cdot L_{bal}}} \tag{76}$$

$$r_{\mathrm{bal}} = \sqrt[3]{\frac{3\cdot 0{,}583\cdot 40{,}25}{2\cdot 7850\cdot 165}} \cong 30[mm]$$

Second step - crankshaft counterweight calculation:

The counterweights are attached to the both webs for each cylinder as it is shown in Figure 87.

$$F_{counterweight}^1 = \frac{1}{2}\cdot F_S^1 \tag{77}$$

If total number of counterweight is 4 then:

$$4\cdot m_{counterweight}\cdot r_{\mathrm{T}_{\mathrm{counterweight}}} = \frac{1}{2}(2\cdot m_{S_{cylinder}}\cdot r_K) \tag{78}$$

Distance between crankshaft axis and center of mass of counterweight $r_{\mathrm{T}_{\mathrm{counterweight}}}$ *was* obtained by NX 10 from CAD model of the counterweights (Figure 87)

Name	Abbreviation	Value	Unit
Distance between crankshaft axis and center of mass of counterweight	$r_{\mathrm{T}_{\mathrm{counterweight}}}$	44,5	mm

Table 14 Calculation of the counterweight - input data

Then:

$$m_{counterweight} = \frac{m_{S_{cylinder}} \cdot r_K}{4 \cdot r_{\mathrm{T}_{\mathrm{counterweight}}}} = \frac{0{,}583 \cdot 40{,}25}{4 \cdot 44{,}5} = 0{,}132[kg] \tag{79}$$

The concept design of the counterweights for reciprocating mass is shown in Figure 87.

9 Conclusion

The main goal of the thesis is a conceptual design of a 4 stroke, 2 cylinder in-line turbocharged engine for an hybrid electric vehicle. During the design process, a few main parts of the engine were recognized as most important and vital for the concept. These parts (included crankshaft assembly, a cylinder head and an engine block), were later designed according the literature in order to achieve high efficiency and low mechanical losses.

The construction of the engine is based on the given parameters. This specification (Table 15) was used to calculate pressure related to crank angle at different engine speed. These data were obtained from 1D engine simulation. The simulation was performed in the company Ricardo Prague. The data were essential for modeling and design parts of the combustion.

Specifications	Value
Fuel	Gasoline/CNG
Strokes	4
Engine Type	V2
Displacement	0.9 L
Injection System	DI/PFI
Induction System	TwinScroll
Valves/Cylinder	4
Bore	80.5 mm
Stroke	80 mm
Connecting Rod Length	133.55 mm
Compression Ratio	10 mm
Intake Valve Max. Lift	8.9 mm
Exhaust Valve Max. Lift	8.9 mm
Intake Valve Diameter	29.8 mm
Exhaust Valve Diameter	25.4 mm
RPM Range	1000 to 6000
Peak Power	63/59 kW @ 5500 rpm
Peak Torque	145/140 N*m @ 2000-3500 rpm
BSFC at Peak Eff.	242/233 g/kW/h

Table 15 Given parameters of the conceptual engine

Thesis includes also a background research of the various HEV powertrain configuration. The designed engine is developed as a part of a propulsion unit for series Hybrid Electric vehicle. More precisely, it will be a part of Plug-in hybrid electric vehicle with increased energy storage capacity. Using the advantages of both series and plug-in HEV. The engine speed will be controlled independently of vehicle speed. This provides operation of the engine at its optimum speed to achieve the best fuel economy. Thanks to this configuration, it also provides capability of all wheel-drive of a vehicle.

The calculation analysis is mainly focused on the connection-rod stress analysis. It was necessary to performed many calculations to obtain input data for stress analysis. That includes calculation of the basic crank mechanism quantities, calculation of crankshaft drive kinematics etc. The analysis shows that the shank of the rod is the part with the highest stress intensity. The stress in this area is between 160 MPa and 300 MPa, and the loads are evenly distributed over the beam section. The maximum value of the stress is 387MPa.

Internal combustion engine is extremely complex system, which has been developing and improving for more than 140 years. Design process of the ICE is demanding and time consuming. The description of the process modeling is not exhaustive due to complexity of each part. This is the reason that some parts are simplified just to show geometry. It is not possible to design a whole ICE within a given time for a diploma thesis. Valve –gear assembly could be the next step in the conceptual design.

.

Reference

[1]. **Husain, I.** *Electric and Hybrid Vehicles - Design Fundametnals.* místo neznámé : CRC PRESS, 2005.
[2]. **Gscheidle, R.** Příručka pro automechanika. Praha : Sobotáles, 2002. ISBN 80-85920-83-2.
[3]. tumblr. [Online] [Cited: 29. 12 2015.].
www.tumblr.com.
[4]. Encyklopedia Britannica. [Online] [Cited: 29. 12 2015.].
http://www.britannica.com/.
[5] **C.Mi, Abul Masrur and David Wenzhong Gao**. *Hybrid Electric Vehicles.* Wiley, 2011.
[6] **S.S. Williamson.** *Energy Management Strategies for Electric and Plug-in Hybrid Electric Vehicles.* Canada : Springer, 2013. ISBN 978-1-4614-7710-5.
[7]. Motion video motorsport. [Online] [Cited: 29. 12 2015.]
http://www.motionvideo.co.nz/.
[8]. **English, Andrew.** *Popularmechanics.* [Online] 23. 7 2013. [Cited: 29. 12 2015.]
http://www.popularmechanics.com/.
[9]. Dictionoary of Automotive Terms. [Online] [Cited: 29. 12 2015.]
http://www.motorera.com/.
[10]. **V.A.W. Hillier**. *Fundatmentals of Motor Vehicle Technology.* Cheltenham : Stanley Thornes Ltd, 201. ISBN 0 7487 0531 7.
[11]. What-when-how. *Crankshaft Lubrication.* [Online] [Cited: 29. 12 2015.]
http://what-when-how.com/.
[12]. **Schreier, L**. *Tension and Compression in Connecting Rods*. [Online] 29. 12 2015.
http://emweb.unl.edu/.
[13]. Engine Types and Their Operation. [Online] [Cited: 25. 3 2016.]
http://howautowork.com/.
[14]. **Nice, K.** How Turbochargers Work [Online] [Cited: 25. 3 2016.]
(http://auto.howstuffworks.com/turbo3.htm). Auto.howstuffworks.com.
[15]. The Downsizing Agenda. *HoneyWell Turbo Technologies.* [Online] [Cited: 25. 3 2016.]
http://turbo.honeywell.com/turbo-basics/the-downsizing-agenda/.
[16]. **Hiereth, H a Prenninger, P**. *Charging the internal combustion engine.* Austria : Springer Wien New York, 2003. ISBN 978-3-211-33033-3.
[17]. **Stone, R a Ball, J. K**. *Automotive Engineering Fundamentals.* USA : SAE International, 2004. ISBN 0-7680-0987-1.
[18]. Turbocharging . Autozine Technical School. [Online] [Cited: 29. 12 2015.]
http://www.autozine.org/technical_school/engine/Forced_Induction_3.html
[19]. **Veltman, T**. Variable-Geometry Turbochargers. [Online] 24. 10 2010. [Cited: 29. 12 2015.]
http://large.stanford.edu/courses/2010/ph240/veltman1/.
[20] . **Vlk, František.** *Vozidlové spalovací motory 1.* Brno : Vlk, 2003. ISBN 8023887564
[21]. **Rober Bosch GmbH.** *Automotive Handbook,9th edition.* Wiley, 2014. ISBN: 978-1-119-03294-6.
[22]. **Etsion, I. a Sher, E.** *Improving fuel efficiency with laser surface textured piston rings*. Elsevier, 2008.
[23]. Auto-innovations. [Online] [Cited: 5. 4 2016.]
http://www.auto-innovations.com/site/images1b/fiattwinair1.jpg
[24]. Wikipedia. [Online] [Cited: 5. 4 2016.]
https://upload.wikimedia.org/wikipedia/commons/a/aa/Straight%20
twin_engine_with_different_crank_shaft_angles.gif"
[25]. CARiD. [Online] [Cited: 5. 4 2016.]
http://www.carid.com/images/motorad/info/images/cooling-system2.jpg
[26] . **Kožoušek.** *Výpočet a konstrukce spalovacích motorů 2.* Praha : SNTL, 1983.

List of figures

List of tables

Appendix

Drawings : Crankshaft (ZCU-DT-001)

Connection rod (ZCU-DT-002)